

INFORMATION TO USERS

This manuscript has been reproduced from the microfilm master. UMI films the text directly from the original or copy submitted. Thus, some thesis and dissertation copies are in typewriter face, while others may be from any type of computer printer.

The quality of this reproduction is dependent upon the quality of the copy submitted. Broken or indistinct print, colored or poor quality illustrations and photographs, print bleedthrough, substandard margins, and improper alignment can adversely affect reproduction.

In the unlikely event that the author did not send UMI a complete manuscript and there are missing pages, these will be noted. Also, if unauthorized copyright material had to be removed, a note will indicate the deletion.

Oversize materials (e.g., maps, drawings, charts) are reproduced by sectioning the original, beginning at the upper left-hand corner and continuing from left to right in equal sections with small overlaps.

Photographs included in the original manuscript have been reproduced xerographically in this copy. Higher quality 6" x 9" black and white photographic prints are available for any photographs or illustrations appearing in this copy for an additional charge. Contact UMI directly to order.

ProQuest Information and Learning
300 North Zeeb Road, Ann Arbor, MI 48106-1346 USA
800-521-0600

UMI[®]

University of Alberta

Fractionation of Softwood TMP

by

Wei Li



**A thesis submitted to the Faculty of Graduate Studies and Research in partial
fulfillment of the requirement for the degree of Master of Science**

Department of Chemical and Materials Engineering

Edmonton, Alberta

Spring 2002



**National Library
of Canada**

**Acquisitions and
Bibliographic Services**

**395 Wellington Street
Ottawa ON K1A 0N4
Canada**

**Bibliothèque nationale
du Canada**

**Acquisitions et
services bibliographiques**

**395, rue Wellington
Ottawa ON K1A 0N4
Canada**

Your file Votre référence

Our file Notre référence

The author has granted a non-exclusive licence allowing the National Library of Canada to reproduce, loan, distribute or sell copies of this thesis in microform, paper or electronic formats.

L'auteur a accordé une licence non exclusive permettant à la Bibliothèque nationale du Canada de reproduire, prêter, distribuer ou vendre des copies de cette thèse sous la forme de microfiche/film, de reproduction sur papier ou sur format électronique.

The author retains ownership of the copyright in this thesis. Neither the thesis nor substantial extracts from it may be printed or otherwise reproduced without the author's permission.

L'auteur conserve la propriété du droit d'auteur qui protège cette thèse. Ni la thèse ni des extraits substantiels de celle-ci ne doivent être imprimés ou autrement reproduits sans son autorisation.

0-612-69728-2

Canada

University of Alberta

Library Release Form

Name of Author: Wei Li

Title of Thesis: Fractionation of Softwood TMP

Degree: Master of Science

Year this Degree Granted: 2002

Permission is hereby granted to the University of Alberta Library to reproduce single copies of this thesis and to lend or sell such copies for private, scholarly, or scientific research purposes only.

The author reserves all other publication and other rights in association with the copyright in the thesis, and except as hereinbefore provided, neither the thesis nor any substantial portion thereof may be printed or otherwise reproduced in any material form whatever without the author's prior written permission.



APT #303 10710-85AVE

Edmonton, Alberta

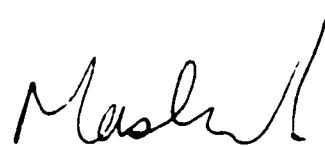
Canada T6E 2K8

Jan. 28th, 2002

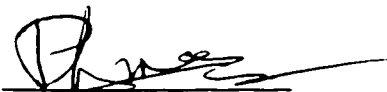
University of Alberta

Faculty of Graduate Studies and Research

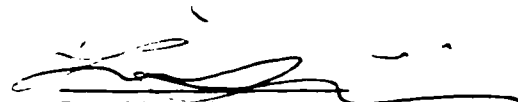
The undersigned certify that they have read, and recommend to the Faculty of Graduate Studies and Research for acceptance, a thesis entitled *Fractionation of Softwood TMP* by Wei Li in partial fulfillment of the requirement for the degree of Master of Science.



Dr. Jacob H. Masliyah
(Co-Supervisor)



Dr. Philip A.J. Mees
(Co-Supervisor)



Dr. Shijie Liu

Jan 28th, 2002



Dr. David J. Wilson

**This thesis is dedicated to my dear wife Mrs. Joyce Chen and my parents Mrs.
Fengshen Wang and Mr. Baosheng Li for their everlasting love and
encouragement.**

ABSTRACT

The objective of this study is to determine whether softwood thermo-mechanical wood pulp (TMP) can be fractionated on the basis of fibre length and fibre coarseness using a rotating cone fractionator, a continuous flotation cell and an air sparged hydrocyclone.

The rotating cone fractionator was found capable of fractionating softwood TMP fibres according to fibre length and fibre coarseness. A rough cone surface and a lower feed consistency improved fractionation performance. The continuous flotation cell was proved to be successful for fractionating softwood TMP fibres according to fibre length and fibre coarseness. A lower feed consistency and a lower feed flow rate improved fractionation performance. The air sparged hydrocyclone was found capable of separating about 5 wt% of long fibres from feed softwood TMP fibre suspension. A lower feed consistency and a higher air flow rate improved fractionation performance.

Based on the fractionation performance comparison, the continuous flotation cell was found to give the best fractionation performance for either removing fines or recovering long fibres from the feed softwood TMP fibre suspension at feed consistency of 0.15 wt%.

ACKNOWLEDGEMENTS

I would like to thank my co-supervisor Dr. Jacob H. Masliyah for his excellent guidance and immense encouragement throughout this project.

I would like to thank my co-supervisor Dr. Philip A.J. Mees for his great guidance and continuous support on this project.

A special thanks goes to Mr. Artin Afacan for his technical support and tremendous effort on thesis correction. A special thanks also goes to Dr. Shijie Liu, my colleagues and the support staff in the department for their support and help.

Finally, I would like to thank the Mechanical Wood-pulps Network of Centres of Excellence for providing the funding which made this thesis possible.

TABLE OF CONTENTS

Chapter 1

Introduction	1
1.1 Fibre fractionation	1
1.1.1 Characteristics of pulp fibres	1
1.1.2 Fractionation of wood pulp fibres.....	4
1.2 Objectives of present study.....	5

Chapter 2

Measurements	7
2.1 Fibre length measurement	7
2.1 Fibre coarseness measurement	9
2.2.1 Introduction	9
2.2.2 Sample preparation.....	10
2.2.3 Measurement in Fibre Quality Analyzer (FQA)	13
2.3 Consistency measurement	13
2.4 Cumulative fibre length and coarseness.....	14

Chapter 3

Rotating cone fractionator.....	18
3.1 Introduction.....	18
3.2 Experimental set-up.....	21
3.3 Results and discussion	24
3.3.1 Effect of feed consistency	24
3.3.2 Effect of feed flow rate	28
3.3.3 Effect of cone rotational speed	32
3.3.4 Effect of cone surface roughness	35
3.4 Conclusions	38

Chapter 4

Continuous flotation cell	39
4.1 Introduction.....	39
4.2 Experiment set-up.....	42
4.3 Results and discussion	44
4.3.1 Effect of feed consistency.....	44
4.3.2 Effect of feed flow rate.....	48
4.3.3 Effect of air flow rate.....	51
4.3.4 Effect of surfactant concentration.....	54
4.3.5 Effect of impeller rotation speed.....	57

4.4	Conslusions	57
-----	-------------------	----

Chapter 5

Air sparged hydrocyclone	60
5.1 Introduction.....	60
5.2 Experimental set-up.....	64
5.3 Results and discussion	66
5.3.1 Effect of feed consistency.....	66
5.3.2 Effect of feed flow rate.....	70
5.3.3 Effect of split ratio of overflow to feed.....	73
5.3.4 Effect of air flow rate.....	76
5.4 Conclusions.....	79

Chapter 6

Fractionation performance.....	80
6.1 Fractionation performance.....	81
6.2 Fractionation parameters.....	92

Chapter 7

Summary	94
---------------	----

Chapter 8

Recommendations for future work.....97

References.....98

Appendix

Data for all the figures included in this thesis.....102

NOMENCLATURE

A	cone angle, (degree)
A_L	fibre arithmetic mean length, (mm)
c	fibre slurry weight percentage consistency, (wt%)
C	fibre coarseness, (mg/100m)
L	arc length of fibre from one end to the other, (mm)
L_L	length weighted mean length, (mm)
L_w	weight weighted mean length, (mm)
h_f	vertical location of feed distributor from cone surface, (mm)
m	fibre mass, (mg)
N	crowding factor
n	fibre count
w	weight of the moisture-free fibre pad, (g)
f	weight of the moisture-free filter paper, (g)
g	weight of the fibre slurry, (g)
R	radius of rotating cone, (mm)
r_f	radial location of feed distributor from axis of rotation, (mm)

LIST OF FIGURES, TABLES AND PHOTOGRAPHS

Figures

- Figure 2.1 Two-stage washing process
- Figure 2.2 Variation of fibre coarseness at different washing time intervals
- Figure 2.3 Fibre fractionation system
- Figure 3.1 Axial zone collection of partical cloud near a rotating vaneless disk (Oroskar and Crosby, 1986)
- Figure 3.2 Rotating cone fractionator (RCF)
- Figure 3.3a Effect of feed consistency on fibre fractionation by fibre length
- Figure 3.3b Effect of feed consistency on fibre fractionation by fibre coarseness
- Figure 3.4a Effect of feed flow rate fibre on fractionation by fibre length
- Figure 3.4b Effect of feed flow rate fibre on fractionation by fibre coarseness
- Figure 3.5a Effect of cone rotational speed on fibre fractionation by fibre length
- Figure 3.5b Effect of cone rotational speed on fibre fractionation by fibre coarseness
- Figure 3.6a Effect of cone surface roughness on fibre fractionation by fibre length
- Figure 3.6b Effect of cone surface roughness on fibre fractionation by fibre coarseness
- Figure 4.1 Fibres in water layer of froth
- Figure 4.2 Continuous flotation cell (CFC) experimental set-up
- Figure 4.3a Effect of feed consistency on fibre fractionation by fibre length
- Figure 4.3b Effect of feed consistency on fibre fractionation by fibre coarseness

Figure 4.4a	Effect of feed flow rate on fibre fractionation by fibre length
Figure 4.4b	Effect of feed flow rate on fibre fractionation by fibre coarseness
Figure 4.5a	Effect of air flow rate on fibre fractionation by fibre length
Figure 4.5b	Effect of air flow rate on fibre fractionation by fibre coarseness
Figure 4.6a	Effect of surfactant concentration on fibre fractionation by fibre length
Figure 4.6b	Effect of surfactant concentration on fibre fractionation by fibre coarseness
Figure 4.7a	Effect of impeller speed on fibre fractionation by fibre length
Figure 4.7b	Effect of impeller speed on fibre fractionation by fibre coarseness
Figure 5.1	Air sparged hydrocyclone
Figure 5.2	Air sparged hydrocyclone (ASH) experimental set-up
Figure 5.3a	Effect of feed consistency on fibre fractionation by fibre length
Figure 5.3b	Effect of feed consistency on fibre fractionation by fibre coarseness
Figure 5.4a	Effect of feed flow rate on fibre fractionation by fibre length
Figure 5.4b	Effect of feed flow rate on fibre fractionation by fibre coarseness
Figure 5.5a	Effect of split ratio (overflow/feed) on fibre fractionation by fibre length
Figure 5.5b	Effect of split ratio (overflow/feed) on fibre fractionation by fibre coarseness
Figure 5.6a	Effect of air flow rate on fibre fractionation by fibre length
Figure 5.6b	Effect of air flow rate on fibre fractionation by fibre coarseness
Figure 6.1a	Fractionation by fibre length at feed consistency of 0.15 wt% starting with the shortest fraction
Figure 6.1b	Fractionation by fibre coarseness at feed consistency of 0.15 wt% starting with the lowest coarseness fraction
Figure 6.1c	Fractionation by fibre length at feed consistency of 0.15 wt% starting with the longest fraction

- Figure 6.1d Fractionation by fibre coarseness at feed consistency of 0.15 wt% starting with the highest coarseness fraction
- Figure 6.2a Fractionation by fibre length at feed consistency of 0.45 wt% starting with the shortest fraction
- Figure 6.2b Fractionation by fibre coarseness at feed consistency of 0.45 wt% starting with the lowest coarseness fraction
- Figure 6.2c Fractionation by fibre length at feed consistency of 0.45 wt% starting with the longest fraction
- Figure 6.2d Fractionation by fibre coarseness at feed consistency of 0.45 wt% starting with the highest coarseness fraction
- Figure 6.3 The variation of fibre coarseness versus fibre length

Photographs

- Photograph 3.1 Transition arc boundary on the cone surface
- Photograph 3.2 Direct drop formation on the cone surface
- Photograph 3.3 Ligament formation on the cone surface
- Photograph 3.4 Film/ligament formation on the cone surface

Tables

- Table 1.1 Properties of North American pulpwoods (smook 1992)
- Table 3.1 Design details and parameters studied for RCF

CHAPTER 1

INTRODUCTION

1.1 FIBRE FRACTIONATION

1.1.1 Characteristics of pulp fibres

At present, wood provides about 93% of the world's virgin fibre requirement, while non-wood fibre sources, such as bagasse, cereal straws and bamboo, provide the remainder. In North America, modern pulp and paper mills utilize wood as the raw material for pulping and papermaking processes. The characteristics of various wood pulp fibres, such as fibre length, diameter, aspect ratio, wall thickness and coarseness, which is defined as the mass of fibre wall material per 100 meters of fibre length, are dependent not only on the wood raw

material and pulping process employed, but also on subsequent purification, processing and conditioning treatments.

The two different types of wood, namely softwood and hardwood used by pulp manufacturers, have different fibre length and fibre coarseness. In general, softwood fibres are two or three times longer and coarser compared to hardwood fibres (Table 1.1). Softwoods make up 35% of trees worldwide. Hardwoods make up the remaining of 65%. Due to the long fibers in softwood, it is utilized more often than hardwood in papermaking process especially when strength is required.

Table 1.1 Properties of North American pulpwoods (Smook 1992)

Species		Fiber Length (mm)	Fibre Coarseness (mg/100m)
Hardwood	Birch	1.8	5-8
	Red Gum	1.7	8-10
Softwood	Black Spruce	3.5	14-19
	Red Cedar	3.5	15-17
	Douglas-Fir	3.9	25-32
	Southern Pine	4.6	20-30
	Redwood	6.1	25-35

Pulping refers to any process by which wood (or other fibrous raw material) is reduced to a fibrous mass. The pulping process can be accomplished by mechanical, thermal and chemical processes. In a mechanical pulping process, the pulp is produced by first cutting the wood into small, uniform-size chips, and then the chips are defibrillated by stone grinding (SGW) or using a refiner. Refiner Mechanical Pulp (RMP) typically retains more long fibres than stone groundwood pulp and yields stronger paper. Most new installations now employ

thermal presoftening of the chips to modify both the energy requirement and the resultant fibre properties. When the chips are given a pressurized steam pretreatment, the resultant product, called Thermomechanical Pulp (TMP), is significantly stronger than RMP and contains very little screen reject material (Cooper, 1987). In a chemical pulping process, the wood chips are cooked with appropriate chemicals in an aqueous solution at elevated temperatures and pressures. The chemical treatment helps in removing almost all lignin, resulting in a very low yield of 40 to 50% of the original wood mass. However, the fibres produced are longer and more flexible compared to the mechanical pulping process.

Mechanical pulping processes have the advantage of converting up to 95% of the dry weight of the wood into pulp. However, the pulp produced by a mechanical pulping process also contains shives, fibre fragments and fines etc., which increase the difficulty of characterizing the pulp. Klemm (1955) made a systematic attempt to characterize ground-wood mechanical pulps by measuring the freeness, which is a measurement of pulp drainage, and the amount of fines present in the pulp. Klemm (1955) also described a direct method for pulp characterization that involved the passage of a pulp sample through a fibre fractionating screen.

Forgacs (1963) reviewed the literature on pulp characterization and concluded that the fibre length, fibre-specific surface and some fibre shape factor are important properties controlling the finished product properties. The studies by Clark (1942) indicated that for constant fibre coarseness, the tensile strength (the force required to break a narrow strip of paper) of a sheet made from relatively unbeaten pulp (other factors being the same) varies as $L^{1/2}$, the burst (determined by clamping a paper sample over a rubber diaphragm through which pressure is applied at a gradually increasing rate, and noting the pressure at rupture) varies as L , the fold (measured by the number of folds sustained before

rupture occurs) varies as L^5 , and tear (determined by using a falling pendulum to continue a tear in the paper sample when the force is applied perpendicular to the plane of the sheet) as $L^{3/2}$, where L represents fibre length.

Smook (1992) reported that the properties of paper are dependent on some important fibre structural characteristics such as fibre length, cell wall thickness and fibre coarseness. A minimum fibre length is required for interfibre bonding. In general, fibres with relatively thin cell walls collapse readily into ribbons during sheet formation while fibres with thicker cell walls resist collapse and do not contribute to interfibre bonding to the same extent. Fibre coarseness can provide a more specific indication of a fibre's behavior. Coarser fibers tend to produce an open, absorbent, bulky sheet with low burst/tensile strength and high tear resistance (Seth, 1990).

1.1.2 Fractionation of wood pulp fibres

As fibre characteristics have major impact on the properties of the finished paper products, it is beneficial to be able to control the fibre length or coarseness of the wood pulp used in papermaking process. The pulp properties may be tailored towards its end use by performing fractionation and then blending appropriate amounts of fractions with different fibre lengths (Moller, 1979). Fibre fractionation has become increasingly important as industry optimizes the papermaking process in response to improved product quality, raw material shortage, increased recycling and environmental protection demands.

Moller et al. (1979), Behera (1981) and Bliss (1983, 1984, 1987) summarized the reasons and some general applications for fibre fractionation. Fibre fractionation optimizes the usage of fibre resources by separating them into

different fractions to suit different requirements for the final products, suit different paper machine characteristics, suit different beating conditions and recover valuable fibres from waste.

Rewatkar and Masliyah (1996) reviewed wood pulp fractionation and listed a number of possible fractionation devices, including screens, hydrocyclones, plate atomizing wheel, liquid column flow, spouted bed and Jacquelin apparatus. More recently, some new fibre fractionators were investigated: flotation cells (Eckert, 1997), rotating cone fractionator (Rewatkar, 1997) and vertical settler (Chen, 2000). Pressure screens are used in the majority of pulp industries, fractionating fibres mainly according to fibre length. Hydrocyclones primarily separate fibres on the basis of fibre specific surface area. A plate atomizing wheel can be used to fractionate high consistency (6 wt%) pulp according to fibre specific surface area. All other fractionators can be used to separate fibres on the basis of fibre length.

Previous studies were concerned with fibre fractionation of wood pulps on the basis of fibre length or fibre specific surface area. Recently, it is desired to fractionate fibres from a pulp according to fibre coarseness. In the present study, three fractionators, rotating cone, continuous flotation cell, and air sparged hydrocyclone were used to fractionate 100% softwood TMP on the basis of both fibre length and fibre coarseness.

1.2 OBJECTIVES OF PRESENT STUDY

The primary objective of this study is to determine whether softwood TMP can be fractionated on the basis of fibre length and fibre coarseness using a rotating cone fractionator, a continuous flotation cell and an air sparged

hydrocyclone. In the present study, both fibre length and fibre coarseness were used as the indicators of the fractionation performance. Optimizations of operational parameters for all three selected fractionators were investigated.

The second objective of this study is to compare the fractionation performance of the selected fractionators (rotating cone, continuous flotation cell and air sparged hydrocyclone). Fibre classification of feed softwood TMP using Bauer McNett, a lab instrument for fibre length distribution test, was adopted as the ideal fractionation process.

CHAPTER 2

MEASUREMENTS

2.1 FIBRE LENGTH MEASUREMENT

Fibre length is the arc length of the fibre from one end to the other. Microscopic examination and screen classification are two traditional methods used to measure fibre length and length distribution. In the microscopic examination method, the magnified image of a known mass of fibres is projected onto a calibrated grid pattern. The lengths of all the fibres are measured to obtain a length distribution and an average fibre length. In the screening method, a fibre suspension in water is passed through a series of screens having different size openings, and the fraction remaining on each screen is subsequently dried and weighted. The required screen sizes depend upon the probable fibre length

distribution. A lab screening device, the Bauer MacNett classifier uses fibre screens (14, 28, 48, 100 and 200 mesh) to classify a pulp sample. Based on this fibre classifier, fibres are classified into four categories: long fibres (14 mesh), intermediate fibres (28, 48 mesh), short fibres (100, 200 mesh) and fines (fibres passing through 200 mesh screen). This method gives the mass weighted average length of the pulp sample.

These methods are now being displaced by modern optical counting devices such as Kajaani Analyzer. Bichard and Scudamore (1988) carried out a comparative study on the performance of the Kajaani FS-100 and FS-200 fibre analyzers. It was found that the FS-200 model was more sensitive to the length of fibres and had the ability to detect fines in a pulp sample. More recently, a Fibre Quality Analyzer manufactured by OPTEST Equipment (Canada) is capable of measuring fibre length, fibre coarseness and degree of curliness of a fibre. The FQA incorporates a novel flow cell, which uses hydrodynamic focusing to orient curled fibres so that they can be precisely measured in the imaging region.

In this study, an FQA was used to measure average fibre length of feed and fractions. The FQA calculates average fibre length in three different ways: arithmetic mean length, length weighted mean length and weight weighted mean length.

Arithmetic mean length (A_L) is the average contour length of all detected fibres in a given sample. The presence of fines will significantly affect this value.

$$A_L = \frac{\sum n_i L_i}{\sum n_i} \quad (i = 1, 2, \dots, n) \quad (2.1)$$

where n is fibre count and L is the contour length of a fibre.

Length weighted mean length (L_L) is most often used to compare differences between samples. Fines do not have a significant effect on this value. L_{LW} is calculated as the following equation (2.2):

$$L_L = \frac{\sum n_i L_i^2}{\sum n_i L_i} \quad (i = 1, 2, \dots, n) \quad (2.2)$$

Weight weighted mean length (L_W) is defined in equation (2.3). Longer fibres have a significant impact on this value.

$$L_W = \frac{\sum n_i L_i^3}{\sum n_i L_i^2} \quad (i = 1, 2, \dots, n) \quad (2.3)$$

In this study, the length weighted mean length was used to represent the mean lengths of the samples, since fines do not have a significant effect on this value.

2.2 FIBRE COARSENESS MEASUREMENT

2.2.1 INTRODUCTION

Fibre coarseness is the mass of fibres per unit of fibre length. The following equation was used to calculate fibre coarseness:

$$C = \frac{m}{\sum n_i L_i} \times 10^5 \quad (2.4)$$

where C is average fibre coarseness, m is the mass (oven dry) of fibres supplied to the FQA, n is the fibre count and L is the contour length of a fibre.

Previous studies showed that the presence of debris, fibre fragment, ray cell and fines in a pulp sample could interfere with the coarseness measurement. Seth and Chan (1996) studied the fibre coarseness measurement of a chemical pulp using optical fibre length analyzers (Kajaani FS-100 and FS-200). They recommended removing fines using a screen (150 mesh) before the coarseness measurement. Karnis (1994) suggested that it is more meaningful to measure and compare the coarseness of various Bauer McNett fractions than those of the whole pulp. In the present study, Fibre Quality Analyzer (FQA) was used to measure the fibre coarseness of the samples (softwood TMP). The samples were washed using screens (48 and 200 mesh) to remove fines and therefore to minimize some measurement errors.

2.2.2 Sample preparation

As shown in Figure (2.1), a two-stage washing process, which is composed of 48 and 200 mesh screens, was specially designed for fibre coarseness measurement in this study. This set-up can retain most long fibres in the 48 mesh screen and therefore prevent long fibres being accidentally removed. Also, the fines removing process in the 200 mesh screen was sped up significantly.

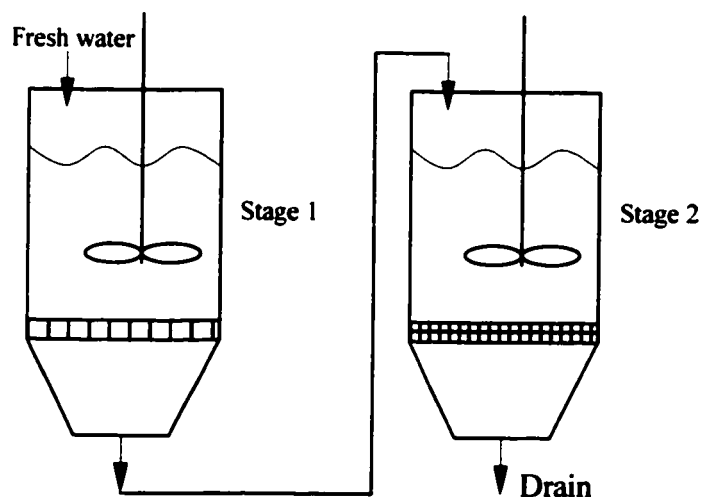


Figure 2.1 Two-stage washing process

In order to determine the sensitivity of fibre coarseness measurements to the percentage of fines, a set of washing tests were carried out to remove fines from the softwood TMP samples. It was found that fibre coarseness decreased significantly during the first two minutes of washing and then reached a stable value. This result indicated that 3 ~ 4 minutes is the suitable washing time interval for softwood TMP samples before coarseness measurement (Figure 2.2).

After being washed, fibres in both 48 and 200 mesh screens were collected and blended together. The washed sample was diluted with water (1L) and kept well mixed. About 500ml pulp slurry was collected for the measurements of fibre length and coarseness using the FQA. The remaining pulp slurry was weighted for consistency measurement, which will be discussed in the following section.

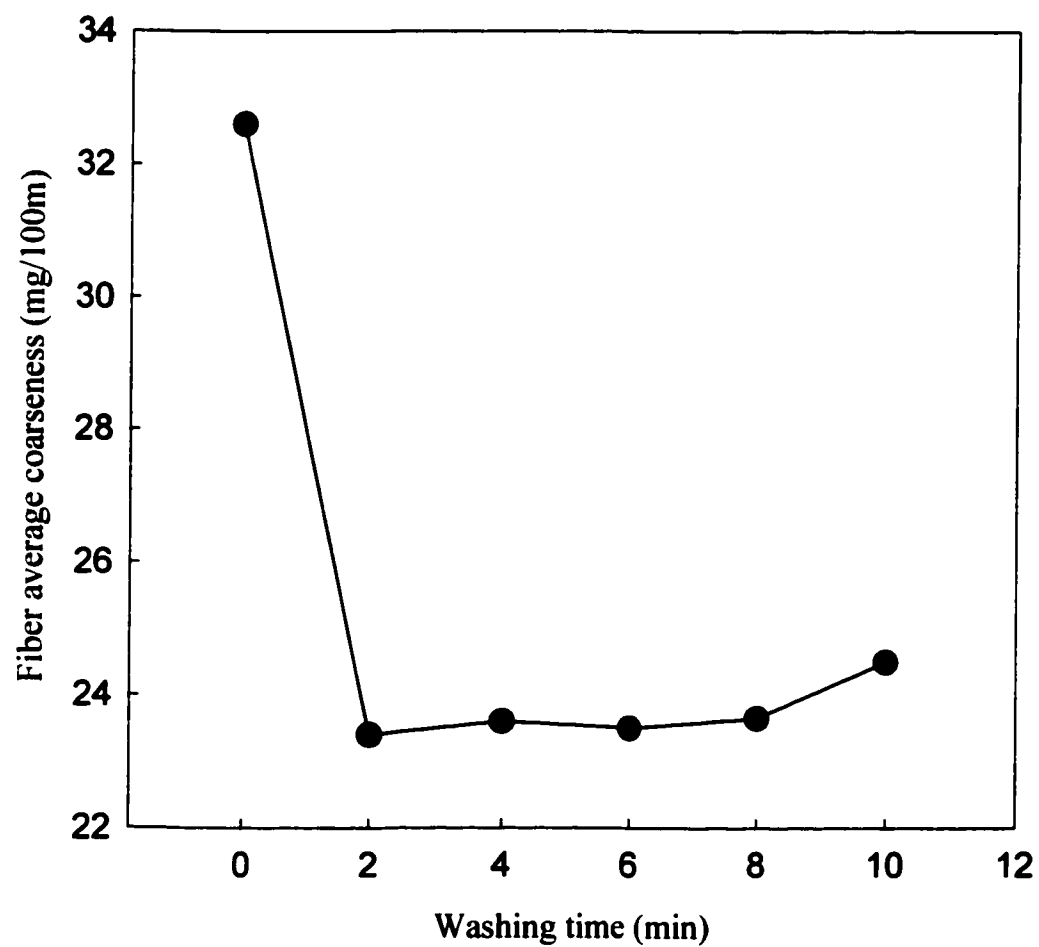


Figure 2.2 Variation of fibre coarseness at different washing time intervals

2.2.3 Measurement in Fibre Quality Analyzer (FQA)

A representative fibre suspension weighing approximately 500g was taken to FQA for coarseness measurement from the diluted sample, which had been washed in the sample preparation stage. Once the fibre mass is entered, the FQA goes through 4 cycles of drawing out fibres from the beaker and diluting the remaining contents. The auto dilution will ensure that only a negligible amount of fibres is left in the beaker at the end of the test. FQA reports coarseness by calculation using Equation (2.4). A fibre frequency of 5 ~ 20 favors the measurement of fibre length and coarseness in FQA.

2.3 CONSISTENCY MEASUREMENT

Pulp consistency is defined as the weight in grams of oven-dry fibre in 100 grams of pulp-water mixture and is expressed in a percentage. In the present study, TAPPI standard T 240 was adopted to measure pulp consistencies of samples. The procedure is as follows:

1. Use a sampling cup to withdraw about 100ml of pulp;
2. Deposit the entire contents in the tared beaker and determine the net weight of the specimen;
3. Place a previously dried, tared filter paper in the Buchner funnel, moisten with water, then apply suction to the flask and filter the specimen from step 2;
4. Remove the resulting fibre pad and filter paper and heat in an oven at a temperature of 103°C;

5. Make successive readings until a constant weight is obtained. Record the weight to the nearest 0.01g.
6. The percentage consistency is then:

$$c = \frac{w - f}{g} \times 100 \quad (2.5)$$

where w is the weight of the moisture-free pad and filter paper, f is the weight of the moisture-free filter paper, and g is the net weight of the original fibre slurry specimen in the beaker.

2.4 CUMULATIVE FIBRE LENGTH AND COARSENESS

For a given fractionation system, samples were collected from both feed and fraction streams during a test. The samples were washed using 48 and 200 mesh screens and then measured for fibre weight, fibre length and fibre coarseness. Figure (2.3) is a schematic diagram of a typical fibre fractionation process, where m represents fibre mass (oven dry), L_L denotes length weighted mean length, and C stands for fibre coarseness.

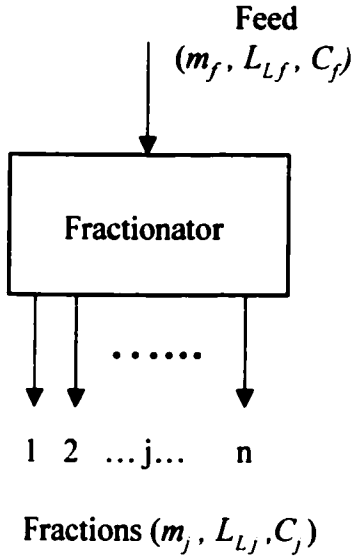


Figure 2.3 Fibre fractionation system

In this study, length weighted fibre length and fibre coarseness defined in Equations (2.2) and (2.4), are the primary fibre properties of the feed and fractions. Cumulative fibre length and fibre coarseness are used to compare the fibre fractionation performance under different experimental conditions. In order to calculate the cumulative fibre length and the cumulative fibre coarseness, two equations were derived in this study.

From Equations (2.2) and (2.4), the length weighted fibre length and the fibre mass of a fraction can be written as the follows:

$$L_{l, fraction-j} = \frac{(\sum n_i L_i^2)_{fraction-j}}{(\sum n_i L_i)_{fraction-j}} \quad (2.6)$$

$$m_{fraction-j} = (\sum n_i L_i)_{fraction-j} \cdot C_{fraction-j} \quad (2.7)$$

where *fraction-j* was the fractions defined by the Fibre Quality Analyzer (FQA).

Equations (2.6) and (2.7) can be rearranged as the follows:

$$(\sum n_i L_i^2)_{fraction-j} = L_{L, fraction-j} \cdot (\sum n_i L_i)_{fraction-j} \quad (2.8)$$

$$(\sum n_i L_i)_{fraction-j} = \frac{m_{fraction-j}}{C_{fraction-j}} \quad (2.9)$$

Combine (2.8) and (2.9), the unknown term $(\sum n_i L_i^2)_{fraction-j}$ is given by the following equation:

$$(\sum n_i L_i^2)_{fraction-j} = L_{L, fraction-j} \cdot \frac{m_{fraction-j}}{C_{fraction-j}} \quad (2.10)$$

Based on definition, the cumulative length weighted fibre length and the cumulative fibre coarseness of fractions can be calculated as the follows:

$$L_{L, Cum.} = \frac{(\sum n_i L_i^2)_{fraction-1} + (\sum n_i L_i^2)_{fraction-2} + \dots + (\sum n_i L_i^2)_{fraction-n}}{(\sum n_i L_i)_{fraction-1} + (\sum n_i L_i)_{fraction-2} + \dots + (\sum n_i L_i)_{fraction-n}} \quad (2.11)$$

$$C_{Cum.} = \frac{m_{fraction-1} + m_{fraction-2} + \dots + m_{fraction-n}}{(\sum n_i L_i)_{fraction-1} + (\sum n_i L_i)_{fraction-2} + \dots + (\sum n_i L_i)_{fraction-n}} \quad (2.12)$$

Equations (2.11) and (2.12) cannot be used directly to calculate the cumulative length weighted fibre length and cumulative fibre coarseness of

fractions due to some unknown terms. However, the following equations can be derived by combining Equations (2.9), (2.10).

$$L_{L,Cum.} = \frac{L_{L,fraction-1} \cdot \frac{m_{fraction-1}}{C_{fraction-1}} + L_{L,fraction-2} \cdot \frac{m_{fraction-2}}{C_{fraction-2}} + \dots + L_{L,fraction-n} \cdot \frac{m_{fraction-n}}{C_{fraction-n}}}{\frac{m_{fraction-1}}{C_{fraction-1}} + \frac{m_{fraction-2}}{C_{fraction-2}} + \dots + \frac{m_{fraction-n}}{C_{fraction-n}}} \quad (2.13)$$

$$C_{Cum.} = \frac{m_{fraction-1} + m_{fraction-2} + \dots + m_{fraction-n}}{\frac{m_{fraction-1}}{C_{fraction-1}} + \frac{m_{fraction-2}}{C_{fraction-2}} + \dots + \frac{m_{fraction-n}}{C_{fraction-n}}} \quad (2.14)$$

Equations (2.13) and (2.14) can be further written as follows:

$$L_{L,Cum.} = \frac{\sum \frac{L_{L,fraction-j} \cdot m_{fraction-j}}{C_{fraction-j}}}{\sum \frac{m_{fraction-j}}{C_{fraction-j}}} \quad (2.15)$$

$$C_{Cum.} = \frac{\sum m_{fraction-j}}{\sum \frac{m_{fraction-j}}{C_{fraction-j}}} \quad (2.16)$$

Equations (2.15) and (2.16) can be used to calculate the cumulative length weighted fibre length of fraction mixtures that exhibit a wide range of fibre length and fibre coarseness distribution. Equations (2.15) and (2.16) will be used to compare the fibre length and fibre coarseness of the feed sample with the 100% cumulative fibre length and coarseness of fractions at the following chapters.

CHAPTER 3

ROTATING CONE FRACTIONATOR

3.1 INTRODUCTION

The atomization by a rotating disk is widely used for spray drying and a promotor of chemical reaction or absorption between a gas and a liquid. Moller et al. (1979) developed the technique of a plate-atomizing wheel, which was found successful for fibre fractionation at feed consistency as high as 6 wt%. As shown in Figure 3.1, the equipment consisted of an atomizing disk and collection chambers. A saucer type plate was used for atomizing pulp slurry in a similar way as that of a spray dryer. Fractionation is realized by collection of various axial zones of the circular particle cloud near the disk periphery. For the processing of sediment pulps containing 3 wt% solids, generally it was found that (i) fine cellulose and clay particles were concentrated near the top of the cloud, (ii) good

pulp fibre was concentrated near the middle and upper middle of the cloud, and (iii) sand grains, nonfibrous wood particles, and bark particles were concentrated near the bottom of the cloud. Without exception, the smaller and less dense particles were concentrated near the top of the cloud.

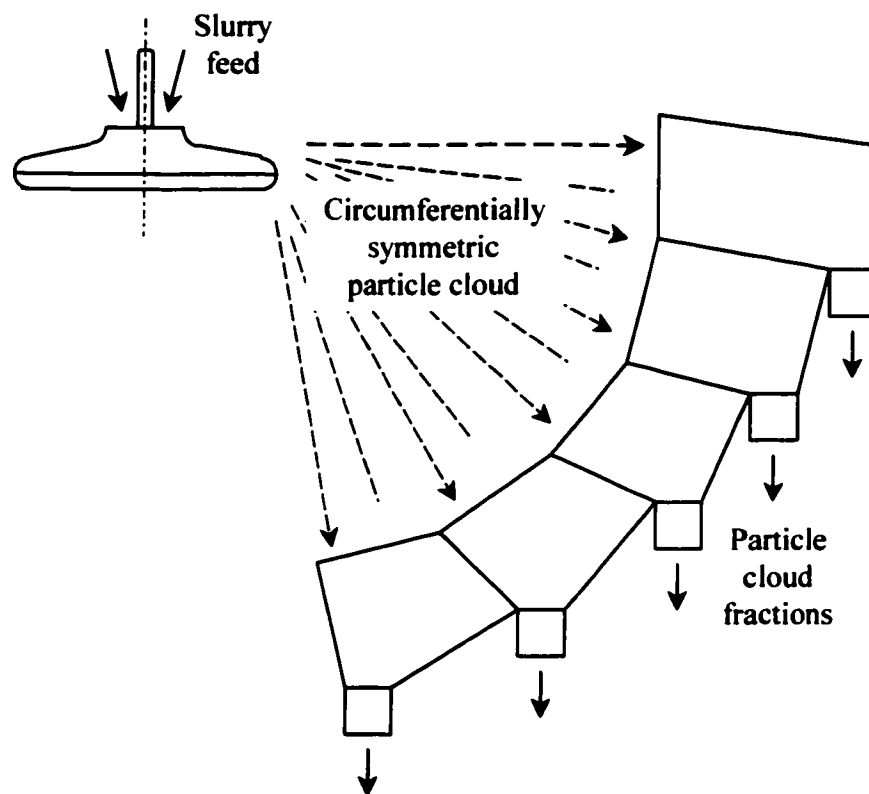


Figure 3.1 Axial zone collection of particle cloud near a rotating vaneless disk (Oroskar and Crosby, 1986)

Oroskar and Crosby (1986) studied various design and operating parameters for fibre fractionation using an atomizing disk. They found that the fibres were separated at the disk edge primarily by fibre diameter. The success of this classification scheme for pulp fibres was attributed to the extremely intense shear that exists within the liquid film passing over the disk surface and to the centrifugal force acting normal to the film near the edge of the disk.

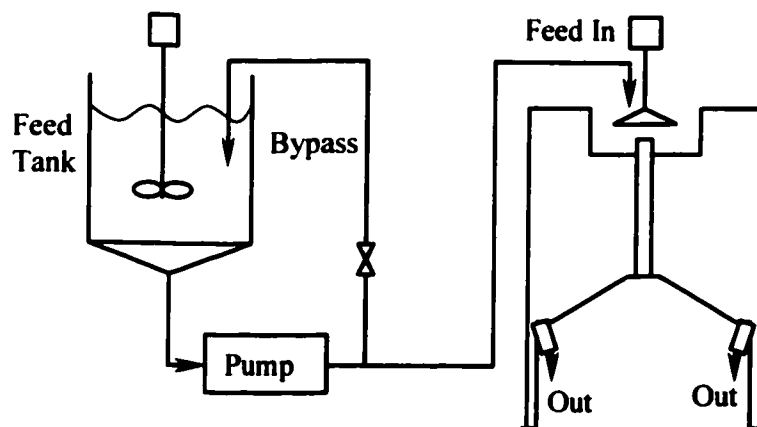
The need of a large diameter disk and high rotational speeds would limit the commercial use of the plate-atomizing disk. Rewatkar and Masliyah (1997) designed the rotating cone fractionator (RCF) based on similar principles as that of the plate-atomizing disk. The unique feature of the rotating cone fractionator is that it can carry out fibre fractionation at low rotational speeds. The cone surface is constructed from a sieve mesh, thereby introducing a rough surface. The feed pipe is located at an off-centre position to the axis of rotation. The fractions are collected at different angular locations (Figure 3.2).

Rewatkar (1997) studied a rotating cone fractionator for fibre fractionation of mechanical pulp fibres, and found that the rotating cone fractionator separate fibres on the basis of fibre length. Chen (1998) found that the rotating cone fractionator could be used to fractionate nylon fibres according to fibre length. They also found that fractionation performance varied with the atomization mode on the cone surface and that ligament formation showed excellent fibre fractionation.

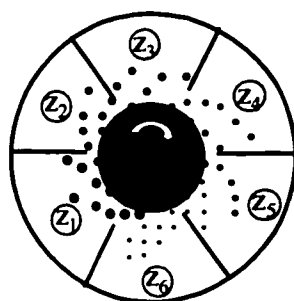
The objective of the present study is to determine whether softwood TMP fibres could be fractionated using a rotating cone fractionator on the basis of fibre length and fibre coarseness. Optimization of operating parameters was also investigated.

3.2 EXPERIMENTAL SET-UP

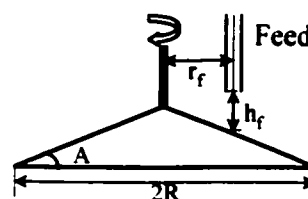
Figure (3.2 A) shows a schematic diagram of the RCF experimental set-up used in this study. The feed fibre suspension (softwood TMP) was prepared in the feed tank and was kept in a well-mixed condition with the help of a stirrer. During the test, the fibre suspension was pumped at a constant feed flow rate using a peristaltic pump that was calibrated. The feed flow rate and cone rotational speed were controlled using variable speed drives on the feed pump and the rotating cone. For all tests, the feed delivery point was off-centre. The feed fibre suspension flowed over the conical surface. At the rim of the cone it was dispersed into the air. The dispersed spray was collected by a specially designed circumferential assembly as shown in Figure (3.2 B). The circumferential collection assembly consisted of six equally divided compartments built within a cylindrical vessel. The bottom of the cylindrical vessel was made up of an inverted cone for easy removal of the fibre suspension. Each compartment was provided with its own outlet at the bottom of the vessel. Collection zone numbers were assigned according to the transition boundary of suspension film appearing on the conical surface. All the experiments were carried out by adjusting the collection assembly in such a way that the dispersed spray originating from the transition boundary at the rim of the cone was captured by the first collection zone. The subsequent zone numbers were assigned based on their angular location compared with that of the first collection zone. Figure (3.2 C) and table 3.1 show the cone design details and the experimental conditions of the rotating cone fractionator used in this study. Photograph 3.1 shows the transition boundary on the cone surface.



(A) Experimental Set-up

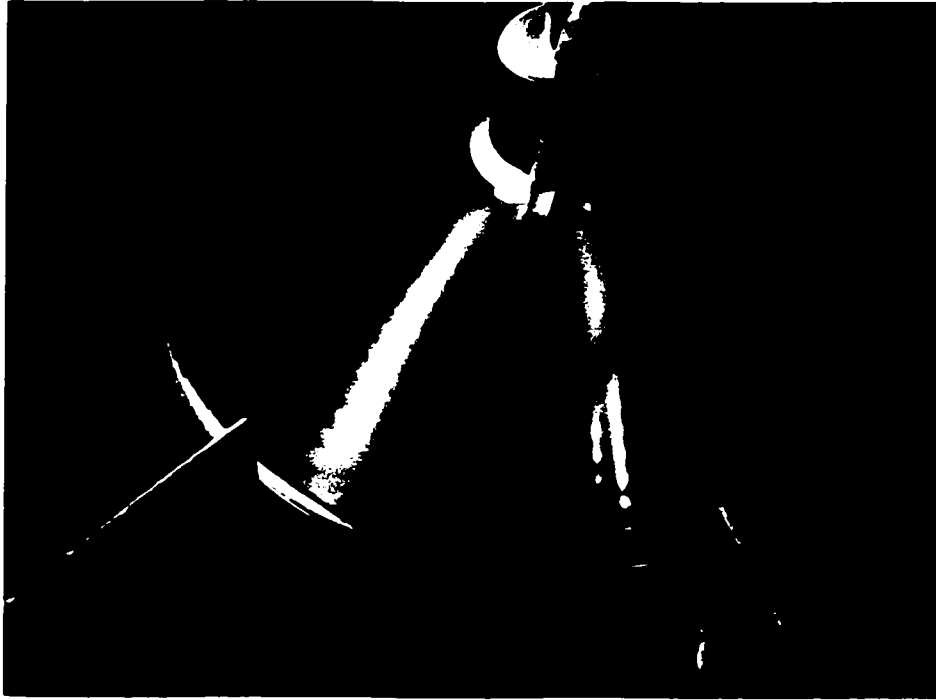


(B) Top View of RCF



(C) Rotating Cone Detail

Figure 3.2 Rotating cone fractionator (RCF)



Photograph 3.1 **Transition arc boundary on the cone surface**

Table 3.1 Design details and parameters studied for RCF

	Range of value studied	
Operating parameters	Feed consistency (%)	0.15 – 0.95
	Feed flow rate (L/min)	1.2 – 3.6
	Cone rotational speed (rpm)	200 – 600
	Cone surface roughness (mesh)	Smooth, 20 mesh
Cone design details	Cone angle (A)	30°
	Cone radius (R, mm)	90
	Distributor location	$r_f = 10$ mm
	(r_f, h_f mm)	$h_f = 15$ mm

For each test, feed and six fraction samples were collected and measured for fibre mass and consistency. All samples were then washed using the 2-stage washing process to remove fines. After measuring the consistency, the washed samples were taken to the Fibre Quality Analyzer to determine fibre length and fibre coarseness.

3.3 RESULTS AND DISCUSSION

In the following sections, the effects of feed consistency, feed flow rate, cone rotational speed, and cone surface roughness on fractionation performance will be discussed in some detail.

3.3.1 Effect of feed consistency

In the present study, tests on the effect of feed consistency were carried out using a 30° 20-mesh cone with a 90mm radius. The feed consistency was varied from 0.15 wt% to 0.95 wt%. The feed flow rate was 2.4 L/min. The cone rotational speed was 450 rpm. In order to compare the fractionation performance under different operating conditions, the cumulative fibre length and the cumulative fibre coarseness calculated from Equations (2.15) and (2.16) were plotted against cumulative amount of fibre collected for each run. Variations of the cumulative average fibre length with cumulative percentage feed are shown in Figure 3.3a, in which all curves start with the fraction having the shortest fibre length. As shown in Figure 3.3b, variations of the cumulative average fibre coarseness with cumulative percentage feed are plotted in the similar way as that in Figure 3.3a. The values of the 100% cumulative fibre length and fibre coarseness should approach the value of the feed sample. The accuracy of fibre

length and coarseness measurements would then manifest themselves in these plots. The lowest curve represents the best fractionation performance, since any point on this curve represents a fraction mixture either having the shortest fibre length (or lowest fibre coarseness) as compared to the feed mixture.

It can be observed that within the range of the feed consistency investigated, a lower feed consistency favors fibre fractionation and the best fractionation performance occurs at feed consistency of 0.15 wt%.

The effect of feed consistency on fractionation performance may be explained by relating the consistency of the feed pulp to the crowding factor as defined by Kerekes and Schell (1992). The crowding factor can be considered a measure of the intimacy of fibre-to-fibre contact. Kerekes and Schell gave the following approximate equation for crowding factor, N :

$$N \approx 5cL^2 / C \quad (3.1)$$

where c is the pulp consistency, L is the length of the fibres in meter, and C is the fibre coarseness in kg/m. Kerekes and Schell characterized the fibre contact regimes as follows: (i) $N < 1$, the suspension is considered dilute, with little chance of fibre contact, (ii) $1 < N < 60$, the suspension is referred to as semiconcentrated, with forced collisions between fibres, (iii) $N > 60$, the suspension is concentrated and had continuous fibre contact. The crowding factors were 28, 75, and 178 for the feed consistencies of 0.15 wt%, 0.40 wt%, and 0.95 wt%, respectively. The lowest feed consistency (0.15 wt%) was in the considered semiconcentrated regime. The higher feed consistencies (0.40 wt% and 0.95 wt%) were in the concentrated regime and had continuous fibre contact between fibres. Therefore, a better fractionation performance would be expected in the lowest feed consistency.

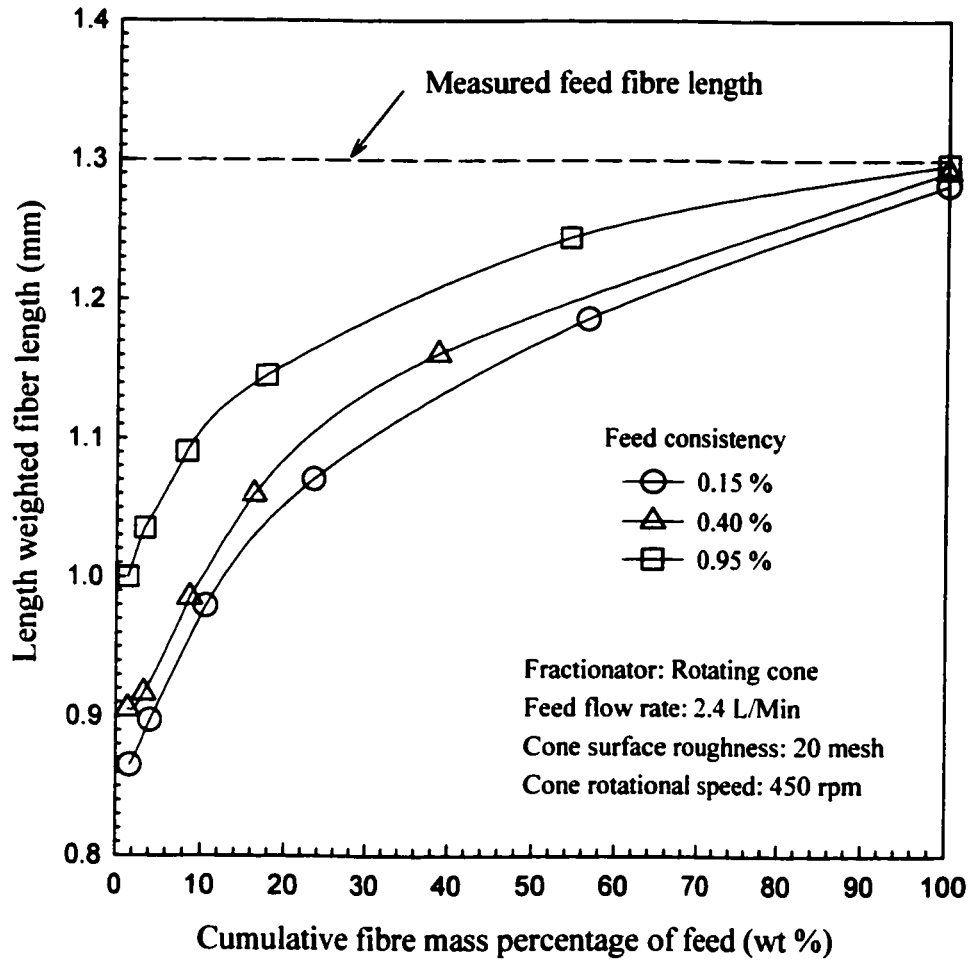


Figure 3.3a Effect of feed consistency on fibre fractionation by fibre length

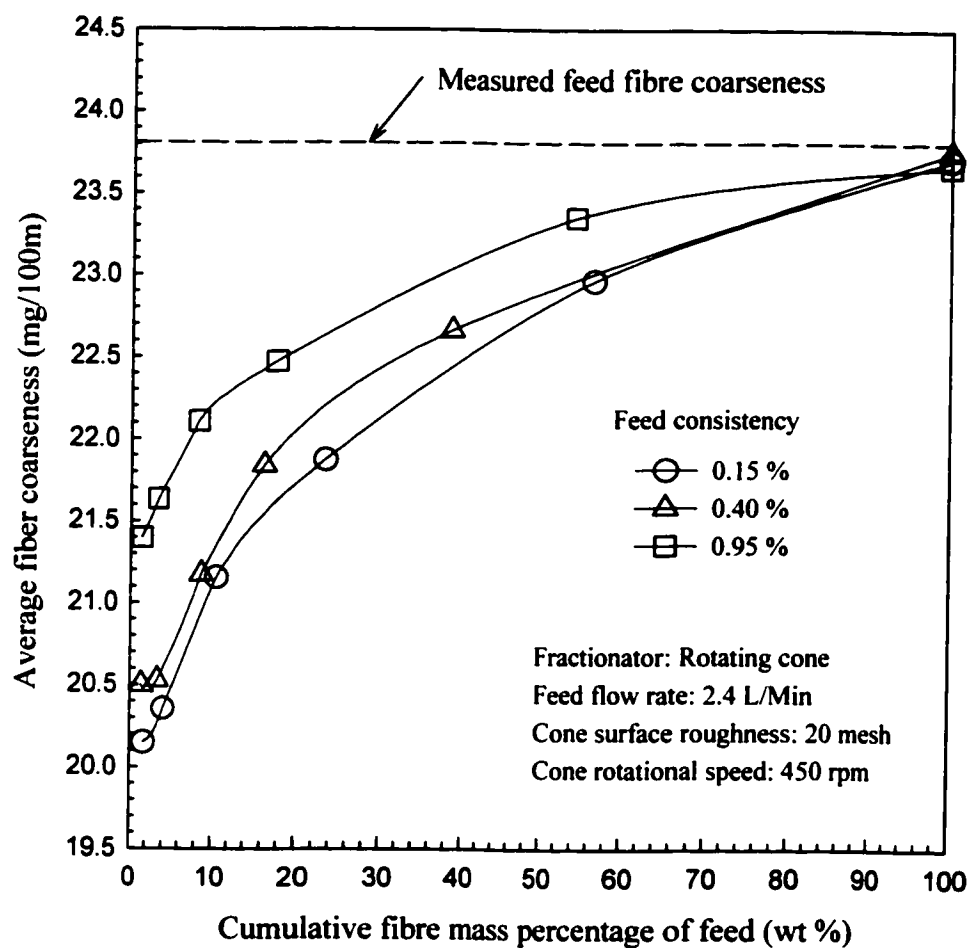


Figure 3.3b Effect of feed consistency on fibre fractionation by fibre coarseness

3.3.2 Effect of feed flow rate

The effect of feed flow rate was studied using a 20-mesh cone. The feed flow rate was varied from 1.2 to 3.6 L/min. The feed consistency was 0.15 wt%. The cone rotational speed was 450 rpm. Variations of the cumulative average fibre length with cumulative percentage feed are shown in Figure 3.4a. Variations of the cumulative average fibre coarseness with cumulative percentage feed are shown in Figure 3.4b. It can be observed that within the range of the feed flow rate studied, the fractionation performance improves with an increase in feed flow rate from 1.2 to 2.4 L/min. However, with a further increase in feed flow rate to 3.6 L/min, the fractionation performance deteriorates. This suggests that an optimal feed flow rate exists while other operating parameters are fixed.

The results confirmed the conclusion of previous studies (Rewatkar, 1997). At a constant cone rotational speed, three different atomization modes could be observed with an increase in feed flow rate: direct drop formation, ligament formation and film/ligament formation. The ligament formation, which occurred at feed flow rate of 2.4 L/min, showed the best fractionation performance. Photograph 3.2 - 3.4 showed the different atomization modes at different feed flow rates.

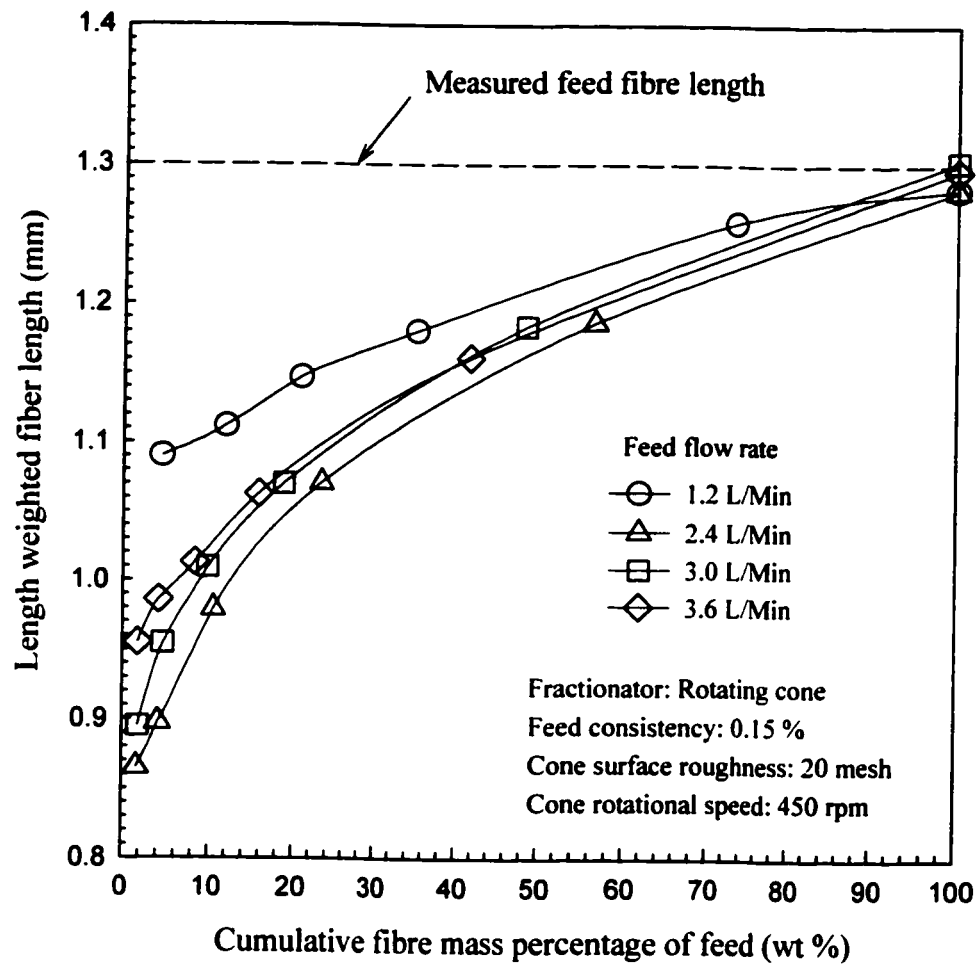


Figure 3.4a Effect of feed flow rate on fibre fractionation by fibre length

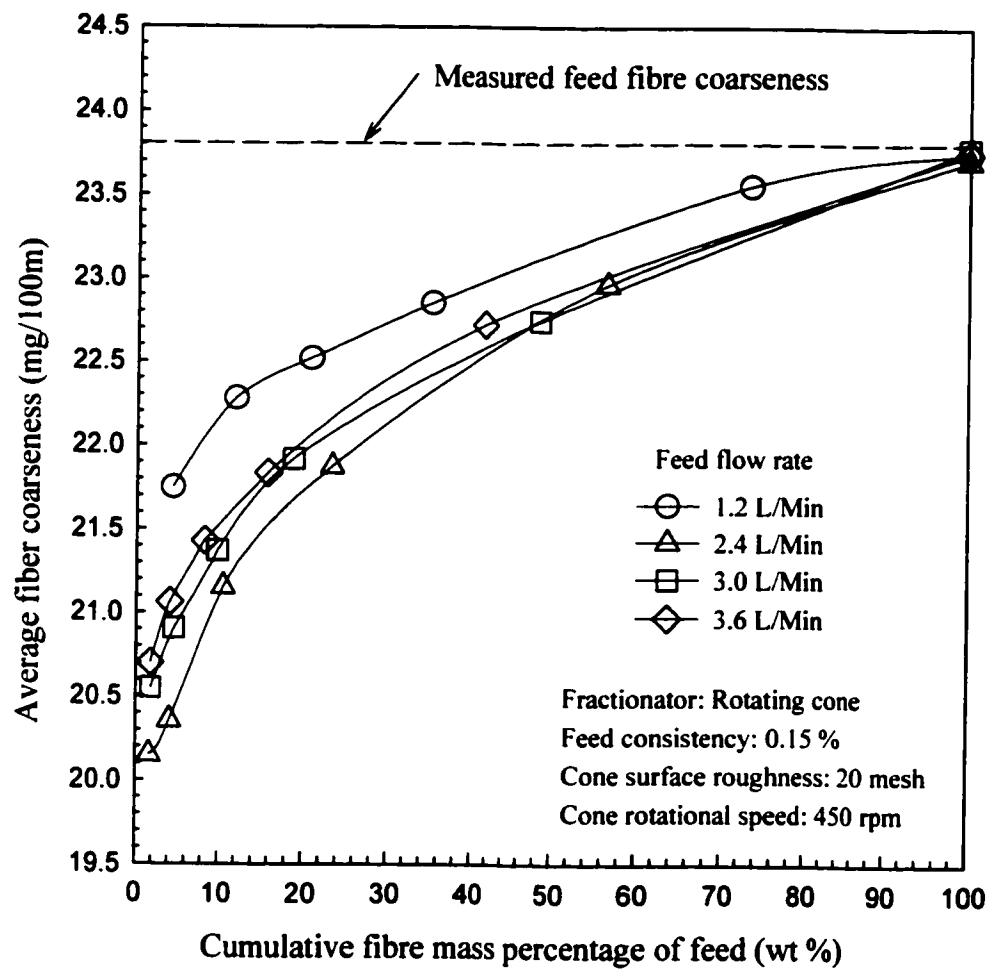
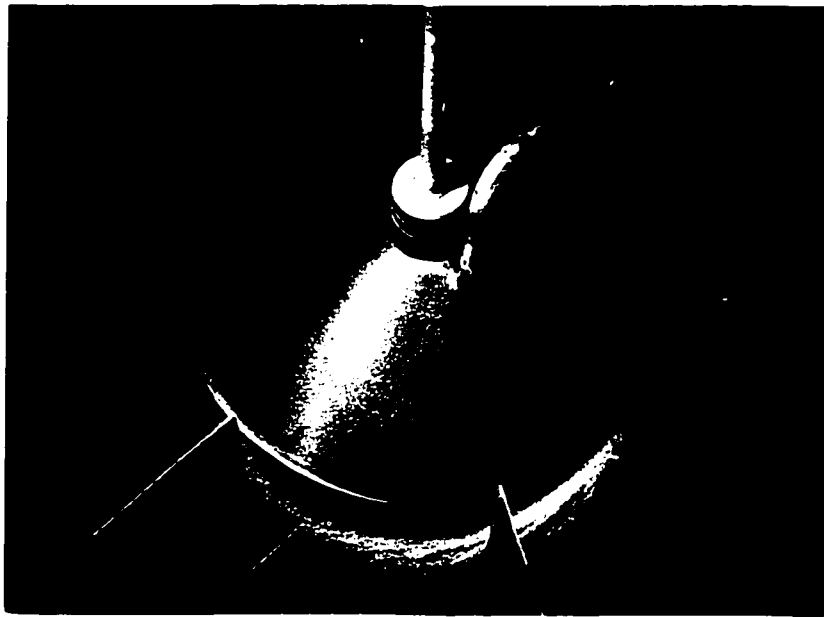


Figure 3.4b Effect of feed flow rate on fibre fractionation by fibre coarseness



Photograph 3.4 Film/ligament formation on the cone surface

3.3.3 Effect of cone rotational speed

The effect of feed flow rate was studied using a 20-mesh cone. The cone rotational speed varied from 200 to 600 rpm. The feed consistency was 0.15 wt%. The feed flow rate was 2.4 L/min. Variations of the cumulative average fibre length with cumulative percentage feed are shown in Figure 3.5a. Variations of the cumulative average fibre coarseness with cumulative percentage feed are shown in Figure 3.5b. It can be observed that within the range of the cone rotational speed studied, the fractionation performance improves with an increase in cone rotational speed from 200 to 300 rpm. With a further increase in cone rotational speed to 600 rpm, there is a decrease in the fractionation performance. This suggests that an optimal cone rotational speed exists while other parameters are constants.

The atomization modes varied with an increase in cone rotational speed at a constant feed flow rate. Observation and the experimental results showed that the ligament formation gave the best fractionation performance.

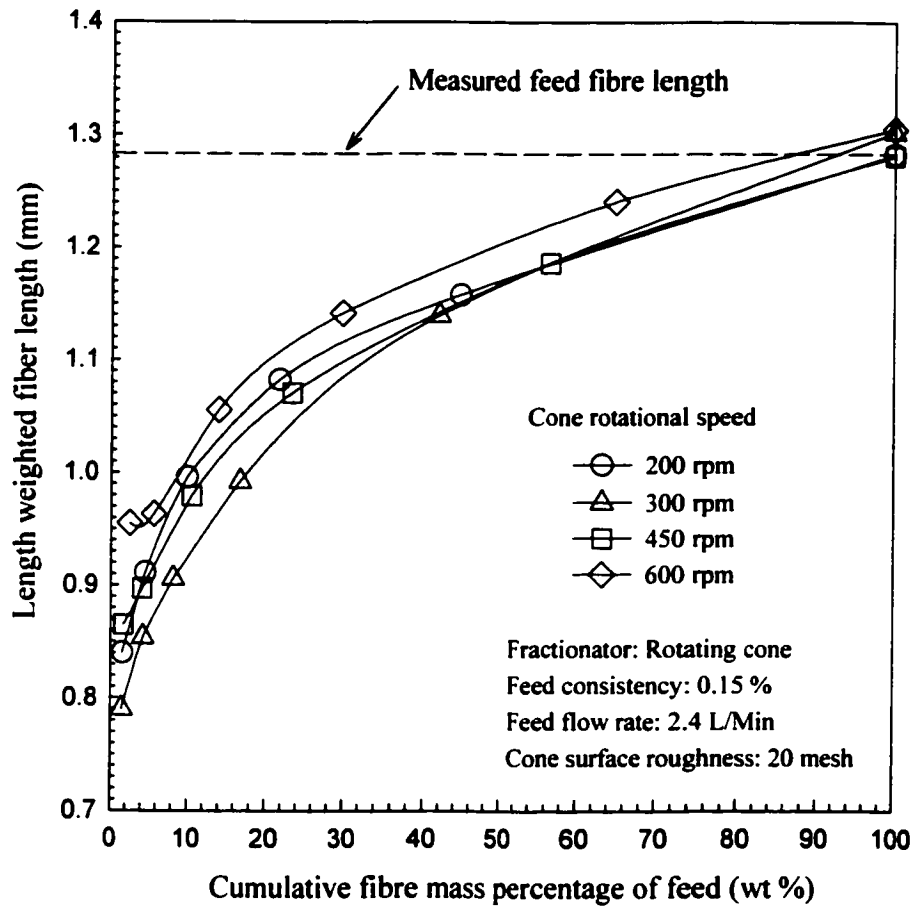


Figure 3.5a Effect of cone rotational speed on fibre fractionation by fibre length

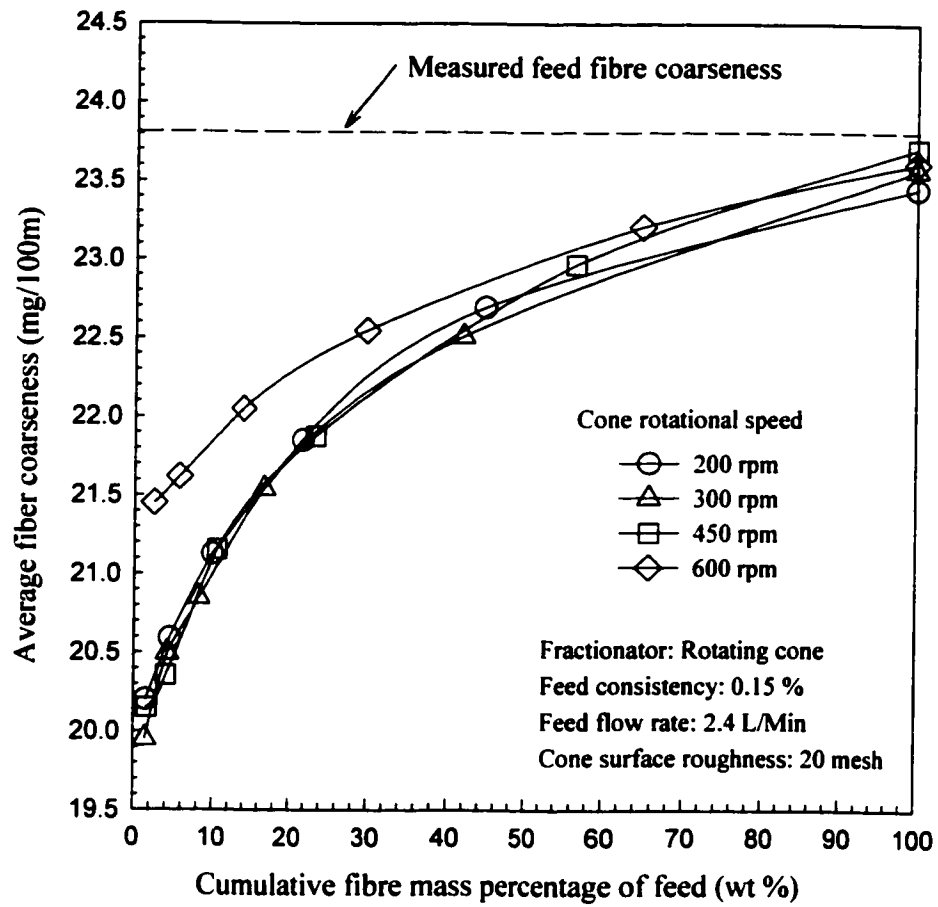


Figure 3.5b Effect of cone rotational speed on fibre fractionation by fibre coarseness

3.3.4 Effect of cone surface roughness

The effect of cone surface roughness was studied for a cone of 90 mm radius. The cone surface roughness was varied from smooth to a rough surface. The rough surface cone was constructed simply by using a 20-mesh screen. For the 20-mesh surface studied, the wire diameter was 474 μm and the opening was 798 μm . The openings of the mesh sieve were blocked using adhesive tape on the lower side of the cone surface. The cone rotational speed was 450 rpm; the feed consistency was 0.15 wt%; and the feed flow rate was 2.4 L/min. Variations of the cumulative average fibre length with cumulative percentage feed are shown in Figure 3.6a. Variations of the cumulative average fibre coarseness with cumulative percentage feed are shown in Figure 3.6b. It can be observed that the fractionation performance improves significantly with the 20-mesh surface as compared to that of the smooth cone.

With increasing cone surface roughness, the transition arc generated by the feed fibre suspension was found to shift in the direction of rotation. This shift of transition with an increase in surface roughness was due to increased drag acting on the flowing suspension. This shift of transition in the direction of rotation leads to an increase in the residence time of the suspension on the cone surface, thereby enhancing the fractionation process.

Rewatkar (1997) studied the effect of surface roughness on fractionation of wood fibres. He concluded that a cone having a rough surface gave better fractionation performance as compared to one having a smooth surface. The optimum rough surface was found to be dependent on the fibre length of the feed sample. Chen (1998) also studied the effect of surface roughness on fractionation of nylons fibres. She found that fibre deposition on the screen would limit the use of a rough surface on fractionation of nylon fibres.

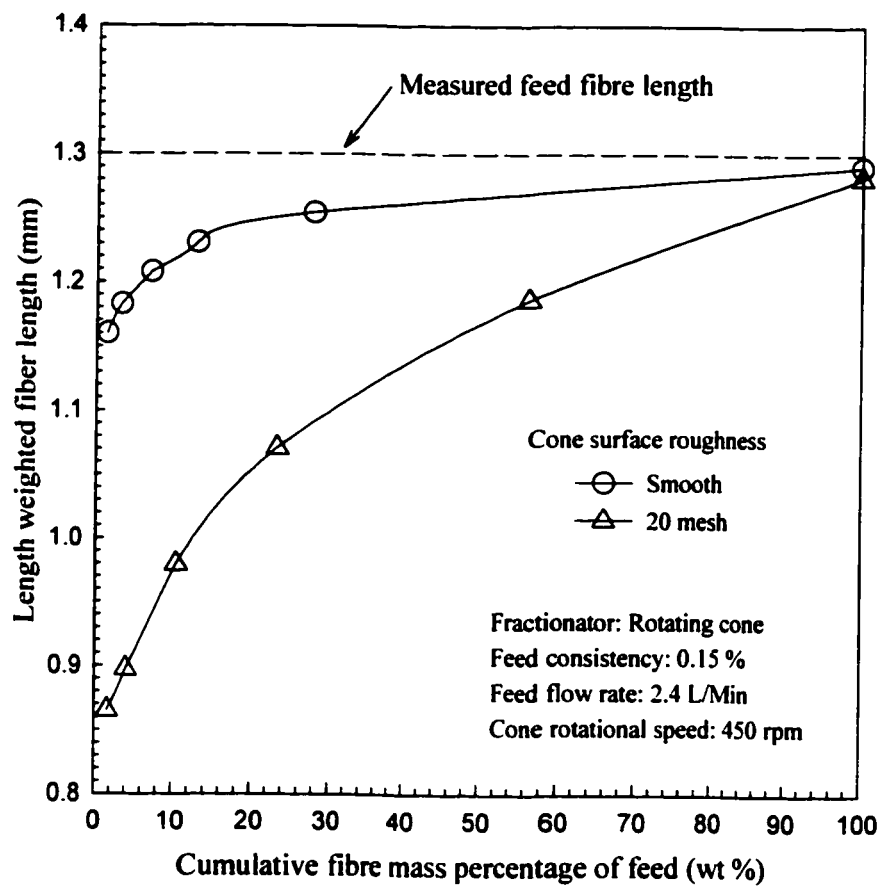


Figure 3.6a Effect of cone surface roughness on fibre fractionation by fibre length

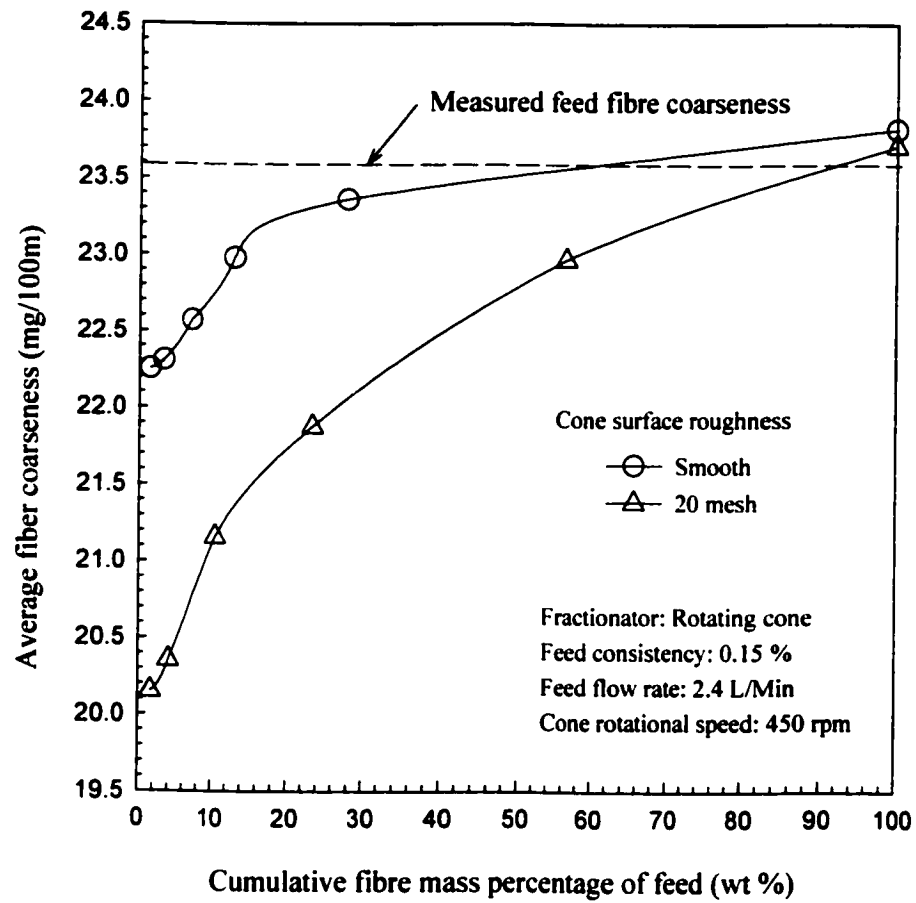


Figure 3.6b Effect of cone surface roughness on fibre fractionation by fibre coarseness

3.4 CONCLUSIONS

In the present study, a rotating cone fractionator was found to be useful in fractionating softwood TMP fibres according to both fibre length and fibre coarseness. The atomization mode in the ligament formation along with a clear transition boundary on the cone surface was found to give the best fractionation performance. The ligament formation occurred either at an optimum feed flow rate or an optimum cone rotational speed while other operating parameters were fixed. A rotating cone having a rough surface was found to give much better fractionation performance as compared to a smooth surface. Lower feed consistency favored better fractionation performance. The rotating cone fractionator was found to fractionate softwood TMP fibres at consistency as high as 0.95 wt%.

CHAPTER 4

CONTINUOUS FLOTATION CELL

4.1 INTRODUCTION

In the mineral processing industry, froth flotation is used to float certain minerals, allowing for the separation of valuable minerals from the less desirable minerals or unwanted minerals (gangue). This is normally accomplished by the addition of a reagent referred to as a collector, which alters the surface characteristics of selected mineral particles. If the desired mineral particles can be made more hydrophobic than the other minerals present, then they will have a greater tendency to attach themselves to an air bubble and will have a higher concentration in the froth. As the air bubbles rise through a slurry, they tend to entrain both the valuable minerals and gangue in the froth. As the froth layer

builds up in thickness, much of the entrained liquid drains back through the froth, carrying the unattached gangue particles with it (Jameson, 1984).

Recently, some researchers started to investigate the applications of froth flotation in fibre fractionation process. Li et al. (1995) reported their results of fractionation of chemical and mechanical pulps using froth flotation. They found that chemical pulps with low lignin content floated more freely than the mechanical pulps. Eckert et al. (1997) studied fibre fractionation of softwood TMP using a batch flotation process. They found that fractionation occurred on the basis of fibre length and the length of fibres trapped in the froth could be related to the size of bubbles generated in the flotation cell. Eckert et al. (1998) also successfully demonstrated fractionation of softwood TMP using a continuous flotation process. The results indicated a strong correlation between the mean bubble diameter and the length of fibres captured in the froth. The surfactant concentration added to the feed stream had the greatest effect on the bubble size, while the impeller speed and air flow rate had the least.

Eckert et al. (1997) confirmed the conclusions from Ajersch and Pelton (1995) that entrapment of longer fibres in froth was the primary mechanism of separation, rather than surface activity of the fibres. They found that if the froth was removed as soon as it was formed, the fibre length distribution in the captured froth was similar to the feed pulp. However, if the froth layer was allowed to build and drain before removal, the fibre length distribution was significantly different from that of the feed pulp. As shown in Figure 4.1, the air bubbles entrain fibres while rising through pulp slurry. As the water film between the bubbles drains and returns to the pulp slurry, it carries the fines and shorter fibres with it. The longer fibres in the froth are unable to negotiate the tortuous path of the liquid and remain trapped by the bubbles. The drained froth therefore carries with it a fibre distribution consisting of a much higher proportion of long fibre than the original feed pulp. It would appear that fibre length, rather than

surface activity, is the most important parameter in this flotation process, since fibres were fractionated on the basis of fibre length.

The objective of the present study is to fractionate softwood TMP using a continuous flotation cell on the basis of fibre length and fibre coarseness.

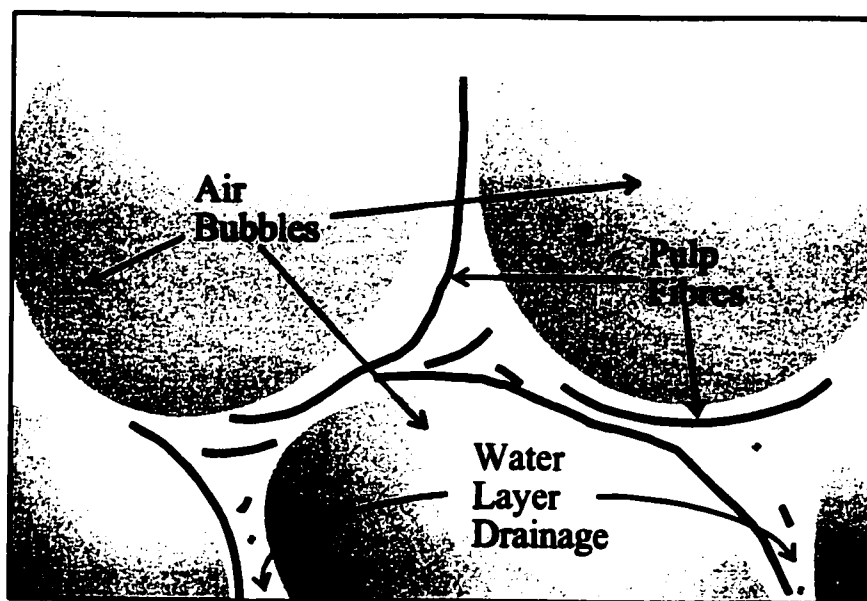


Figure 4.1 Fibres in water layer of froth

4.2 EXPERIMENTAL SET-UP

A modified Wemco laboratory flotation cell was used in the present study. A schematic of the experimental set-up is shown in Figure 4.2. The feed flow rate and impeller speed were controlled using variable speed drives on the feed pump and impeller motors. The air flow rate was measured and controlled using a rotameter. The feed flow rate was measured using a magnetic flow meter and the impeller speed was measured through a mechanical tachometer attached to the drive shaft.

The feed softwood TMP was prepared in the feed tank and was kept in a well-mixed condition with the help of a stirrer. Surfactant (pine oil) was added, and then the pulp was allowed to mix for 1 to 2 hours before the experiment was run. For the initial fill, about 4.5 litres of pulp was pumped from the feed tank into the 5.5 litre flotation cell. A sample of the feed in the cell was taken, and then the air was turned on to the desired flow rate. The impeller motor was turned on and set to the appropriate rotation speed. A timer was started when the froth first flowed over the lip of the cell. The froth and the tailing were collected in two-minute intervals over a twenty-minute time span of the test. At the end of a test, the mass and consistency of the selected froth, tailing and feed samples were measured and recorded. After the 2-stage washing process, the mass and consistency of the washed samples were measured and recorded. The washed samples were then analyzed using the Fibre Quality Analyzer (FQA) to determine the fibre length and coarseness.

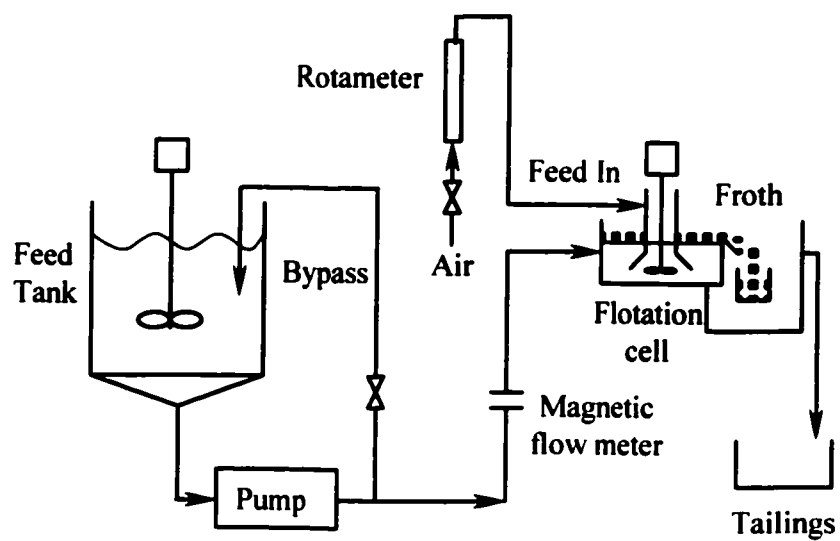


Figure 4.2 Continuous flotation cell experimental set-up

4.3 RESULTS AND DISCUSSION

In the following sections, the effects of operating parameters on fractionation performance are discussed. The fibre length and coarseness of the fractions were plotted against the fibre mass of the fractions. The values of the 100% cumulative fibre length (or fibre coarseness) calculated from Equations (2.15) and (2.16) were also plotted on the same figure and they should approach the values of the feed sample when the measurement error is small.

4.3.1 Effect of feed consistency

The effect of feed consistency on fractionation performance was investigated at the mass feed consistency ranging between 0.15 wt% and 0.40 wt%. Other operating parameters were kept constant. The feed flow rate was 0.15 L/min, the air flow rate was 44.4 L/min, the impeller speed was 1800 rpm and the surfactant concentration was 0.0004 vol%. The fibre lengths of fractions collected at different feed consistencies were plotted versus the fibre mass percentage of feed as shown in Figure 4.3a. The fibre length of the fibres in the froths decreased significantly with an increase in the feed consistency, while the fibre mass percentage of the froth increased with an increase in the feed consistency. On the other hand, the fibre length of the tailing increased with an increase in the feed consistency, while the fibre mass percentage of the tailings decreased with an increase in the feed consistency. The results indicated that more fibres were captured in the froth fraction at higher feed consistency. The lowest feed consistency (0.15 wt%) gave the longest average fibre length in the froth.

The fibre coarsenesses of fractions collected at different feed consistencies were plotted against the fibre mass percentage of feed as shown in Figure 4.3b. Basically, Figure 4.3b shows the same trends as that in Figure 4.3a. The fibre coarseness of the fibres in the froth decreased significantly with an increase in the feed consistency, while the fibre coarseness of the fibres in the tailing increased with an increase in the feed consistency. The lowest feed consistency (0.15 wt%) gave the highest average fibre coarseness in the froth.

The results agreed with the conclusions of Eckert et al. (1998) that, as the feed consistency was increased, the recovery (fibre mass percentage of feed) of feed fibres to the froth increased significantly. However, the grade (average fibre length) of the froth decreased with an increase in the feed consistency. The change in fractionation performance with the feed consistency could be attributed to two factors (Eckert et al., 1998). A higher feed consistency results in a higher level of naturally occurring surfactants, which decreases air bubble size and fractionation performance. Also, a higher consistency results in a higher crowding factor as defined by Kerekes and Schell (section 3.3.1). For pulp consistencies of 0.15 wt%, 0.30 wt%, and 0.40 wt%, the corresponding crowding factors are 1, 2, and 3. The lowest feed consistency (0.15 wt%) was in the considered dilute regime. The higher feed consistencies (0.30 wt% and 0.40 wt%) were in the semi-concentrated regime with forced collisions between fibres. Therefore, better fractionation performance should be expected at the lowest feed consistency.

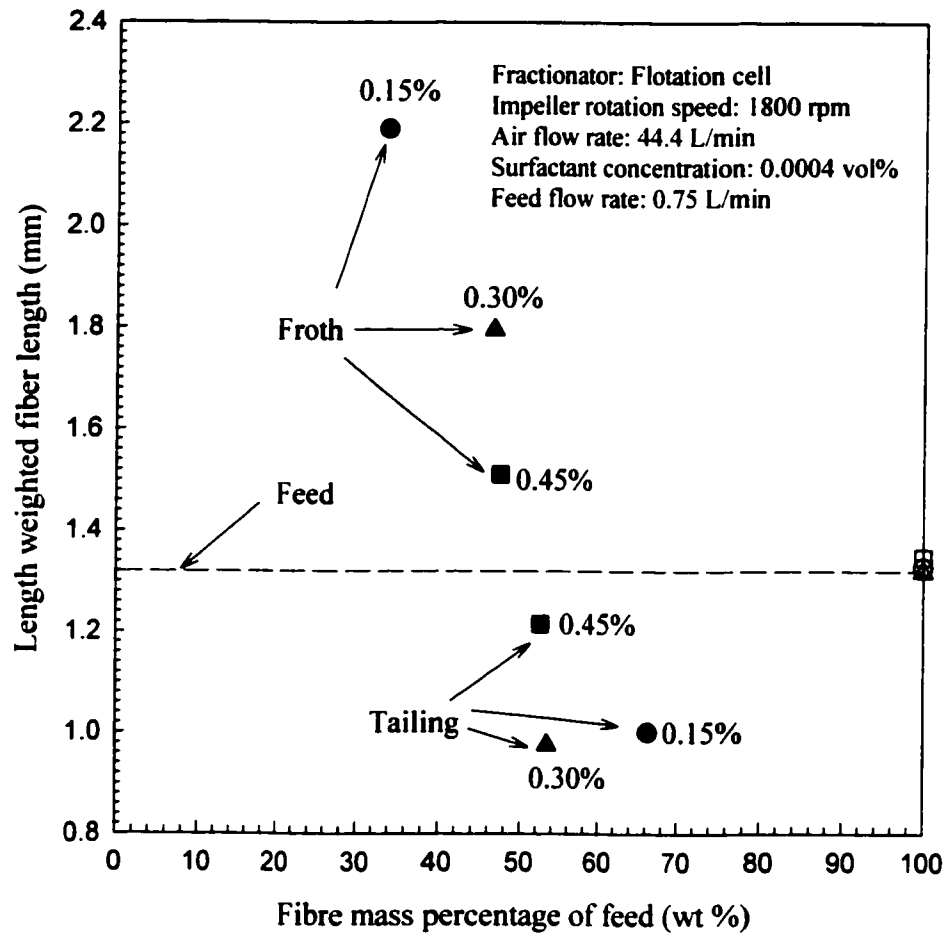


Figure 4.3a Effect of feed consistency on fibre fractionation by fibre length

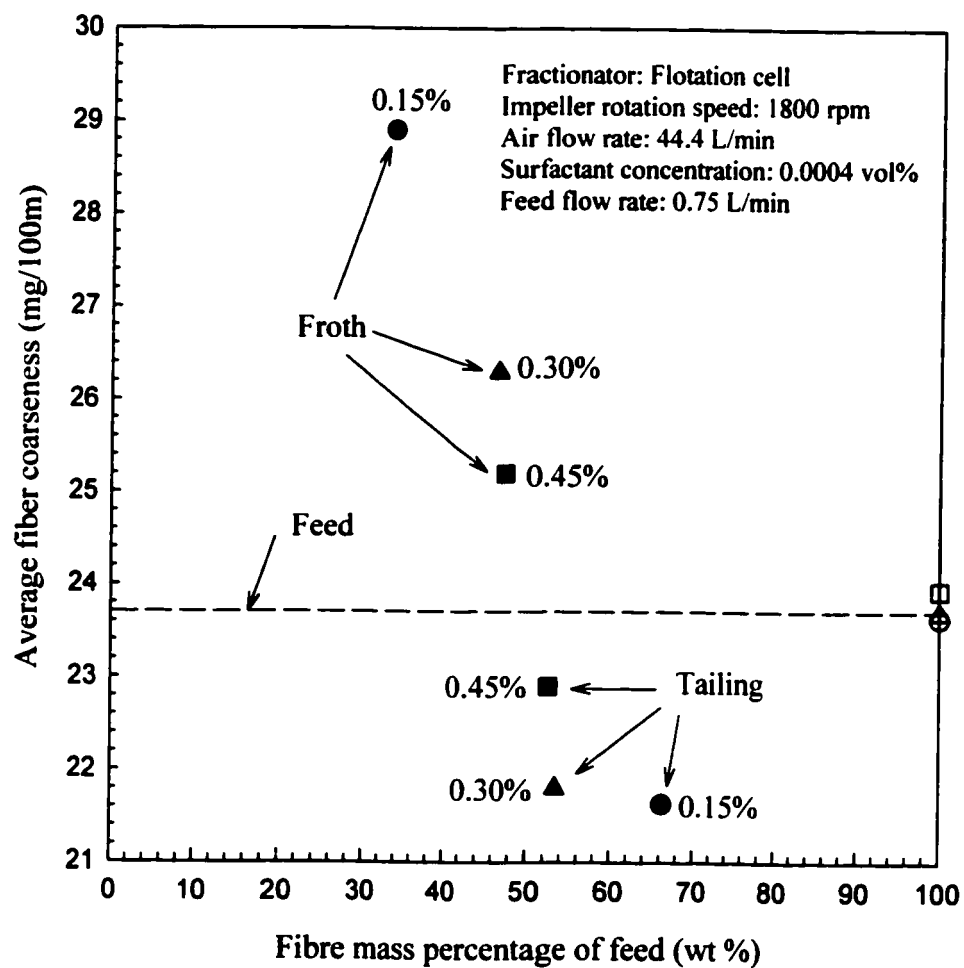


Figure 4.3b Effect of feed consistency on fibre fractionation by fibre coarseness

4.3.2 Effect of feed flow rate

The effect of feed flow rate was determined by testing three different feed flow rates of 0.44, 0.75 and 1.58 L/min, at constant feed consistency, air flow rate, impeller speed and surfactant concentration of 0.15 wt%, 44.4 L/min, 1800rpm and 0.0004 vol%, respectively.

The variation of length weighted fibre lengths of the fibres captured in the froths and tailings with different feed flow rates is shown in Figure 4.4a. The lowest feed flow rate (0.44 L/min) gave the longest average fibre length captured in the froth. The average fibre length captured in the froths decreased significantly with an increase of feed flow rate. The variation of fibre coarsenesses of the fibres captured by froths and tailings with different feed flow rates is shown in Figure 4.4b. The lowest feed flow rate gave the highest average fibre coarseness captured in the froth. Also, the average fibre coarseness captured in the froths decreased with an increase in the feed flow rate whereby approaching the feed value.

Due to the reduced mean residence time, a decrease in the fractionation performance is expected with increased feed flow rate. Also, a higher feed flow rate would quickly replenish the surfactant during the run and a higher surfactant concentration would be expected in the bulk of the flotation cell at steady state. Therefore, the decreased fibre length and coarseness of the fibres in the froth was attributed to smaller bubbles being generated.

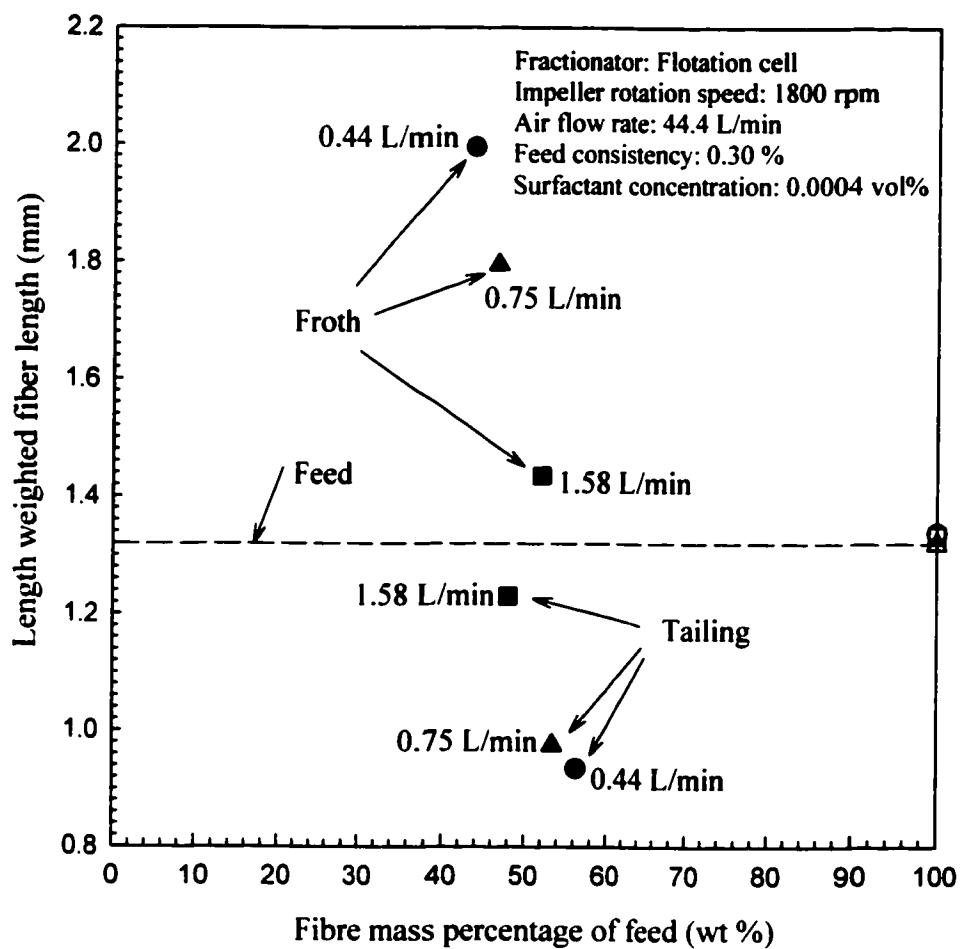


Figure 4.4a Effect of feed flow rate on fibre fractionation by fibre length

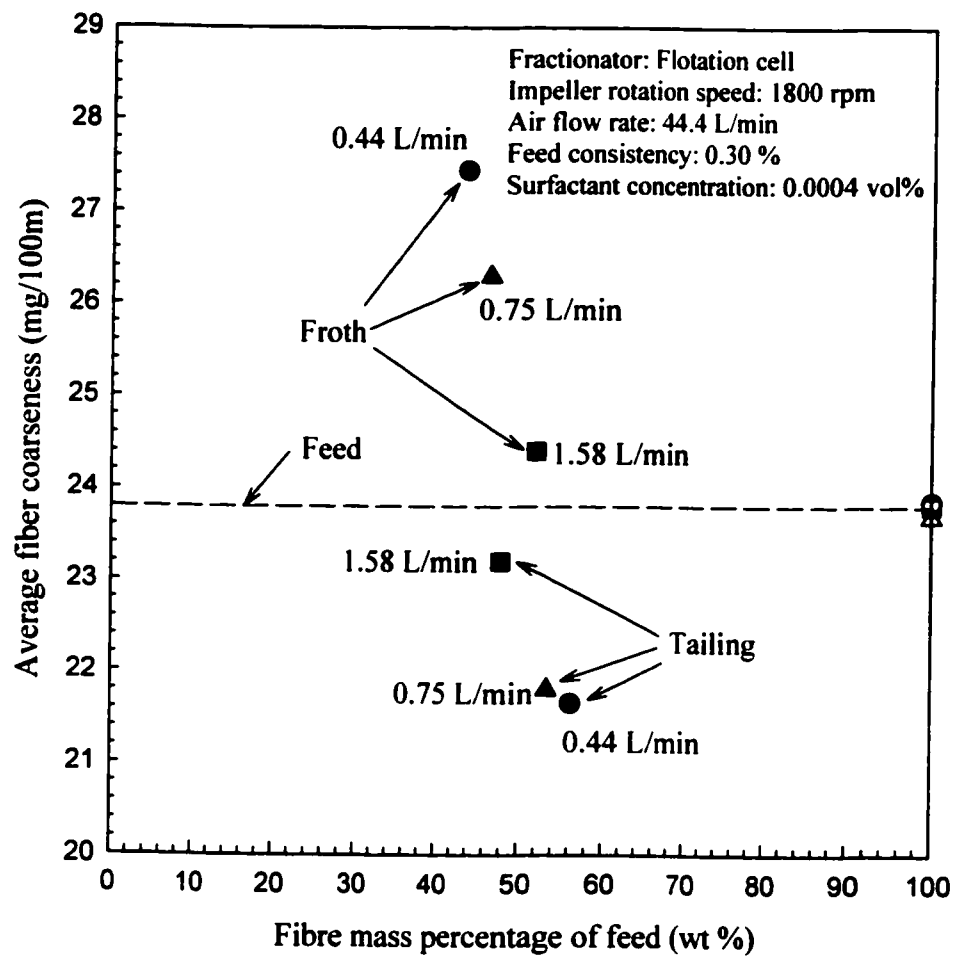


Figure 4.4b Effect of feed flow rate on fibre fractionation by fibre coarseness

4.3.3 Effect of air flow rate

The effect of air flow rate was determined by testing two air flow rates of 28.4 and 44.4 L/min. The maximum air flow rate that could be achieved was 44.4 L/min. For these tests, the feed consistency, the feed flow rate, the impeller speed and the surfactant concentration were 0.30 wt%, 0.75L/min, 1800rpm and 0.0004 vol%, respectively.

The variation of length weighted fibre length of the fibres captured in the froths and tailings at different air flow rates is shown in Figure 4.5a. The higher air flow rate (44.4 L/min) gave longer average fibre length captured in the froth. The average fibre length captured in the froths increased slightly with an increase in the air flow rate. The variation of the fibre coarsenesses of the fibres captured in the froths and tailings with different air flow rates is shown in Figure 4.5b. The higher air flow rate gave the higher average fibre coarseness captured in the froth. Also, the average fibre coarseness captured in the froths increased slightly with an increase in the air flow rate. These results indicated that air flow rate does not have significant effect on the fractionation performance.

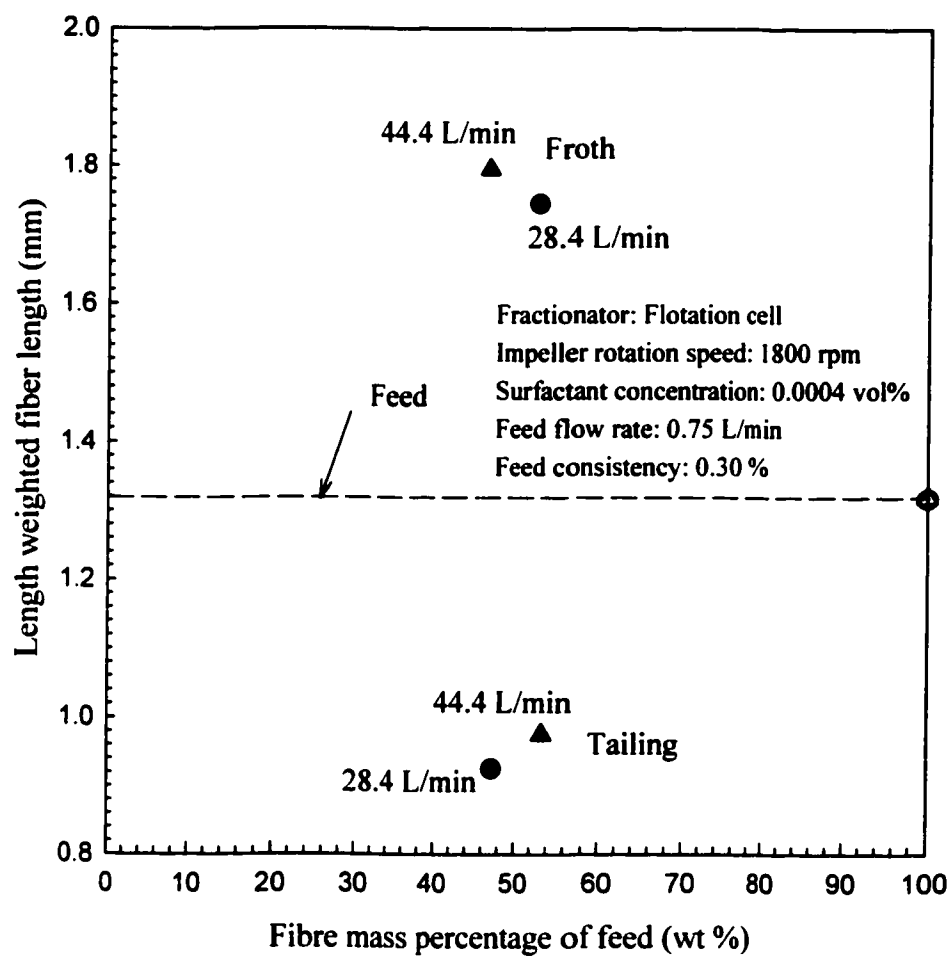


Figure 4.5a Effect of air flow rate on fibre fractionation by fibre length

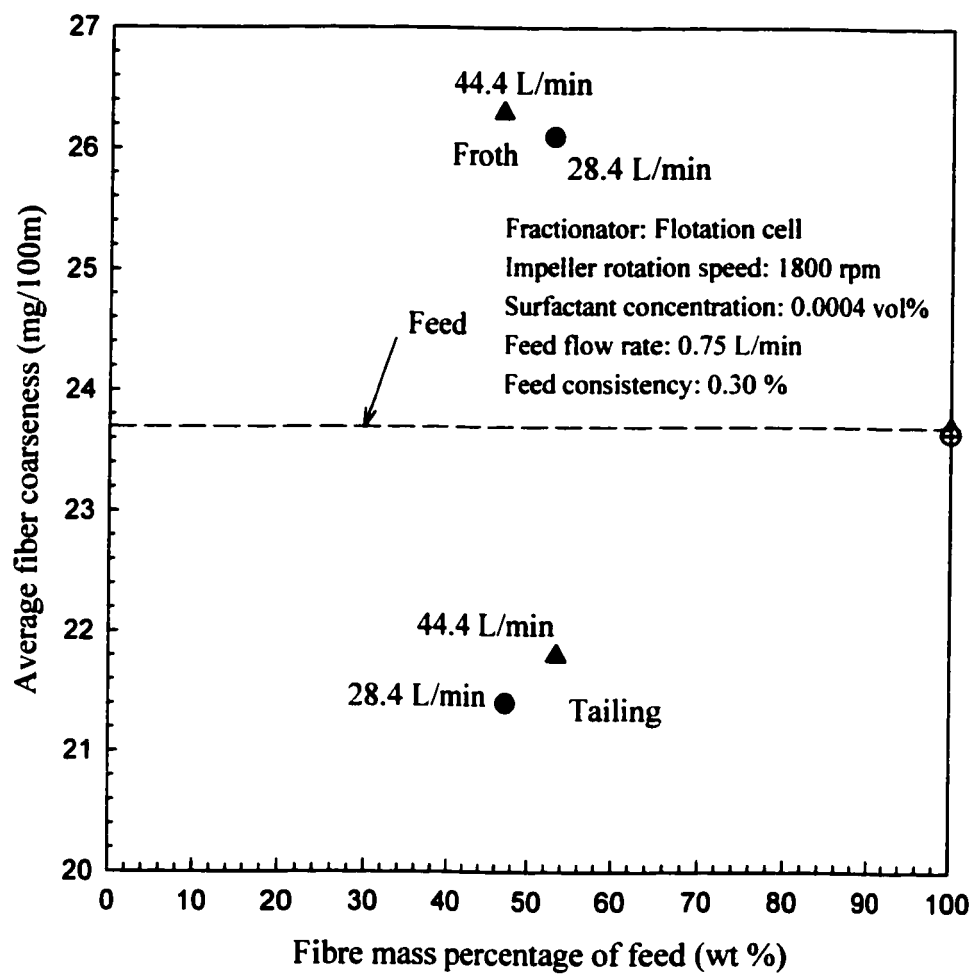


Figure 4.5b Effect of air flow rate on fibre fractionation by fibre coarseness

4.3.4 Effect of surfactant concentration

The exact concentration of surfactant in the feed was not known, since the wood fibre contained natural surfactants. In the present study, the surfactant concentration was defined as the concentration of added surfactant, rather than total surfactant in the feed.

The effect of surfactant concentration was tested at added surfactant concentrations of 0, 0.0004 and 0.0008 vol%. For these tests, the feed consistency, the feed flow rate, the air flow rate and the impeller speed were 0.30 wt%, 0.75L/min, 44.4 L/min and 1800rpm, respectively.

The variation of length weighted fibre length of the fibres captured in the froths and tailings with different surfactant concentrations is shown in Figure 4.6a. Without any added surfactant, fibres with very high average fibre length were captured in the froth. When the surfactant concentration was 0.0008 vol%, fibres with shortest average fibre length were captured in the froth. The results indicated that the amount of fibres (both long and short fibres) captured in the froths increased with an increase in surfactant concentration. The variation of fibre coarseness of the fibres captured in the froths and tailings with different surfactant concentrations is shown in Figure 4.6b. Without any added surfactant, fibres with very high average fibre coarseness were captured in the froth. When the surfactant concentration was 0.0008 vol%, fibres with the lowest average fibre coarseness were captured in the froth.

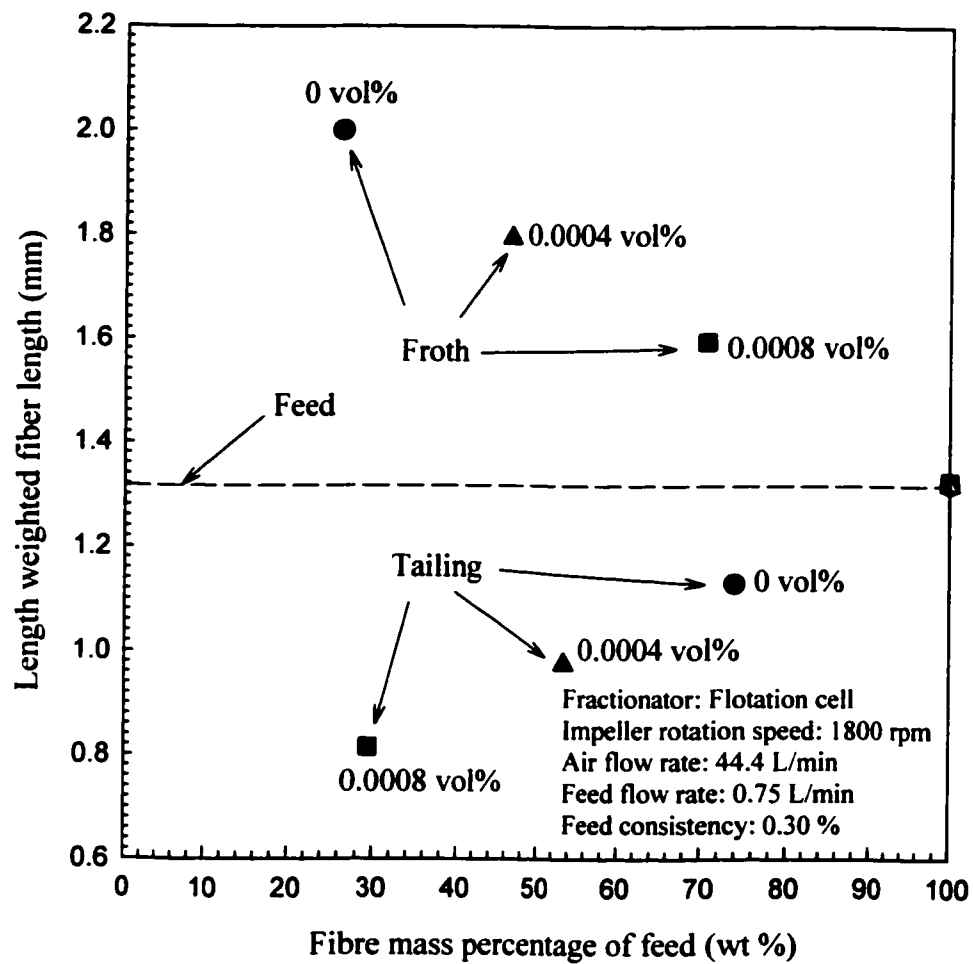


Figure 4.6a Effect of surfactant concentration on fibre fractionation by fibre length

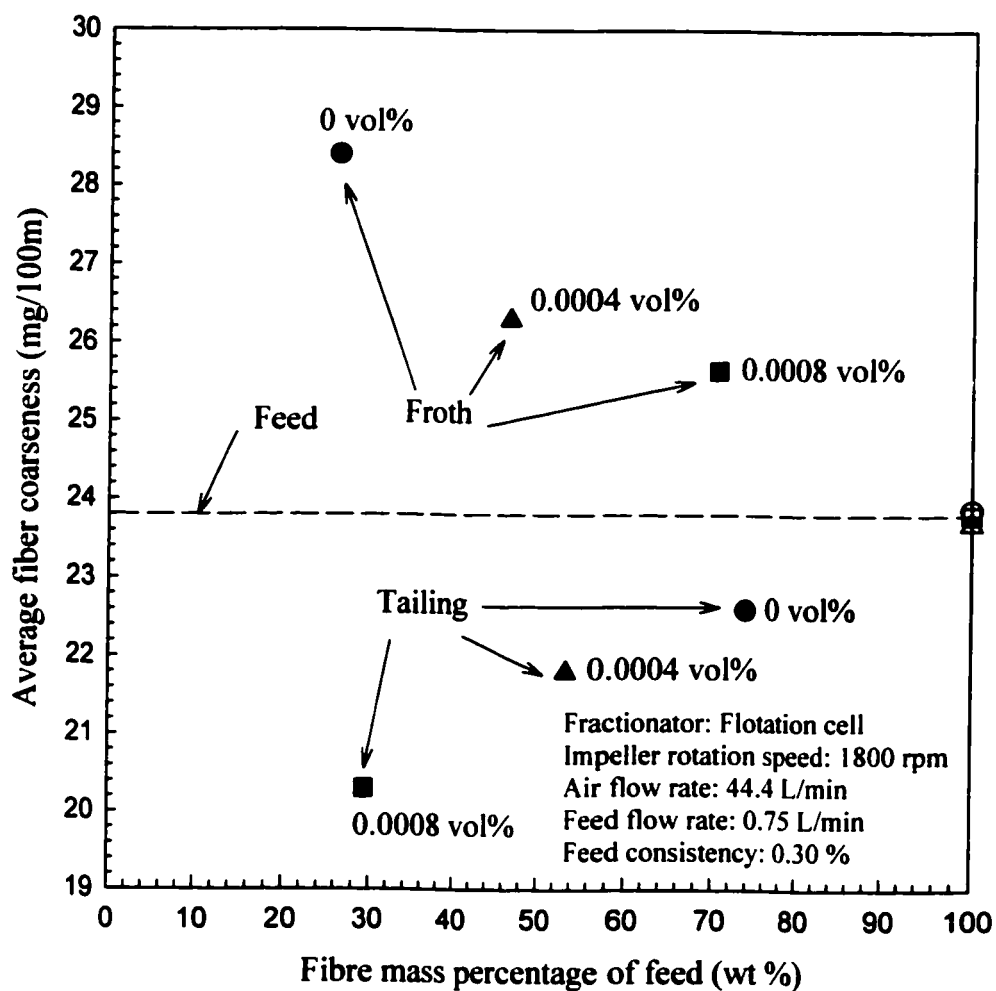


Figure 4.6b Effect of surfactant concentration on fibre fractionation by fibre coarseness

4.3.5 Effect of impeller rotation speed

The effect of impeller rotation speed was tested at speeds of 1250, 1575, and 1800 rpm. For these tests, the feed consistency, the feed flow rate, the air flow rate and the surfactant concentration were 0.30 wt%, 0.75L/min, 44.4 L/min and 0.0004 vol%, respectively.

The variation of length weighted fibre length of the fibres captured in the froths and tailings with different impeller speeds is shown in Figure 4.7a. The impeller speed of 1575 rpm gave a slightly longer average fibre length captured in the froth. The average fibre length captured in the froths was not significantly influenced by the impeller speed. The variation of fibre coarsenesses of the fibres captured in the froths and tailings with different impeller speeds is shown in Figure 4.7b. The impeller speed of 1575 rpm gave a slightly higher average fibre coarseness captured in the froth. The average fibre coarseness captured in the froths was not significantly influenced by the impeller speed.

4.4 CONCLUSIONS

A continuous flotation cell could be used to fractionate 100% softwood TMP fibres according to fibre length and fibre coarseness. Feed consistency, feed flow rate and surfactant concentration had strong effects on the fractionation performance. Impeller rotation speed and air flow rate had slight effects on the fractionation performance. Lower feed consistency and feed flow rate favored better fractionation performance.

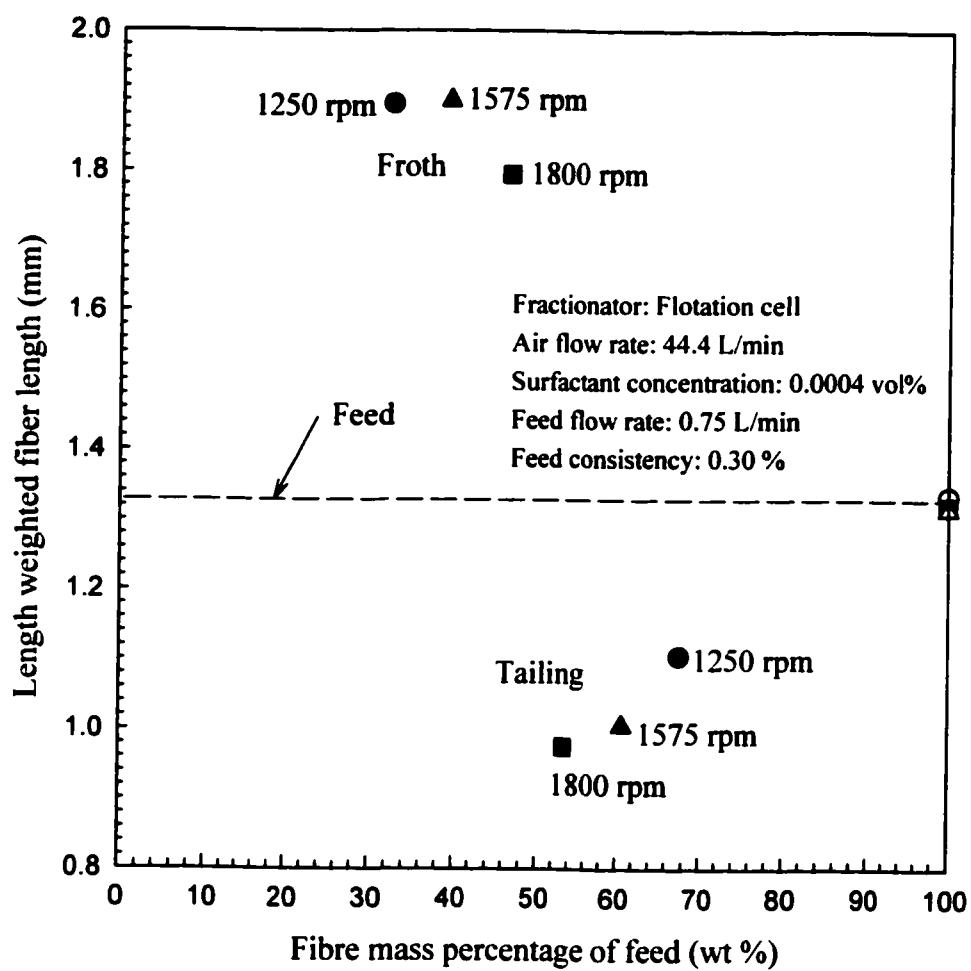


Figure 4.7a Effect of impeller speed on fibre fractionation by fibre length

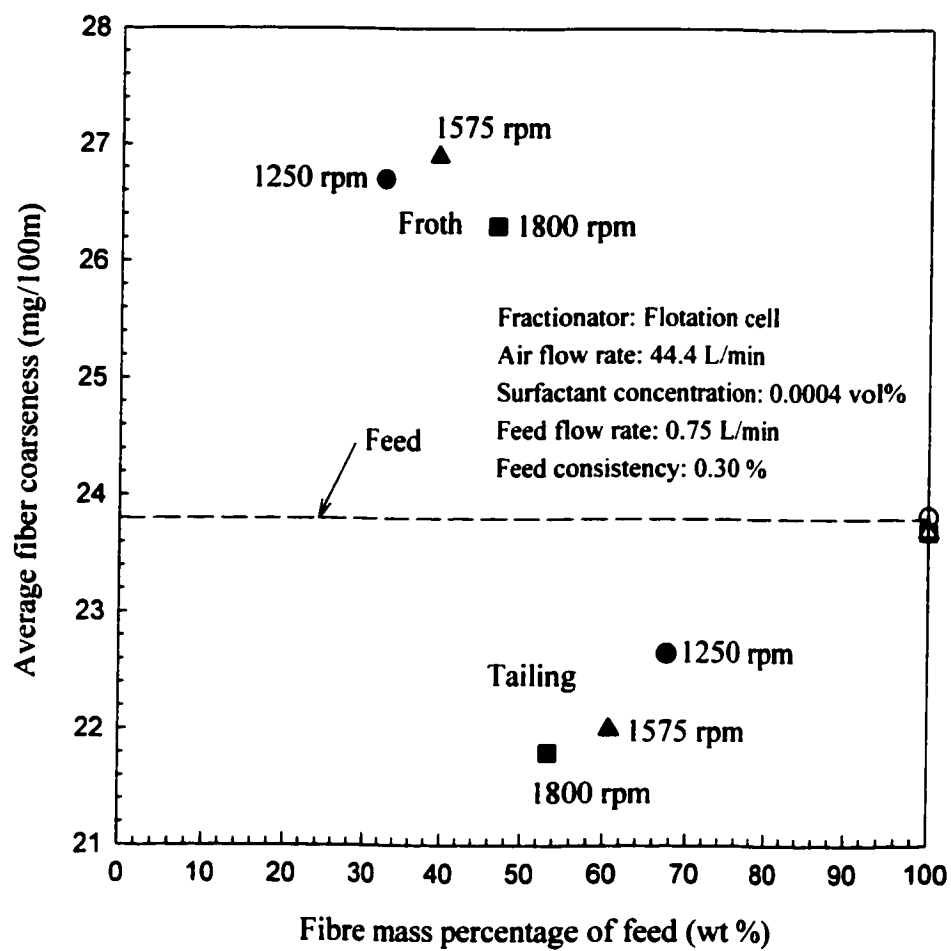


Figure 4.7b Effect of impeller speed on fibre fractionation by fibre coarseness

CHAPTER 5

AIR SPARGED HYDROCYCLONE

5.1 INTRODUCTION

In the pulp industry, hydrocyclones (centrifugal cleaners) have been used for decades to remove dirt particles, plastic contaminants, and shives from pulps (Franko, 1987; Galloway and Branion, 1990; Bliss, 1992). Many researchers found that hydrocyclones can fractionate wood pulp fibres based on their physical properties such as fibre length, fibre wall thickness, specific surface and fibre coarseness (Bliss, 1983, 1984; Gavelin and Backman, 1991; Paavilainen, 1992).

Air sparged hydrocyclone (ASH) flotation is a new technology that has been under development during the past two decades. This technology combines froth flotation principles together with the flow characteristics of a hydrocyclone

system. The most important feature of the air sparged hydrocyclone is its high specific capacity, which corresponds to significant savings in capital cost (equipment and floor space). For example, the air sparged hydrocyclone had a specific capacity of at least 100 times that of conventional flotation equipment. In addition to its unique flow pattern and flotation characteristics being considerably different from conventional flotation machines, another feature of the air sparged hydrocyclone is its ability to operate at high ratio of air to slurry flow rate. A recent development in flotation with the air sparged hydrocyclone is the high air rate flotation in which the volumetric ratio of air flow rate to slurry flow rate is as high as ten to one (Miller, 1989).

During the last few years, it has been shown that effective flotation separations for a variety of mineral commodities can be achieved with the high capacity air sparged hydrocyclone. Attention also has been given to applications of air sparged hydrocyclone flotation technology outside the mineral industry, including the pulp and paper industry and the food industry (Miller, 1995). The most significant development was the announcement by Kamyr in 1991 to construct a 20-million dollar wastepaper recycling plant which uses air sparged hydrocyclone technology for deinking flotation in the production of recycled paper. The plant has twenty 6-inch air sparged hydrocyclone units to handle a flow of about 4000 gpm. In addition to these efforts to commercialize the air sparged hydrocyclone technology, fundamental research has been on-going. As a result of x-ray computed tomography studies (Miller, 1995), a better appreciation of the influence of system variables on the nature of the segregated flow is being developed. In addition, high-speed photography and high-speed video techniques are being used to examine the nature of bubble formation in the swirl flow of the air sparged hydrocyclone and the corresponding bubble size distributions.

In the air sparged hydrocyclone flotation process, the slurry is fed tangentially through a conventional cyclone header into a porous cylinder to

develop a swirl flow and is discharged through the annular opening created between the cylinder wall and a froth pedestal which is located on the cylinder axis at the bottom of the air sparged hydrocyclone (Figure 5.1). Air is sparged through the jacketed porous cylinder wall and is sheared into numerous small bubbles by the high-velocity swirl flow of the slurry. When the air sparged hydrocyclone is used in a mineral flotation process, hydrophobic particles in the slurry collide with the bubbles, and transported radially by the bubbles into a froth phase, which forms in the cylinder central axis region. The froth phase is supported and constrained by the froth pedestal and thus moves towards the vortex finder of the cyclone header, being discharged as an overflow stream. Hydrophilic particles generally remain in the slurry phase and are discharged as an underflow stream through the annulus between the porous cylinder wall and the froth pedestal. When the air sparged hydrocyclone is used in the fractionation process of wood fibres, the entrapment of longer fibres in froth is possible mechanism of separation rather than surface activity of the fibres since all wood fibres are naturally hydrophilic. The air bubbles entrain fibres while moving towards the froth phase. The water film between the bubbles drains and returns to the slurry phase that carries the fines and shorter fibres with it. The longer fibres remain in the froth phase and therefore the drained froth carries a much higher proportion of long fibres than the feed pulp slurry.

The objective of the present study is to determine whether an air sparged hydrocyclone can be used to fractionate softwood TMP fibres on the basis of fibre length and fibre coarseness difference.

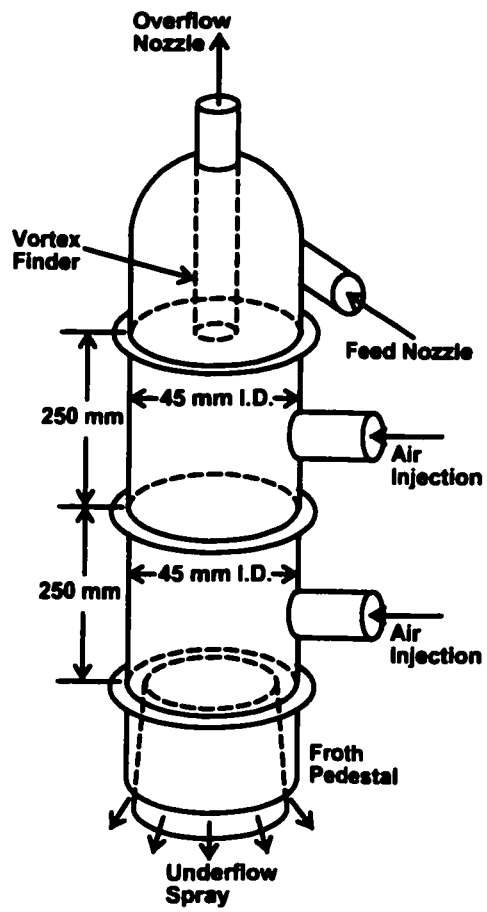


Figure 5.1 Air sparged hydrocyclone

5.2 EXPERIMENTAL SET-UP

In this study, an air sparged hydrocyclone (Advanced Processing Technologies Inc.) was used. Dimensions are shown in Figure 5.1. The cylindrical body was made up of two concentric tubes. Each section measures 250mm in length and 45mm in diameter and is composed of an outer stainless-steel shell, an inner porous tube, a vortex finder at the top, and an adjustable froth pedestal at the bottom of the unit. In the present study, the air sparged hydrocyclone was assembled with one section having an inner porous tube of 100 μm pore diameter.

The schematic of the experimental setup is shown in Figure 5.2. For each test, approximately 200 litres pulp slurry (Softwood TMP, no surfactant added) was prepared in the feed tank and fed tangentially to the top of the air sparged hydrocyclone. Feed flow rate was controlled using a variable speed drive on the feed pump motor, and measured with a magnetic flow meter. Air is supplied at the side of the air sparged hydrocyclone's shell and into the annular spacing between the shell and the porous tube. Air flow rate was controlled and measured by a rotameter. The flow rate of underflow stream was controlled by adjusting the froth pedestal's opening. Samples were collected from feed tank, overflow and underflow streams. The flow rate of the overflow stream was determined by collecting a sample for a fixed time interval. mass collected at a fixed time span. Due to the difficulty with sampling at high flow rate (30–90 L/min), the flow rate of the underflow was calculated from the feed flow rate minus the overflow rate. The weight and consistency of the samples were determined using the 2-stage washing process. Again, after washing, the mass and consistency of the washed samples were examined. The fibre length and coarseness of the washed samples were determined using the Fibre Quality Analyzer (FQA).

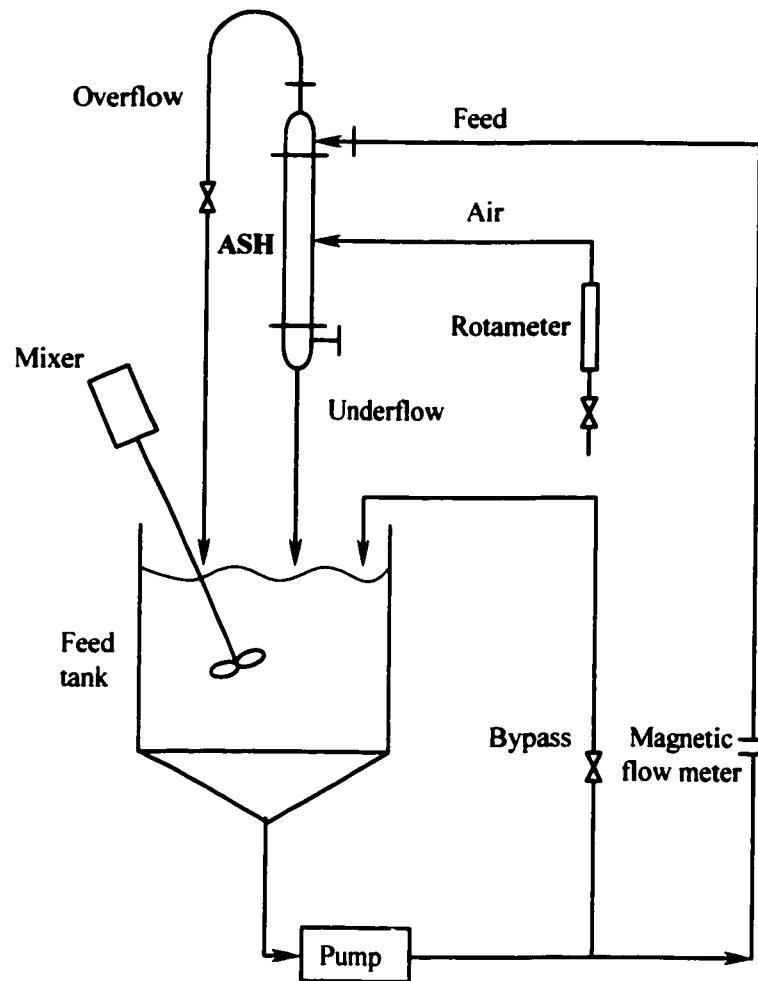


Figure 5.2 Air sparged hydrocyclone (ASH) experimental set-up

5.3 RESULTS AND DISCUSSION

For all the tests conducted in this study, the overflow samples exhibited much longer fibre length and higher fibre coarseness, while the underflow samples showed a slightly shorter fibre length and lower fibre coarseness as compared to those of the feed sample. The overflow rates were below 10% of the feed flow rate due to the design features of the air sparged hydrocyclone used in this study. About 95% of feed pulp slurry left the system by the underflow exit.

In the following sections, the effects of operating parameters on fractionation performance are discussed. The fibre length and coarseness of the fractions were plotted against the fibre mass of the fractions. The values of the 100% cumulative fibre length and coarseness calculated from Equations (2.15) and (2.16) were also plotted on the same figure and they should approach the values of the feed sample when the sampling error is small.

5.3.1 Effect of feed consistency

The feed consistency was varied from 0.15 wt% to 0.45 wt% while other operating parameters were kept constant: the feed flow rate was 60 L/min, the air flow rate was 44.4 L/min, and the ratio of overflow rate to feed flow rate was 5%.

The fibre lengths of overflow and underflow samples collected at different feed consistencies were plotted versus the fibre mass percentage of feed as shown in Figure 5.3a. The fibre length of the fibres in the overflow sample decreases with an increase in the feed consistency. The fibre length of the underflow sample at different feed consistency is very close to that of the feed, since almost 95% of

the feed pulp slurry reports to the underflow stream, and removing a small long fibre fraction (overflow stream) does not make much difference on the average fibre length between the feed stream and the underflow stream. The ratio of the overflow rate to the feed flow rate was kept constant at 5%.

The fibre coarseness of the fractions collected at different feed consistencies was plotted against the fibre mass percentage of feed as shown in Figure 5.3b. Basically, Figure 5.3b shows the same trends as that in Figure 5.3a. The fibre coarseness of the overflow samples decreases with an increase in the feed consistency. The lowest feed consistency (0.15 wt%) gives the longest fibre length and highest fibre coarseness within the overflow stream. The results revealed that better fractionation performance occurs at a lower feed consistency. The results could be explained using the crowding factor theory. At higher feed consistency, air bubbles entrain more short fibres and fines in the froth phase due to continuous fibre contact.

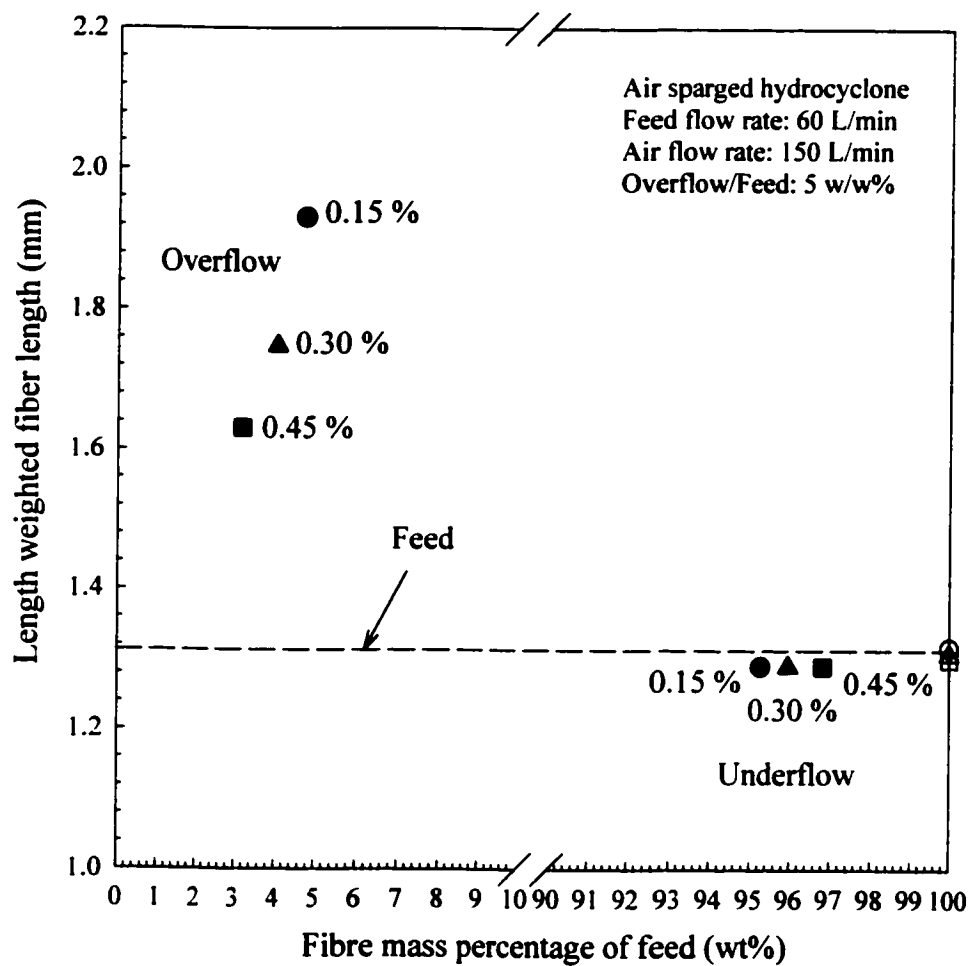


Figure 5.3a Effect of feed consistency on fractionation by fibre length

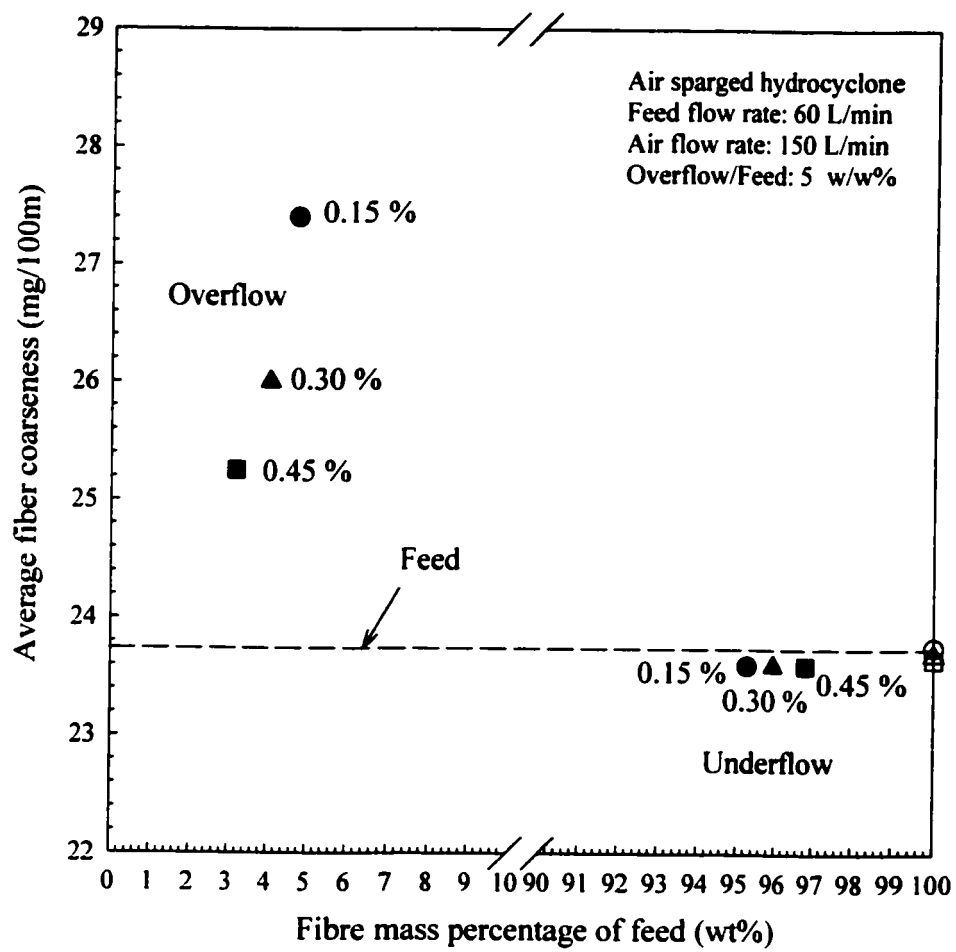


Figure 5.3b Effect of feed consistency on fractionation by fibre coarseness

5.3.2 Effect of feed flow rate

The effect of feed flow rate on fractionation performance was carried out at feed consistency of 0.15 wt%, the air flow rate of 150 L/min, the split ratio of 5% (the overflow rate to the feed flow rate). The feed flow rate was varied from 30 L/min to 75 L/min.

The fibre length of the overflow and underflow samples collected at different feed flow rates was plotted against the fibre mass percentage of feed as shown in Figure 5.4a. The fibre coarseness of the overflow and underflow samples collected at different feed flow rates was plotted against the fibre mass percentage of feed as shown in Figure 5.4b. At the feed flow rate of 45 L/Min, the overflow has the longest fibre length and the highest fibre coarseness as compared to those tests conducted at other feed flow rates. The fibre length and fibre coarseness of underflow samples at different feed consistency are very close to that of the feed due to the low split ratio. The results indicated that an optimum feed flow rate gives the best fractionation performance, which occurs at feed flow rate of 45 L/min.

The feed flow rate is a measure of the slurry velocity entering the cyclone. Miller et al. (1989) found that the effect of feed flow rate on flotation recovery of coarse particles is influenced by the surface chemistry features of the feed particles. Another effect of the feed flow rate is the effect on the swirl motion. The mechanism of the effect of feed flow rate on fractionation performance in this study is not known.

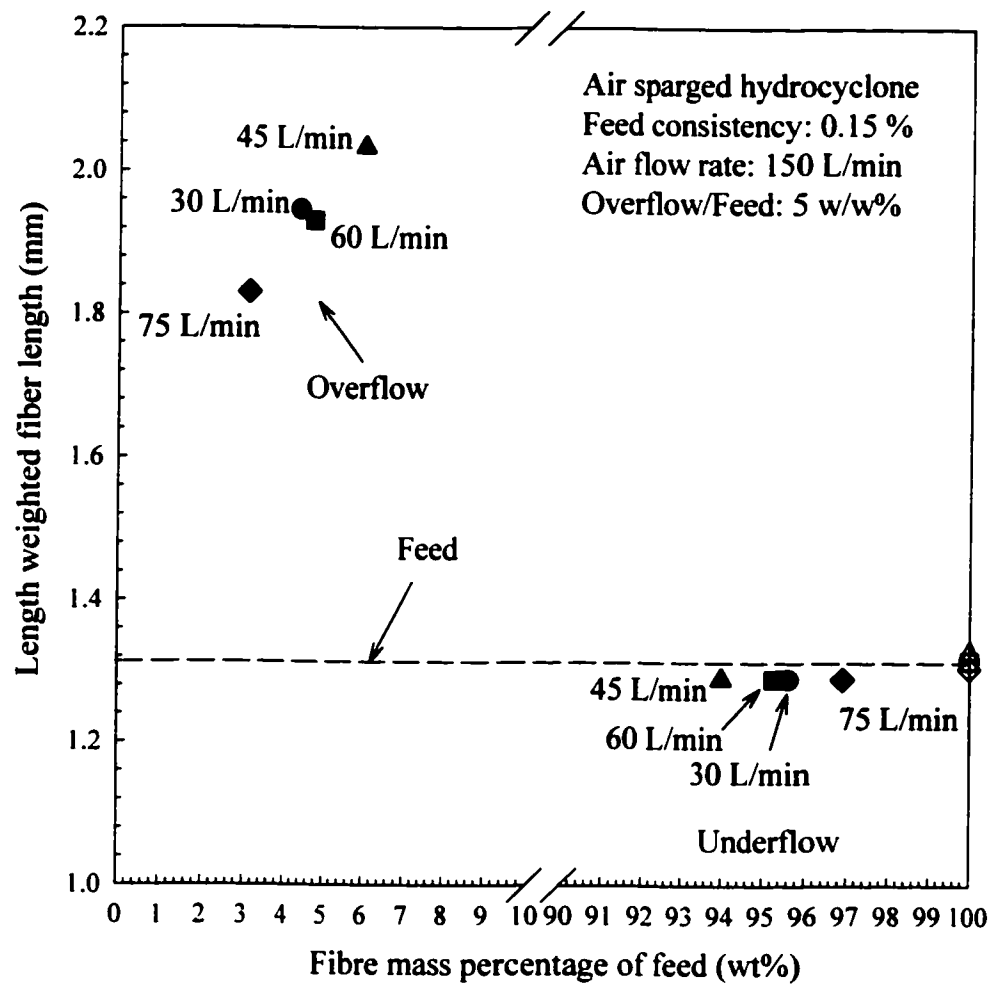


Figure 5.4a Effect of feed flow rate on fractionation by fibre length

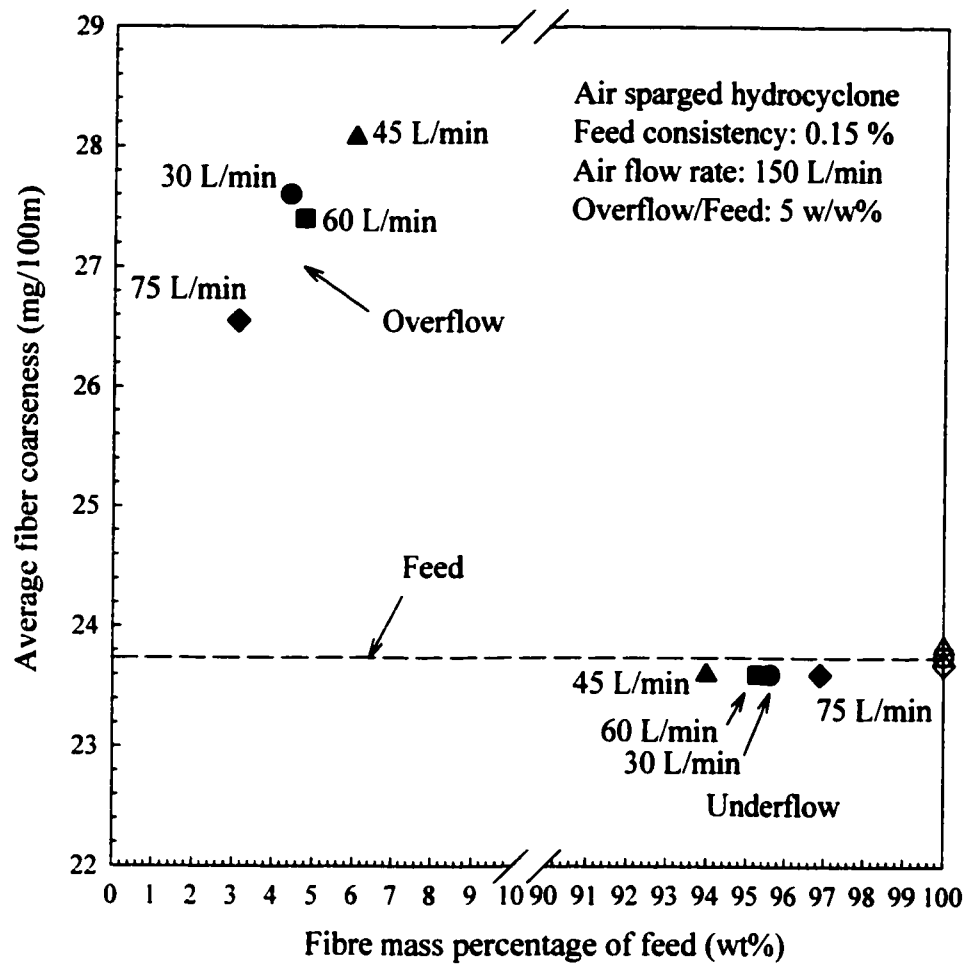


Figure 5.4b Effect of feed flow rate on fractionation by fibre coarseness

5.3.3 Effect split ratio of overflow to feed

The effect of split ratio of the overflow to feed streams on the fractionation performance was carried out at feed consistency of 0.15 wt%, air flow rate of 150 L/min and feed flow rate of 60 L/min. The split ratio of the overflow to feed streams was varied from 1% to 10% by adjusting the overflow valve opening.

The fibre length of the overflow and underflow samples collected at different split ratio was plotted against the fibre mass percentage of feed as shown in Figure 5.5a. The fibre coarseness of the overflow and underflow samples collected at different split ratio was plotted against the fibre mass percentage of feed as shown in Figure 5.5b. At a split ratio of 3%, the overflow stream has the longest fibre length and the highest fibre coarseness as compared to those tests at other split ratios. With a slightly decrease in the split ratio of 3%, the fibre length and fibre coarseness of the overflow stream decreased dramatically. The fibre length and fibre coarseness of the overflow stream decreased slightly and then remained stable at a split ratio of over 3%. The fibre length and fibre coarseness of underflow samples at different split ratio are close to that of the feed. The results suggested that an optimum split ratio gives the best fractionation performance, which occurs at 3%.

The results indicated that the froth characteristics of the air sparged hydrocyclone are quite different and more complex than that of conventional flotation system. The flotation efficiencies achieved with the air sparged hydrocyclone significantly depended on the froth stability and flow rate values.

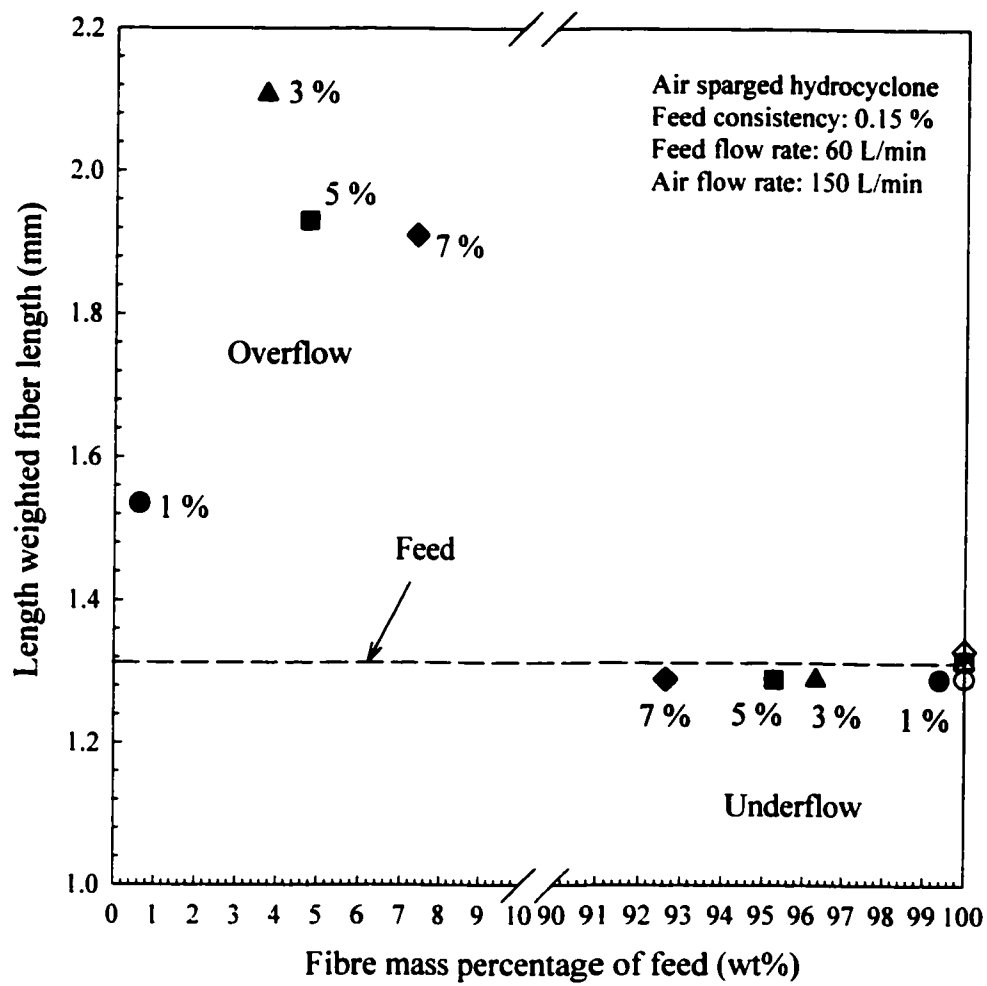


Figure 5.5a Effect of split ratio (overflow/feed) on fractionation by fibre length

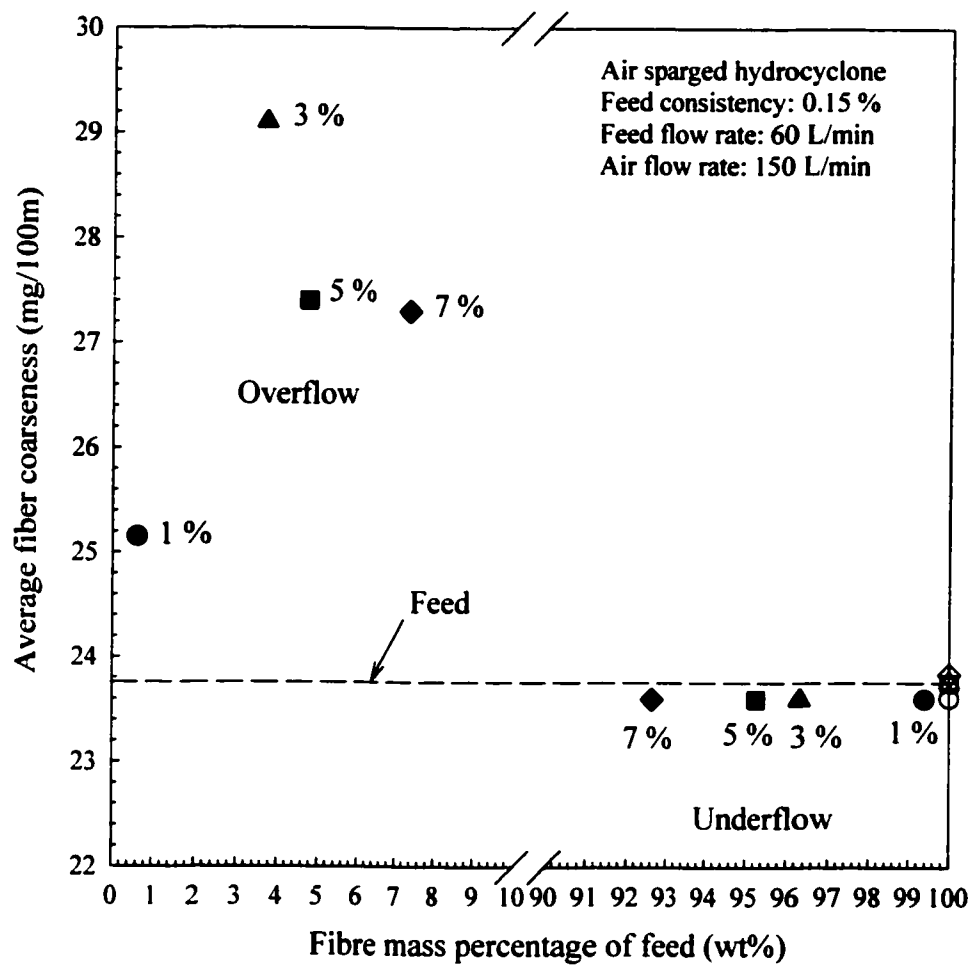


Figure 5.5b Effect of split ratio (overflow/feed)
 on fractionation by fibre coarseness

5.3.4 Effect of air flow rate

The effect of air flow rate on fractionation performance was studied at feed consistency of 0.30 wt%, feed flow rate of 60 L/min, split ratio of 5% (the overflow rate to the feed flow rate). The air flow rate was varied from 100 L/min to 200 L/min. The fibre length of the overflow and underflow samples collected at different air flow rates was plotted against the fibre mass percentage of feed as shown in Figure 5.6a. The fibre coarseness of the overflow and underflow samples collected at different air flow rates were plotted against the fibre mass percentage of feed as shown in Figure 5.6b. At the highest air flow rate of 200 L/min, the overflow had the longest fibre length and the highest fibre coarseness as compared to those tests at lower feed flow rates. However, the fibre length and coarseness of the overflow streams only slightly decreased with a decrease in the air flow rate. The fibre length and fibre coarseness of the underflow samples at different air flow rates are close to that of the feed. The results suggested that higher air flow rate gives better fractionation performance, which occurs at an air flow rate of 200 L/min in this study.

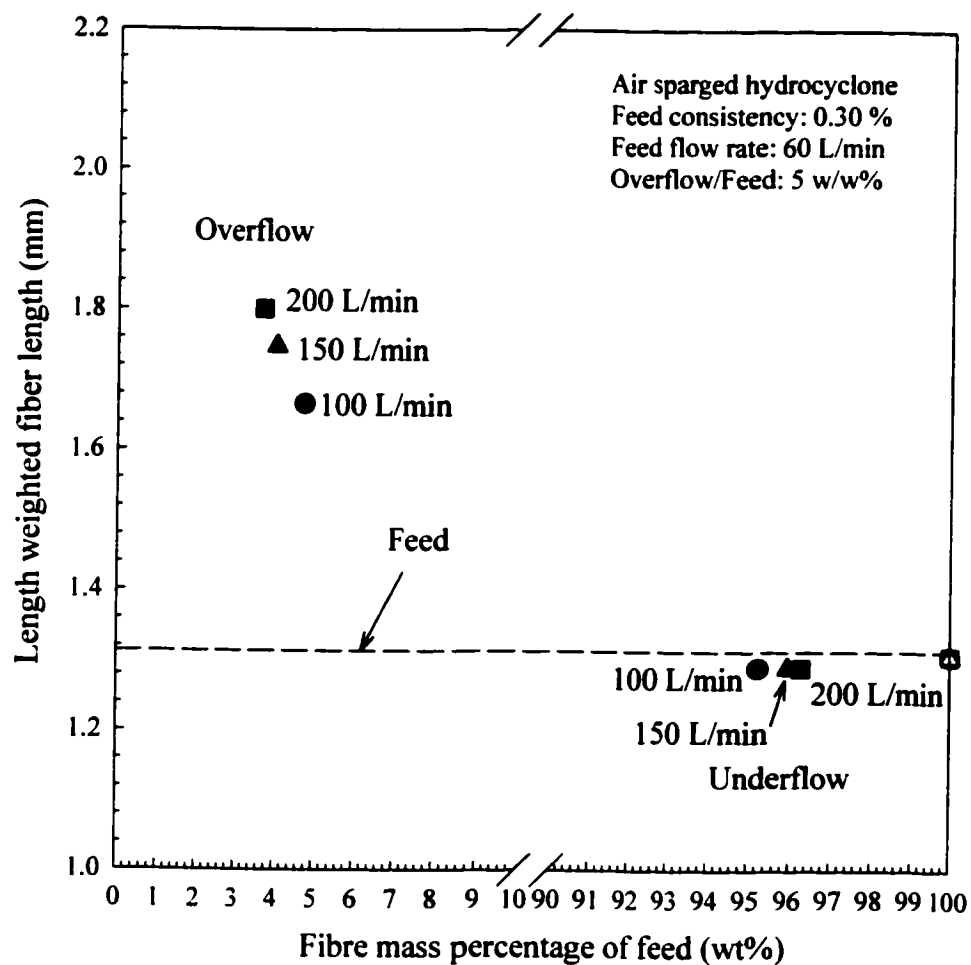


Figure 5.6a Effect of air flow rate on fractionation by fibre length

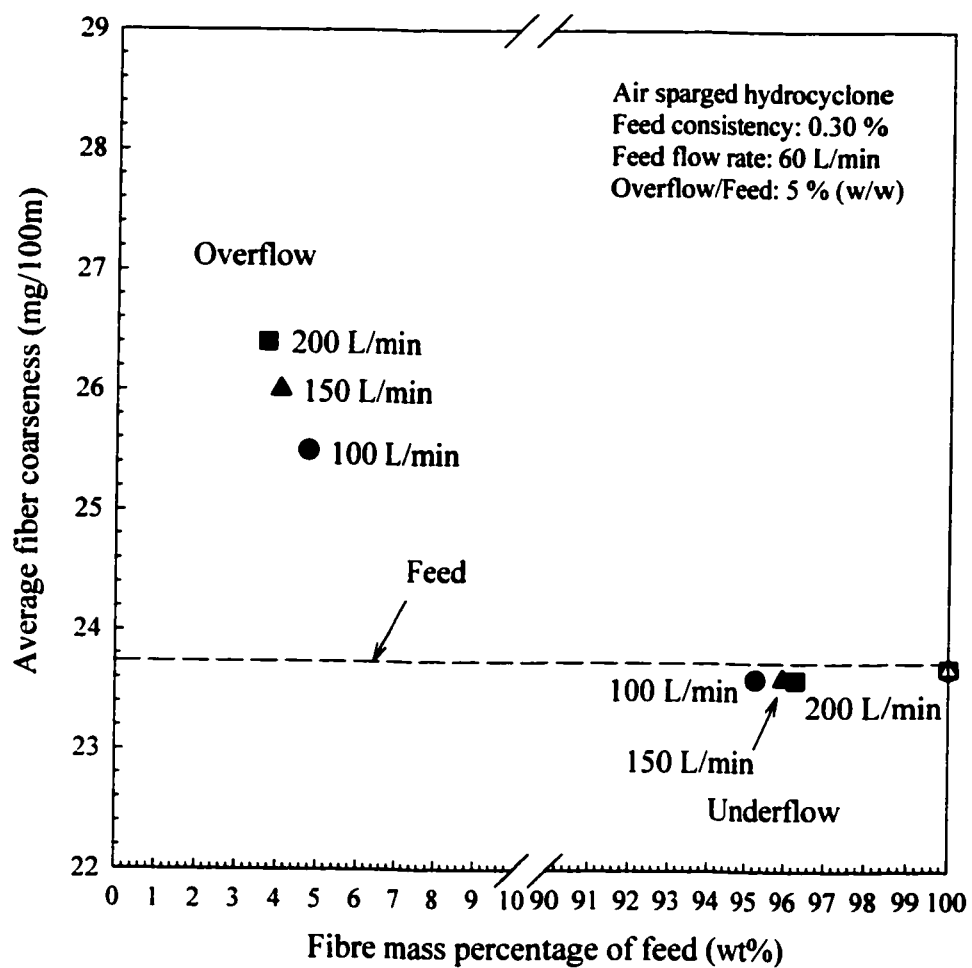


Figure 5.6b Effect of air flow rate on fractionation by fibre coarseness

5.4 CONCLUSIONS

An air sparged hydrocyclone was used to fractionate softwood TMP fibres on the basis of fibre length and fibre coarseness. About 5 wt% of the long fibres reported to the overflow stream, while the remaining 95 wt% fibres went to the underflow stream with the average fibre length and fibre coarseness close to those of the feed. Feed consistency, feed flow rate and split ratio of overflow to feed had strong effects on the fractionation performance. A lower feed consistency and a higher air flow rate favored better fractionation performance. An optimum feed flow rate and an optimum split ratio of the overflow to feed streams improved fractionation performance, since they had strong effects on froth stability.

CHAPTER 6

FRACTIONATION PERFORMANCE

In the present study, the rotating cone fractionator, continuous flotation cell and air sparged hydrocyclone were found capable of fractionating softwood TMP fibres. The results strongly suggested that low feed consistencies favor fibre fractionation. In this section, attempts were made to evaluate the fractionation performance of the selected devices at the same feed consistency. The fractionation performances of different devices were compared by comparing cumulative plots of fibre length and fibre coarseness. The fibre coarseness was also plotted versus the fibre length of fractions collected to examine the correlation between fibre length and fibre coarseness for softwood TMP fibres. The later approach might reveal more information about the primary parameter of fractionation (either fibre length or fibre coarseness). The following sections will discuss these approaches in detail.

The Bauer MacNett classifier, which uses five screens (14, 28, 48, 100 and 200 mesh) to classify a pulp sample, was adopted as an ideal fractionation device. Softwood TMP fibres are classified into five fractions. The cumulative fibre length and fibre coarseness of the five fractions represent the best fractionation performance curve on the fractionation performance figures.

6.1 FRACTIONATION PERFORMANCE

In the present study, the rotating cone was designed to generate six fractions while the continuous flotation cell and the air sparged hydrocyclone gave two fractions. In order to compare the fractionation performance of devices giving more than two fractions, the cumulative fibre length and fibre coarseness of the fractions collected from the rotating cone and Bauer McNett classifier, which were calculated from Equations (2.15) and (2.16) starting off with either the shortest or the longest fraction, were plotted versus the cumulative fibre mass percentage of the feed. The fibre length and fibre coarseness of fractions collected from the continuous flotation cell and the air sparged hydrocyclone were plotted against fibre mass percentage of the feed on the same figure. The values of 100% cumulative fibre length and fibre coarseness were plotted on the same figure and should approach the value of the feed sample when the measurement error is small.

At the feed consistency of 0.15 wt%, the cumulative fibre length and fibre coarseness (rotating cone, Bauer McNett) were plotted against the cumulative fibre mass percentage of feed as shown in Figure 6.1a and Figure 6.1b, respectively. The cumulative curves started off with the shortest fractions. The fibre length and fibre coarseness of the shortest fractions collected by the continuous flotation cell and the air sparged hydrocyclone were also plotted

against the fibre mass percentage of the feed on the same figures. As shown in Figure 6.1a, the upper bound is the feed line that indicates no fractionation, and the lower bound is the Bauer McNett cumulative fibre length curve, which represents the “best” fractionation performance. The rotating cone fractionator was capable of removing a small amount (less than 10 wt%) of fines from the feed, while the air sparged hydrocyclone could not remove any fines from the feed. The continuous flotation cell had the ability to remove a large amount (about 70 wt%) of short fibres and fines from the feed. These results indicated that the continuous flotation cell had the best fractionation performance of removing fines from the feed among the three selected devices at the feed consistency of 0.15 wt%. As shown in Figure 6.1b, the continuous flotation cell had the best fractionation performance on removing the low coarseness fibres from the feed at the feed consistency of 0.15 wt%.

In order to compare the fractionation performance of recovering valuable long fibres, the cumulative fibre length and fibre coarseness were plotted versus fibre mass percentage of the feed starting off with the longest fractions. As shown in Figure 6.1c, the air sparged hydrocyclone was capable of recovering a small amount (less than 5 wt%) of long fibres from the feed, while the rotating cone fractionator could not recover long fibres from the feed. The continuous flotation cell had the ability to remove about 30 wt% of long fibres from the feed. These results indicated that the continuous flotation cell had the best fractionation performance of recovering valuable long fibres among the three selected devices at the feed consistency of 0.15 wt%. As shown in Figure 6.1d, the continuous flotation cell had the best fractionation performance on recovering the high coarseness fibres from the feed at the feed consistency of 0.15 wt%.

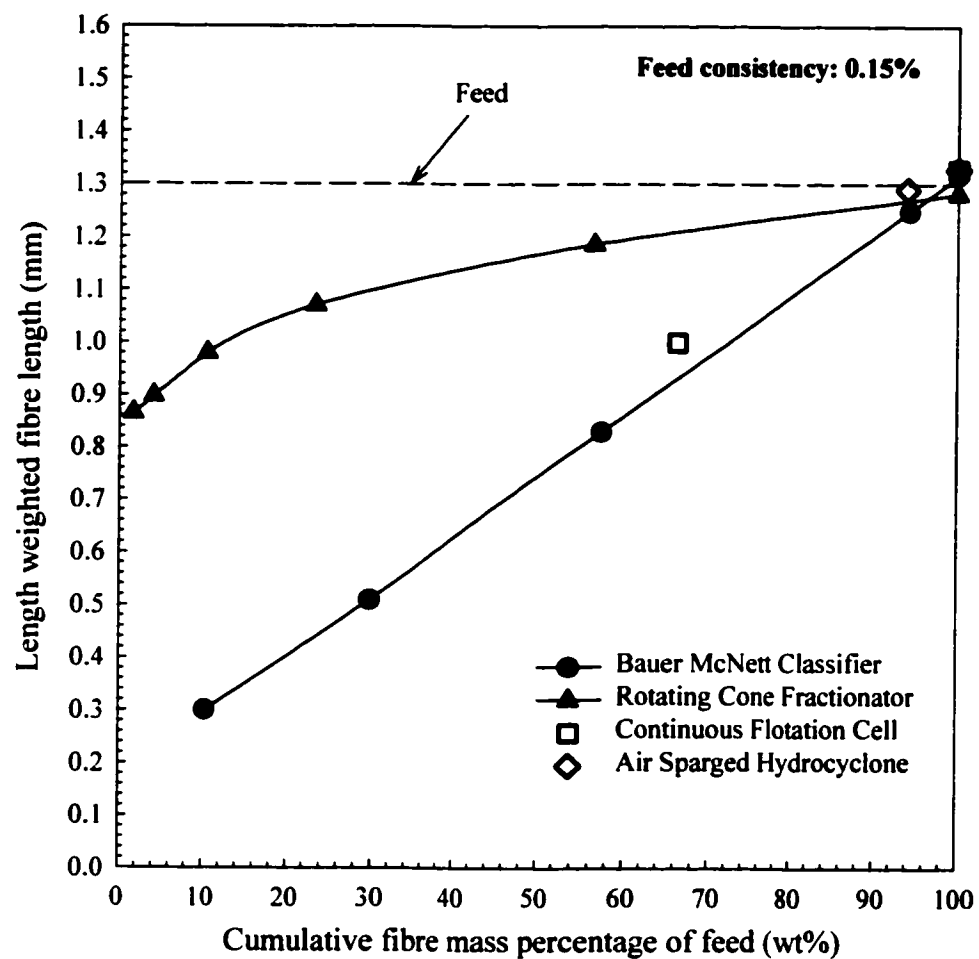


Figure 6.1a Fractionation by fibre length at feed consistency of 0.15 wt% starting with the shortest fraction

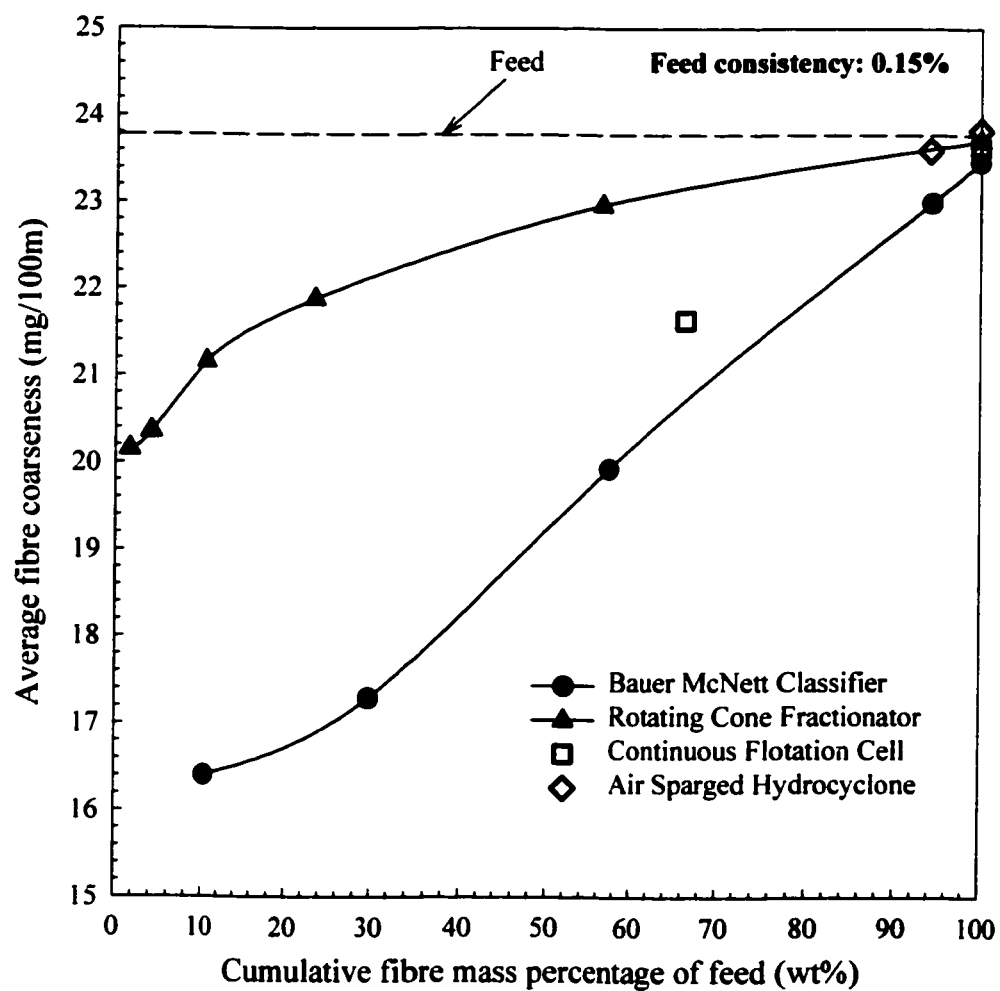


Figure 6.1b Fractionation by fibre coarseness at feed consistency of 0.15 wt% starting with the lowest coarseness fraction

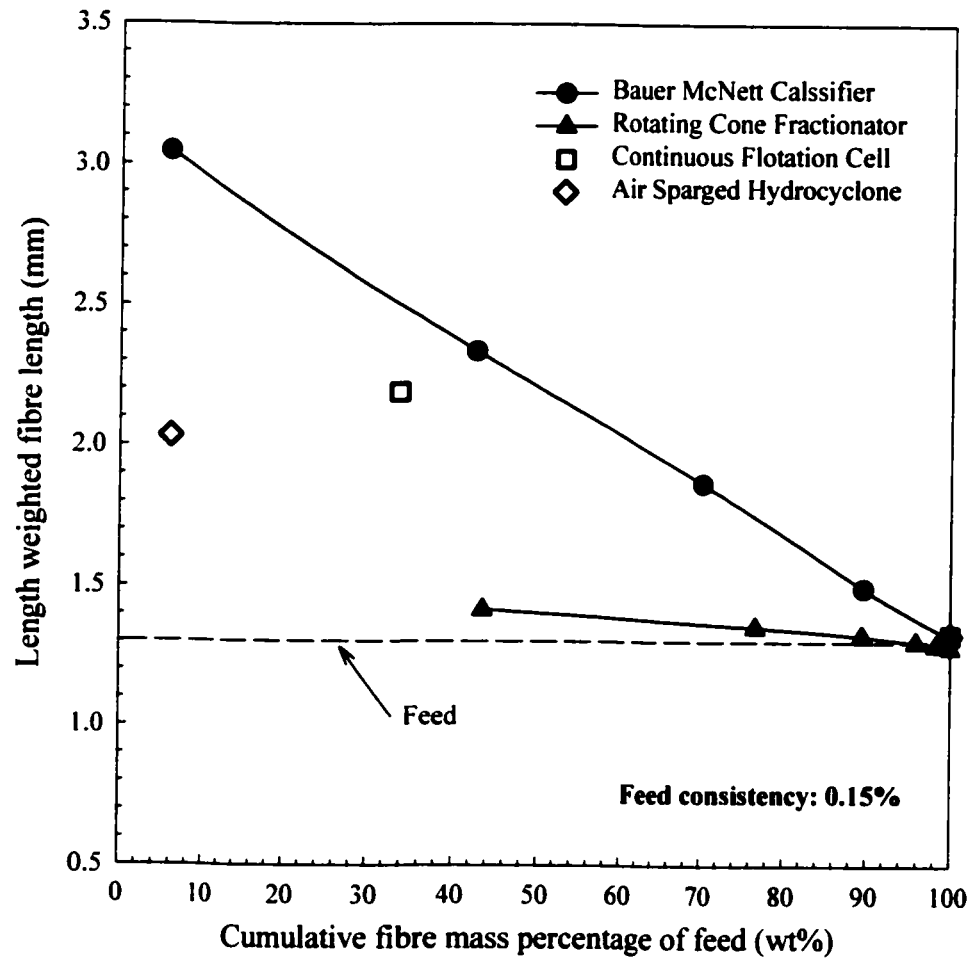


Figure 6.1c Fractionation by fibre length at feed consistency of 0.15 wt% starting with the longest fraction

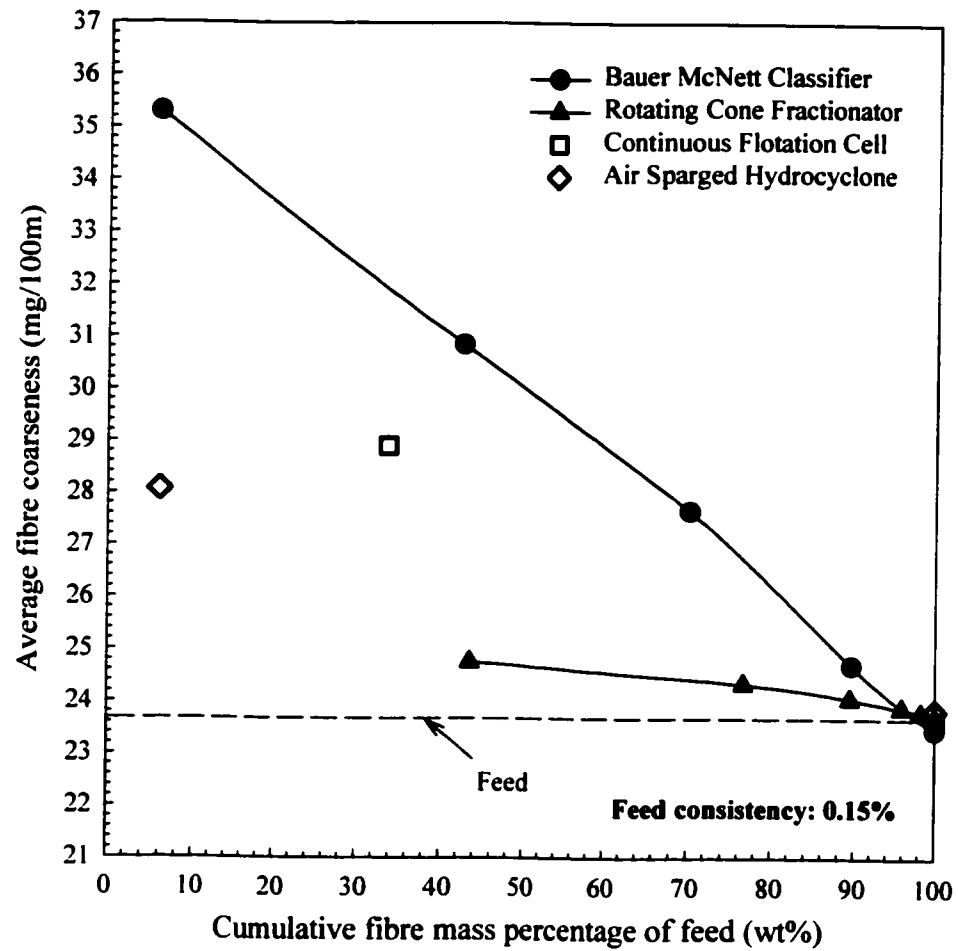


Figure 6.1d Fractionation by fibre coarseness at feed consistency of 0.15 wt% starting with the highest coarseness fraction

Comparisons of the cumulative fibre length and fibre coarseness versus the cumulative fibre mass percentage at a feed consistency of 0.45 wt% are shown in Figures 6.2a - 6.2d. The cumulative curves in Figures 6.2a and 6.2b started off with the shortest fraction, while the cumulative curves in Figures 6.2c and 6.2d started off with the longest fraction. It was found that the three selected devices had a similar fractionation performance at a feed consistency of 0.45 wt%, since the data points of both the continuous flotation cell and the air sparged hydrocyclone aligned themselves with the cumulative curve of the rotating cone fractionator. This result confirmed the previous conclusion that fractionation performance decreased with an increase in feed consistency, and that low feed consistency favors fibre fractionation.

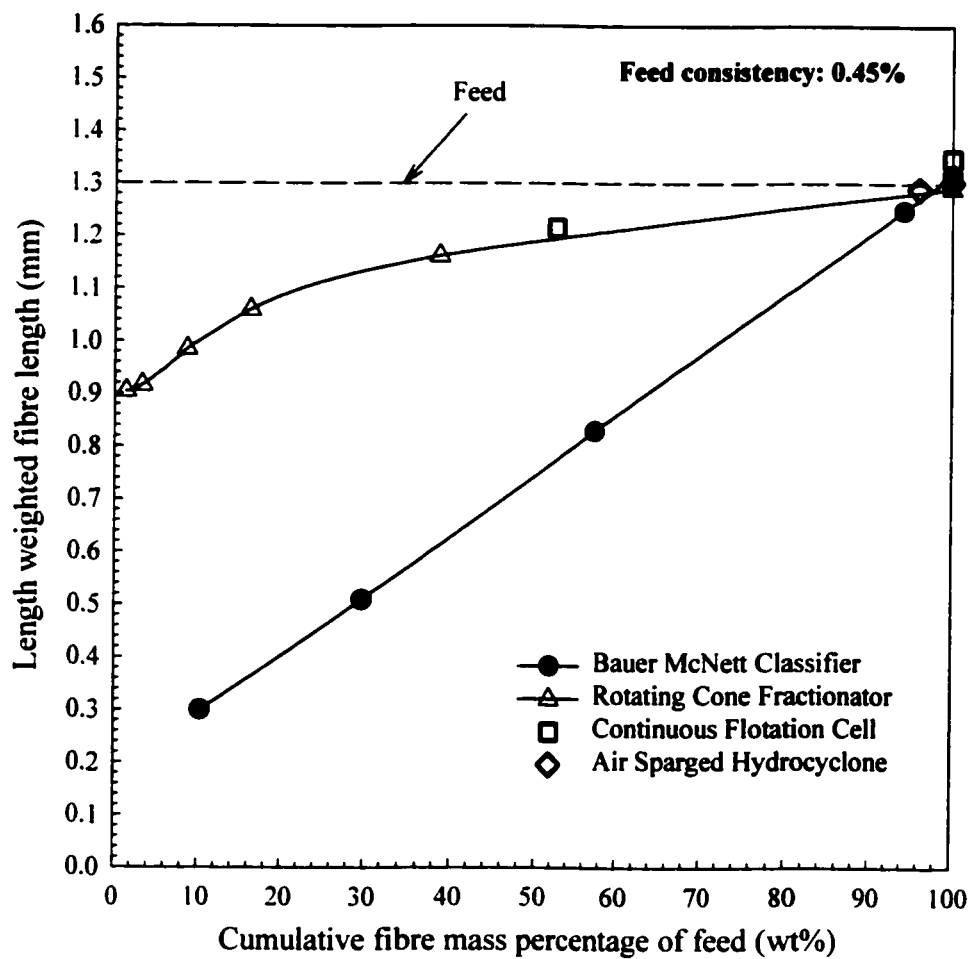


Figure 6.2a Fractionation by fibre length at feed consistency of 0.45 wt% starting with the shortest fraction

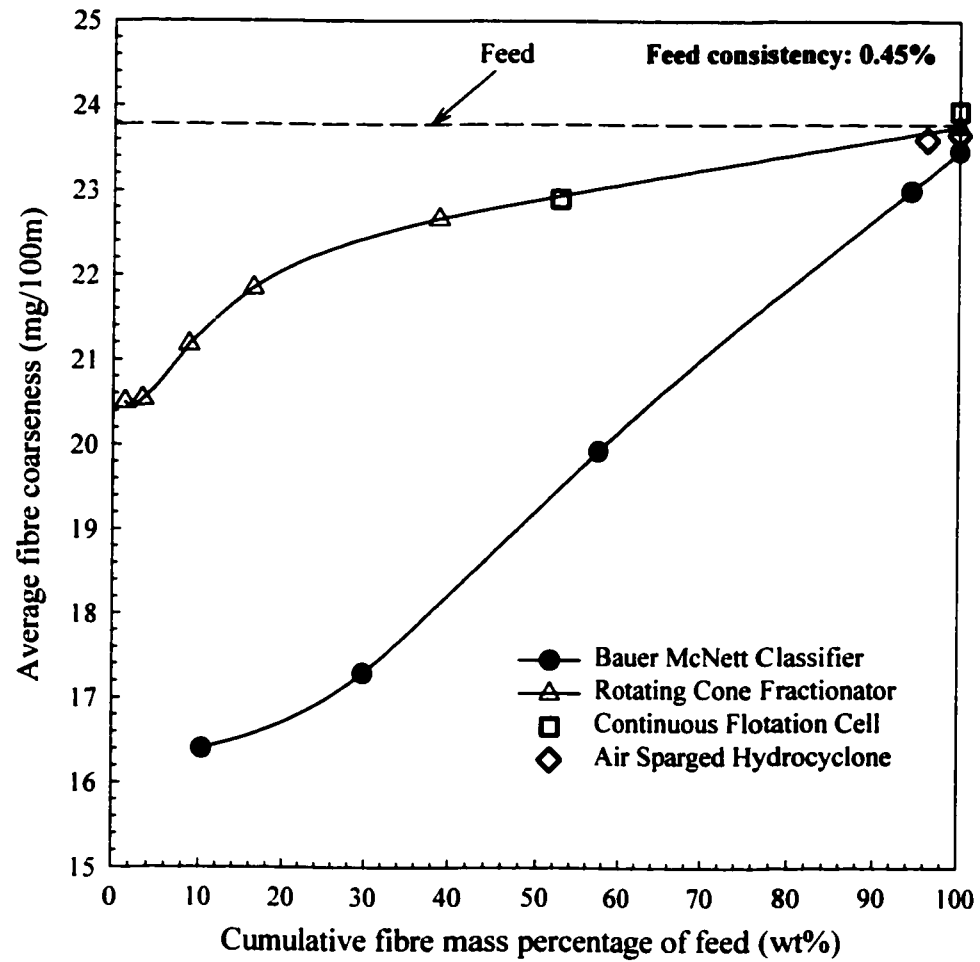


Figure 6.2b Fractionation by fibre coarseness at feed consistency of 0.45 wt% starting with the lowest coarseness fraction

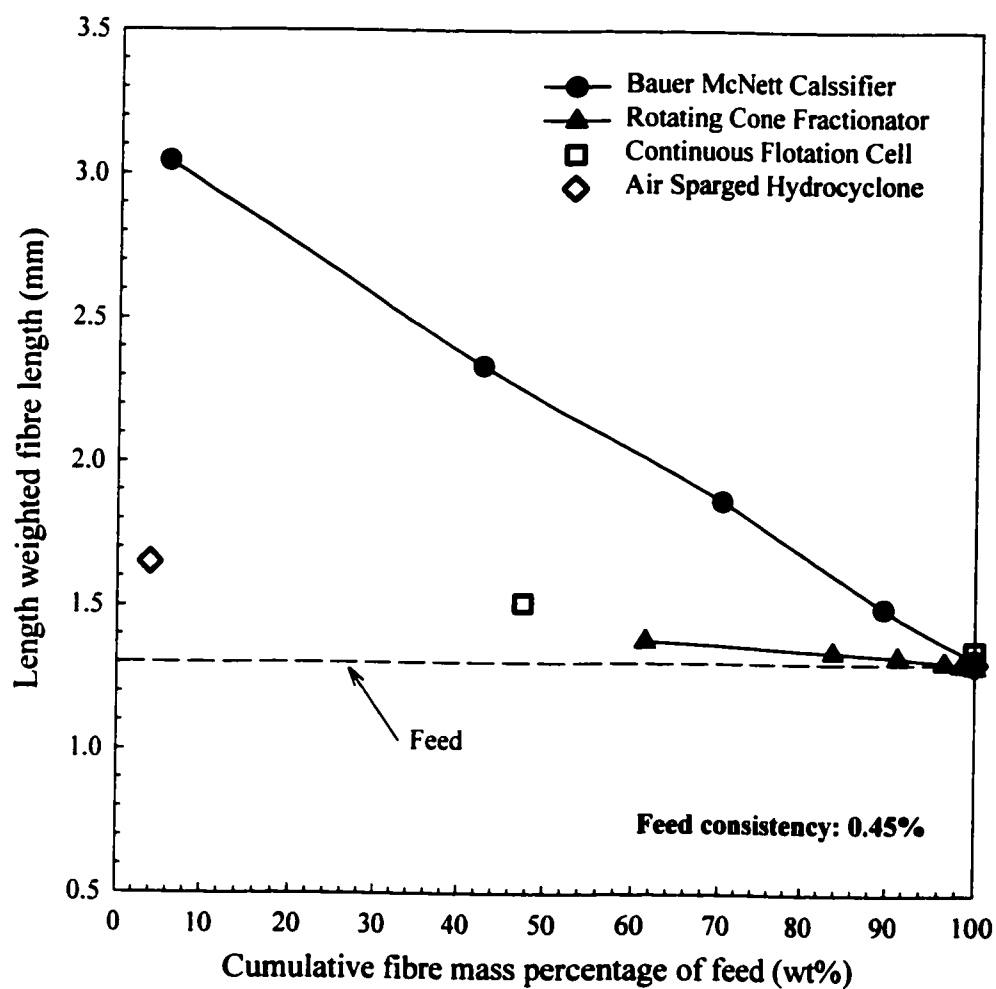


Figure 6.2c Fractionation by fibre length at feed consistency of 0.45 wt% starting with the longest fraction

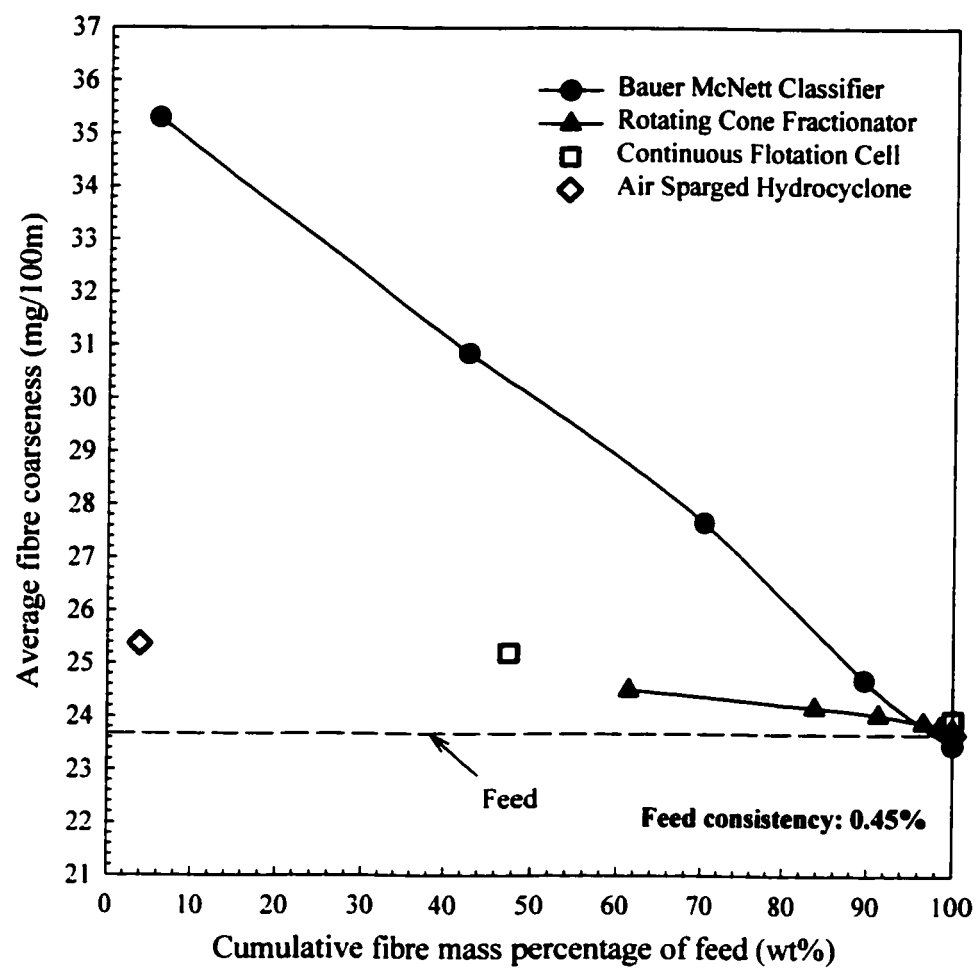


Figure 6.2d Fractionation by fibre coarseness at feed consistency of 0.45 wt% starting with the highest coarseness fraction

6.2 FRACTIONATION PARAMETERS

In the present study, both fibre length and fibre coarseness were used as indicators for fractionation performance. It was found that the longer fibre fractions exhibit higher coarseness. Therefore it is difficult to conclude the primary fractionation parameter as being either the fibre length or the fibre coarseness. However, the Bauer McNett classifier fractionates fibre primarily on the basis of fibre length, since fibres will only pass through the screen if their length is less than twice the screen opening (TAPPI standard T233 cm-95).

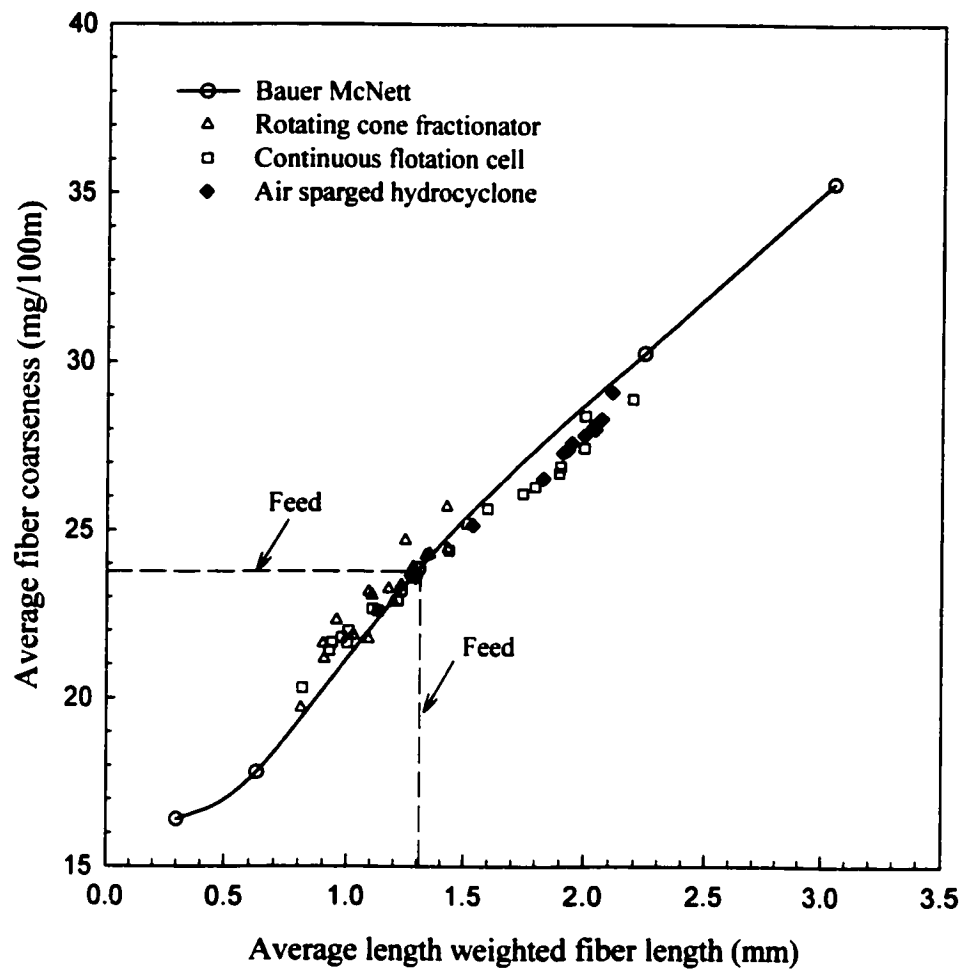


Figure 6.3 The variation of fibre coarseness versus fibre length

CHAPTER 7

SUMMARY

Since fibre length and coarseness have major impact on the properties of the finished paper products, it is beneficial to perform fibre fractionation to control fibre length or coarseness of the wood pulp used in the papermaking process. Previous studies were concerned with fibre fractionation of wood pulps on the basis of fibre length and fibre specific surface area. In the present study, more attention was focused on fractionating fibres from a pulp according to both fibre length and fibre coarseness. Three fractionators, rotating cone, continuous flotation cell, and air sparged hydrocyclone were investigated to fractionate 100% softwood TMP. The Bauer McNett fibre classifier was adopted as an ideal lab scale fractionator, which separates fibres mainly on the basis of fibre length.

In the present study, the rotating cone fractionator was found to be capable of fractionating softwood TMP fibres according to both fibre length and fibre

coarseness. The atomization mode in the form of ligaments along with a clear transition boundary on the cone surface was found to give the best fractionation performance. The ligament formation occurred either at an optimum feed flow rate or an optimum cone rotational speed while other operating parameters were fixed. A rotating cone having a rough surface was found to give a much better fractionation performance as compared to a smooth surface. Lower feed consistency favored better fractionation performance. However, the rotating cone fractionator could fractionate softwood TMP fibres at consistency as high as 1 wt%.

A continuous flotation cell was proved to be successful for fractionating 100% softwood TMP fibres according to fibre length and fibre coarseness at low feed consistencies (0.15 wt%~0.30 wt%). The feed consistency, feed flow rate and surfactant concentration had strong effects on the fractionation performance. Impeller rotation speed and air flow rate had slight effects on the fractionation performance. Lower feed consistency and feed flow rate favored better fractionation performance.

An air sparged hydrocyclone was used to fractionate softwood TMP fibres on the basis of fibre length and fibre coarseness. About 5 wt% of long fibres reported to the overflow stream, while the remaining 95 wt% fibres reported to the underflow stream with the average fibre length and fibre coarseness close to those of the feed. Feed consistency, feed flow rate and split ratio of overflow to feed streams had strong effects on the fractionation performance. A lower feed consistency and a higher air flow rate favored better fractionation performance. An optimum feed flow rate and an optimum split ratio of overflow to feed streams favored fractionation, since they had strong effects on froth stability.

The continuous flotation cell was found to give the best fractionation performance for either removing fines or recovering long fibres from the feed at low feed consistencies (0.15 wt%).

CHAPTER 8

RECOMMENDATIONS

FOR FUTURE WORK

- In the present study, there was no surfactant added for the tests carried out using the air sparged hydrocyclone. The effect of surfact concentration on fractionation performance should be investigated.
- Fibre length was found directly related to fibre coarseness for softwood TMP fibres studied. Further study should follow to investigate fibre fractionation according to coarseness.

REFERENCES

1. Abubakr, S.M., G.M., and Klungness, J.H., "Fibre Fractionation as a Method of Improving Handsheet Properties after Repeated Recycling", Tappi J. 78 (5): 123-126 (1995)
2. Ajersch, M and Pelton, R., "Mechanism of Stock Loss in Flotation Deinking", 3rd Research Forum on Recycling, CPPA, 27 – 40 (1995)
3. Behera, N.C., and Basu, S., "Studies on the Improvement of Pulp Strength by Fibre Fractionation and Blending Technique", Appita 34 (6): 485-491 (1981)
4. Bichard, W, and Scudamore, P., "Evaluation of the Comparative Performance of the Kajaani FS-100 and FS-200 Fibre Length Analyzers, " TAPPI Journal 71 (12), 149 (1988)
5. Bliss, T. L., "A Study of Fibre Fractionation Using Centrifugal Cleaners," M. Sc. Thesis, Dept of Paper Science and Engineering, Miami University, Oxford, Ohio. (1983)
6. Bliss, T. L., "Secondary Fibre Fractionation Using Centrifugal Cleaners," TAPPI Pulping Conference, Proceedings, P217 (1984)
7. Bliss, T., "Centrifugal Cleaning," Chapter XIII in Pulp and Paper Manufacture, Third Edition, Volume 6, Stock Preparation ed. R. W., Hagemeyer and D. W. Manson, Joint Textbook Committee of the Paper Industry. (1992)
8. Chen, J. X., and Masliyah J.H. "Fractionation of Nylon Fibres Using a Vertical Settler" The Canadian Journal of Chemical Engineering, Volume 78, Feb. (2000)

9. Cooper, W. and Kurdin, J.A. "Acronyms for Mechanical Pulp: Understanding the Alphabet Soup" *Tappi Journal* (December 1987)
10. Clark, J.d'A., "The Measurement and Influence of Fibre Length," *Paper Trade J.* 115 (26), 36 (1942)
11. Clark, J. d'A., "Weight Average Fibre Lengths – A Quick Visual Method," *TAPPI* 45 (1), 38 (1962a)
12. Clark, J. d'A., "Effects of Fibre Coarseness and Length," *TAPPI* 45 (8), 628 (1962b)
13. Eckert, W., Maliyah, J. H. and Afacan, A., "Fractionation of Softwood TMP by Flotation", *TAPPI J.*, 80, No. 5, 210-216 (1997)
14. Eckert, W., Afacan, A., and Masliyah J. H. "Fractionation of Softwood TMP by Flotation" *TAPPI J.*, (March, 1998)
15. Franko, A., "Centri-cleaning," Chapter XVI in *Pulp and Paper Manufacture. Third Edition. Volume 2, Mechanical pulping*, ed., R.A. Leaask, Joint Textbook Committee of the Paper Industry, (1987)
16. Galloway, L. R., and Branion, R. M. R., "Separation of Light Weight Particles from Pulp Suspensions with Three Different Commercial Cleaners," *Preprints 1990 Spring Conference, Technical Section, Canadian Pulp and Paper Association*, Jasper, (1990)
17. Gavelin, G., and Backman, J., "Fractionation with Hydrocyclones," *Proceedings TAPPI Pulping Conference*, P753 (1991)
18. Jameson, R.J., in *Principles of Mineral Flotation: The Wark Symposium* (M. H. Jones and J. T. Woodcock, Eds.), *Symposia Series No. 40*, Australasian Institute of Mining and Metallurgy, Parkville, Victoria, Australia, P. 215 (1984)
19. Karnis, A., *J. Pulp and Paper Sci.* 20(10): J280 (1994)
20. Klemm, K.H., "The Interpretation of Roundwood Production by Fiber Technology," *Pulp and Paper Magazine of Canada* 56 (11), 178 (1955).

21. Kerekes, R. J., and Schell, C. J., "Characterization of Fibre Flocculation Regimes by a Crowding Factor", *Journal of Pulp and Paper Science* 18, J32-38 (1992)
22. Li, M. and Muvundamina, M., *Progr. Paper Recycling* 4(3): 32 (1995)
23. Miller, J. D., "Froth Characteristics in Air sparged Hydrocyclones Flotation", *Mineral Processing and Extractive Metallurgy Review*, Vol. 5, P307-329 (1989)
24. Miller, J. D., "The status of Air Sparged Hydrocyclone Flotation Technology" University of Utah (1995)
25. Miller, J. D., "Swirl flow characteristics and froth phase features in air-sparged hydrocyclone flotation as revealed by X-ray CT analysis", *Int. J. Miner Process.* 47 P251 -274 (1996)
26. Miller, J. D., "Flow phenomena and its impact on air sparged hydrocyclone flotation of quartz" *Minerals and Metallurgical Processing*. Feb (1995)
27. Moller K., De Ruvo, A., Norman B., and Felsvang, K., "Screen, Cleaning and Fractionation with an Atomizer", *Paper Technology and Industry* 20 (3), 110 (1979)
28. Oroskar, A. R. and Crosby, E. J., "Vaneless Disk Fractionation of Slurries", *Industrial and Engineering Chemistry, Fundamentals*, 25 (4), 483 (1986)
29. Paavilainen, L., "The Possibility of Fractionation Softwood Sulfate Pulp according to Cell Wall Thickness," *TAPPI* 45 (5), 319 (1992)
30. Rewatkar, V.B. and Masliyah, J.H., "Hardwood Fibre Fractionation Using Rotating Cone", *Can. J. Chem. Eng.* 75, 196-204 (1997)
31. Rewatkar, V.B. and Masliyah, J.H., "Wood Pulp Fibre Fractionation", in "Mixed-Flow Hydrodynamics" *Advances in Engineering Fluid Mechanics Series*, N.P. Cheremisinoff, Ed., Gulf Publishing, Houston, TX, 871-906 (1996)
32. Seth, R.S., "Fibre Quality Factors in Papermaking I – The Importance of Fibre Length and Strength" *Mat. Res. Soc. Symp. Pro. Vol.* 197 (1990)

33. Seth, R.S., "Fibre Quality Factors in Papermaking I – The Importance of Fibre Coarseness" Mat. Res. Soc. Symp. Pro. Vol. 197 (1990)
34. Seth, R.S., Chan, B.K., "Measurement of fibre coarseness with optical fibre length analyzers", TAPPI Journal Vol. 80: No.5 217 (1996)
35. Smook, G.A. "Handbook for Pulp and Paper Technologists", Second Edition, Augus Wilde Publications (1992)

APPENDIX

Data for all figures included in this thesis

Figure 2.2 Variation of fibre coarseness at different washing time intervals

Time interval (min)	0	2	4	6	8	10
Percentage fines (%)	41.43	28.16	26.35	25.99	24.37	23.91
Coarseness (mg/100m)	32.60	23.40	23.60	23.50	23.65	24.50

Figure 3.3a Effect of feed consistency on fibre fractionation by fibre length

Figure 3.3b Effect of feed consistency on fibre fractionation by fibre coarseness

Feed consistency (%)	Lab data	Zone 1	Zone 2	Zone 3	Zone 4	Zone 5	Zone 6
0.15	Fraction mass (g)	10.21	7.772	3.009	1.502	0.568	0.392
	Length (mm)	1.415	1.275	1.150	1.035	0.920	0.865
	Coarseness (mg/100m)	24.75	23.80	22.50	21.70	20.50	20.15
0.40	Fraction mass (g)	25.54	9.296	3.165	2.212	0.793	0.589
	Length (mm)	1.380	1.240	1.150	1.030	0.925	0.905
	Coarseness (mg/100m)	24.50	23.30	22.65	21.60	20.55	20.50
0.95	Fraction mass (g)	34.43	27.52	7.076	3.665	1.493	1.039
	Length (mm)	1.360	1.295	1.195	1.130	1.060	1.000
	Coarseness (mg/100m)	24.05	23.80	22.80	22.45	21.80	21.40

Figure 3.4a Effect of feed flow rate on fibre fractionation by fibre length

Figure 3.4b Effect of feed flow rate on fibre fractionation by fibre coarseness

Feed flow rate (l/min)	Lab data	Zone 1	Zone 2	Zone 3	Zone 4	Zone 5	Zone 6
1.2	Fraction mass (g)	3.197	4.574	1.725	1.063	0.903	0.525
	Length (mm)	1.350	1.335	1.230	1.195	1.125	1.090
	Coarseness (mg/100m)	24.30	24.25	23.35	22.85	22.60	21.75
2.4	Fraction mass (g)	10.21	7.772	3.009	1.502	0.568	0.392
	Length (mm)	1.415	1.275	1.150	1.035	0.920	0.865
	Coarseness (mg/100m)	24.75	23.80	22.50	21.70	20.50	20.15
3.0	Fraction mass (g)	12.27	7.080	2.142	1.240	0.661	0.437
	Length (mm)	1.425	1.260	1.140	1.060	0.995	0.895
	Coarseness (mg/100m)	24.85	23.30	22.55	21.80	21.15	20.55
3.6	Fraction mass (g)	13.25	5.880	1.708	0.953	0.526	0.403
	Length (mm)	1.400	1.225	1.120	1.040	1.010	0.955
	Coarseness (mg/100m)	24.55	23.30	22.30	21.80	21.35	20.70

Figure 3.5a Effect of cone rotational speed on fibre fractionation by fibre length

Figure 3.5b Effect of cone rotational speed on fibre fractionation by fibre coarseness

Cone rotational speed (rpm)	Lab data	Zone 1	Zone 2	Zone 3	Zone 4	Zone 5	Zone 6
200	Fraction mass (g)	12.71	5.275	2.708	1.240	0.682	0.358
	Length (mm)	1.390	1.235	1.160	1.070	0.950	0.840
	Coarseness (mg/100m)	24.10	23.55	22.50	21.60	20.80	20.20
300	Fraction mass (g)	12.90	5.587	1.894	0.867	0.613	0.331
	Length (mm)	1.430	1.245	1.080	0.965	0.890	0.790
	Coarseness (mg/100m)	24.40	23.20	22.25	21.25	20.80	19.95
450	Fraction mass (g)	10.21	7.772	3.009	1.502	0.568	0.392
	Length (mm)	1.415	1.275	1.150	1.035	0.920	0.865
	Coarseness (mg/100m)	24.75	23.80	22.50	21.70	20.50	20.15
600	Fraction mass (g)	7.060	6.995	3.178	1.661	0.631	0.494
	Length (mm)	1.430	1.330	1.220	1.120	0.970	0.955
	Coarseness (mg/100m)	24.40	23.80	23.00	22.35	21.75	21.45

Figure 3.6a Effect of cone surface roughness on fibre fractionation by fibre length

Figure 3.6b Effect of cone surface roughness on fibre fractionation by fibre coarseness

Cone surface roughness	Lab data	Zone 1	Zone 2	Zone 3	Zone 4	Zone 5	Zone 6
Smooth	Fraction mass (g)	23.32	4.810	1.882	1.240	0.609	0.461
	Length (mm)	1.305	1.275	1.260	1.230	1.200	1.160
	Coarseness (mg/100m)	24.00	23.70	23.50	22.80	22.35	22.25
20 mesh	Fraction mass (g)	10.21	7.772	3.009	1.502	0.568	0.392
	Length (mm)	1.415	1.275	1.150	1.035	0.920	0.865
	Coarseness (mg/100m)	24.75	23.80	22.50	21.70	20.50	20.15

Figure 4.3a Effect of feed consistency on fibre fractionation by fibre length

Figure 4.3b Effect of feed consistency on fibre fractionation by fibre coarseness

Feed consistency (%)	Lab data	Froth	Tailing
0.15	Fraction mass (g)	0.878	1.727
	Length (mm)	2.190	1.000
	Coarseness (mg/100m)	28.90	21.63
0.30	Fraction mass (g)	1.346	1.542
	Length (mm)	1.795	0.975
	Coarseness (mg/100m)	26.30	21.80
0.45	Fraction mass (g)	2.008	2.222
	Length (mm)	1.510	1.215
	Coarseness (mg/100m)	25.20	22.90

Figure 4.4a Effect of feed flow rate on fibre fractionation by fibre length

Figure 4.4b Effect of feed flow rate on fibre fractionation by fibre coarseness

Feed flow rate (l/min)	Lab data	Froth	Tailing
0.44	Fraction mass (g)	1.578	2.030
	Length (mm)	1.995	0.935
	Coarseness (mg/100m)	27.45	21.65
0.75	Fraction mass (g)	1.346	1.542
	Length (mm)	1.795	0.975
	Coarseness (mg/100m)	26.30	21.80
1.58	Fraction mass (g)	3.175	2.931
	Length (mm)	1.435	1.230
	Coarseness (mg/100m)	24.40	23.20

Figure 4.5a Effect of air flow rate on fibre fractionation by fibre length

Figure 4.5b Effect of air flow rate on fibre fractionation by fibre coarseness

Air flow rate (l/min)	Lab data	Froth	Tailing
28.4	Fraction mass (g)	2.450	2.192
	Length (mm)	1.745	0.925
	Coarseness (mg/100m)	26.10	21.40
44.4	Fraction mass (g)	1.346	1.542
	Length (mm)	1.795	0.975
	Coarseness (mg/100m)	26.30	21.80

Figure 4.6a Effect of surfactant concentration on fibre fractionation by fibre length

Figure 4.6b Effect of surfactant concentration on fibre fractionation by fibre coarseness

Surfactant concentration (vol %)	Lab data	Froth	Tailing
0	Fraction mass (g)	0.848	2.398
	Length (mm)	2.000	1.130
	Coarseness (mg/100m)	28.40	22.60
0.0004	Fraction mass (g)	1.346	1.542
	Length (mm)	1.795	0.975
	Coarseness (mg/100m)	26.30	21.80
0.0008	Fraction mass (g)	2.028	0.846
	Length (mm)	1.595	0.815
	Coarseness (mg/100m)	25.65	20.30

Figure 4.7a Effect of impeller speed on fibre fractionation by fibre length

Figure 4.7b Effect of impeller speed on fibre fractionation by fibre coarseness

Impeller speed (rpm)	Lab data	Froth	Tailing
1250	Fraction mass (g)	1.498	3.119
	Length (mm)	1.895	1.105
	Coarseness (mg/100m)	26.70	22.65
1575	Fraction mass (g)	1.689	2.606
	Length (mm)	1.900	1.005
	Coarseness (mg/100m)	26.90	22.00
1800	Fraction mass (g)	1.346	1.542
	Length (mm)	1.795	0.975
	Coarseness (mg/100m)	26.30	21.80

Figure 5.3a Effect of feed consistency on fibre fractionation by fibre length

Figure 5.3b Effect of feed consistency on fibre fractionation by fibre coarseness

Feed Consistency (%)	Lab data	Overflow	Underflow
0.15	Fraction mass (g)	3.532	71.05
	Length (mm)	1.930	1.290
	Coarseness (mg/100m)	27.40	23.60
0.30	Fraction mass (g)	4.563	108.1
	Length (mm)	1.747	1.290
	Coarseness (mg/100m)	26.00	23.60
0.45	Fraction mass (g)	6.200	188.9
	Length (mm)	1.630	1.290
	Coarseness (mg/100m)	25.25	23.60

Figure 5.4a Effect of feed flow rate on fibre fractionation by fibre length

Figure 5.4b Effect of feed flow rate on fibre fractionation by fibre coarseness

Feed flow rate (l/min)	Lab data	Overflow	Underflow
30	Fraction mass (g)	1.624	35.42
	Length (mm)	1.945	1.290
	Coarseness (mg/100m)	27.60	23.60
45	Fraction mass (g)	3.376	52.82
	Length (mm)	2.033	1.290
	Coarseness (mg/100m)	28.07	23.60
60	Fraction mass (g)	4.563	108.1
	Length (mm)	1.747	1.290
	Coarseness (mg/100m)	26.00	23.60
75	Fraction mass (g)	2.955	92.29
	Length (mm)	1.830	1.290
	Coarseness (mg/100m)	26.55	23.60

Figure 5.5a Effect of split ratio (overflow/feed) on fibre fractionation by fibre length

Figure 5.5b Effect of split ratio (overflow/feed) on fibre fractionation by fibre coarseness

Split ratio (overflow/feed) (%)	Lab data	Overflow	Underflow
1	Fraction mass (g)	0.456	74.13
	Length (mm)	1.535	1.290
	Coarseness (mg/100m)	25.15	23.60
3	Fraction mass (g)	2.802	73.297
	Length (mm)	2.107	1.290
	Coarseness (mg/100m)	29.10	23.60
5	Fraction mass (g)	4.563	108.1
	Length (mm)	1.747	1.290
	Coarseness (mg/100m)	26.00	23.60
7	Fraction mass (g)	5.566	70.03
	Length (mm)	1.910	1.290
	Coarseness (mg/100m)	27.30	23.60

Figure 5.6a **Effect of air flow rate on fibre fractionation by fibre length**

Figure 5.6b **Effect of air flow rate on fibre fractionation by fibre coarseness**

Air flow rate (l/min)	Lab data	Overflow	Underflow
100	Fraction mass (g)	5.377	107.7
	Length (mm)	1.665	1.290
	Coarseness (mg/100m)	25.50	23.60
150	Fraction mass (g)	4.563	108.1
	Length (mm)	1.747	1.290
	Coarseness (mg/100m)	26.00	23.60
200	Fraction mass (g)	4.161	107.8
	Length (mm)	1.800	1.290
	Coarseness (mg/100m)	26.40	23.60

- Figure 6.1a Fractionation by fibre length at feed consistency of 0.15% starting with the shortest fraction
- Figure 6.1b Fractionation by fibre coarseness at feed consistency of 0.15 wt% starting with the lowest coarseness fraction
- Figure 6.1c Fractionation by fibre length at feed consistency of 0.15 wt% starting with the longest fraction
- Figure 6.1d Fractionation by fibre coarseness at feed consistency of 0.15 wt% starting with the highest coarseness fraction

Device	Fractions	Fraction mass (g)	Length (mm)	Coarseness (mg/100m)
Rotating cone fractionator	Zone 1	10.210	1.415	24.75
	Zone 2	7.772	1.275	23.80
	Zone 3	3.009	1.150	22.50
	Zone 4	1.502	1.035	21.70
	Zone 5	0.568	0.920	20.50
	Zone 6	0.392	0.865	20.15
Continuous flotation cell	Froth	0.878	2.190	28.90
	Tailing	1.727	1.000	21.63
Air sparged hydrocyclone	Overflow	3.532	1.930	27.40
	Underflow	71.05	1.290	23.60
Bauer McNett Fibre Classifier	14 mesh	0.390	3.045	35.30
	14-28 mesh	2.492	2.240	30.25
	28-50 mesh	1.868	1.305	23.85
	50-100 mesh	1.313	0.630	17.80
	100-200 mesh	0.700	0.300	16.40

- Figure 6.2a Fractionation by fibre length at feed consistency of 0.45 wt% starting with the shortest fraction
- Figure 6.2b Fractionation by fibre coarseness at feed consistency of 0.45 wt% starting with the lowest coarseness fraction
- Figure 6.2c Fractionation by fibre length at feed consistency of 0.45 wt% starting with the longest fraction
- Figure 6.2d Fractionation by fibre coarseness at feed consistency of 0.45 wt% starting with the highest coarseness fraction

Device	Fractions	Fraction mass (g)	Length (mm)	Coarseness (mg/100m)
Rotating cone fractionator	Zone 1	34.43	1.360	24.05
	Zone 2	27.52	1.295	23.80
	Zone 3	7.076	1.195	22.80
	Zone 4	3.665	1.130	22.45
	Zone 5	1.493	1.060	21.80
	Zone 6	1.039	1.000	21.40
Continuous flotation cell	Froth	2.008	1.510	25.20
	Tailing	2.222	1.215	22.90
Air sparged hydrocyclone	Overflow	6.200	1.630	25.25
	Underflow	188.9	1.290	23.60
Bauer McNett Fibre Classifier	14 mesh	0.390	3.045	35.30
	14-28 mesh	2.492	2.240	30.25
	28-50 mesh	1.868	1.305	23.85
	50-100 mesh	1.313	0.630	17.80
	100-200 mesh	0.700	0.300	16.40

Figure 6.3 The variation of fibre coarseness versus fibre length

(This figure was plotted using the data listed above.)